AD-A216 089

REPORT DOCUMENTATION PAGE

Form Approved
OMB No. 0704-0188

1. AGENCY USE ONLY (Leave blank)	2. REPORT DATE	3. REPORT TYPE AND DATES COVERED
	October 1984	Final (5-1-83/7-31-84

4. TITLE AND SUBTITLE
BASIS RESEARCH ON PROCESSING OF CERAMICS FOR SPACE STRUCTURES

5. FUNDING NUMBERS
61102F
2303/A3

6. AUTHOR(S)
Professor H. Kent Bowen and Dr. Richard L. Pober

7. PERFORMING ORGANIZATION NAME(S) AND ADDRESS(ES)
Massachusetts Institute of Technology
Materials Processing Center
77 Massachusetts Avenue, Cambridge, MA 021[illegible]

8. PERFORMING ORGANIZATION REPORT NUMBER
AFOSR-TR-
89-1708

9. SPONSORING/MONITORING AGENCY NAME(S) AND ADDRESS(ES)
AFOSR
BLDG 410
BAFB DC 20332-6448

10. SPONSORING/MONITORING AGENCY REPORT NUMBER
AFOSR-83-0192

DTIC
ELECTE
DEC 21 1989
S D
D

11. SUPPLEMENTARY NOTES

12a. DISTRIBUTION/AVAILABILITY STATEMENT

12b. DISTRIBUTION CODE

13. ABSTRACT (Maximum 200 words)

Uniform, composite $Al_2O_3 \cdot ZrO_2$, $Al_2O_3 \cdot TiO_2$, and $SiC \cdot ZrO_2$ were synthesized using a newly developed continuous flow reactor, by metal alkoxide hydrolysis in an alcohol/core particle suspension. Results indicate that coating particles bind to core particles via a chemisorption process. If so, water-wet core particle surfaces may be necessary for composite particle synthesis.

Submicronic, monosize alumina-silica composite particles were synthesized by heterocoagulating separate colloidal dispersions of alumina and silica.

OVER

14. SUBJECT TERMS	15. NUMBER OF PAGES
	138
	16. PRICE CODE

17. SECURITY CLASSIFICATION OF REPORT	18. SECURITY CLASSIFICATION OF THIS PAGE	19. SECURITY CLASSIFICATION OF ABSTRACT	20. LIMITATION OF ABSTRACT
unclassified	unclassified		

NSN 7540-01-280-5500

Standard Form 298 (890104 Draft)
Prescribed by ANSI Std. 239-18
298-01

89 12 20 072

Narrow size distribution, unagglomerated, rounded titania-coated alumina containing 30-60 mole % titania was prepared by stepwise hydrolysis of titanium alkoxide in a colloidal alumina dispersion. The amount of titania coated on alumina depended on the total amount of alkoxide hydrolyzed; powders with varying amounts of titania were reproducibly synthesized.

Fine-size, narrow size distribution, spherical, nonagglomerated anatase TiO_2 was also synthesized, by controlled hydrolysis of titanium tetraethoxide in ethanolic solution, using the continuous flow reactor.

Uniformly-sized, chemically similar alumina-zirconia composite powder particles were also produced in the continuous flow reactor, with zirconia contents as little as (nominally) 4 and 8 weight % (alumina-zirconia composites containing 5-10% zirconia have optimum mechanical characteristics). Autoclaving increased green density and largely eliminated sintering problems, producing better-defined, more closely adhering zirconia layers than could be obtained without autoclaving.

Studies on how slurry characteristics affect alumina consolidation in a colloid press revealed that 1) pH conditions far from a slurry's isoelectric point are preferable, 2) dispersant should not be used, 3) binders can strengthen powder compacts, and 4) blowing gas through specimens under load in the press does not help.

A soluble double metal alkoxide, calcium aluminum ethoxide, was synthesized, but in a gel form rather than as the desired powder.

A second double alkoxide, of magnesium and aluminum, was prepared and converted to spinel, $MgAl_2O_4$. This was used in a partially successful attempt to produce cordierite: a gel formed, rather than the desired powder, consisting of 75% cordierite and 25% spinel.

One study concentrated on synthesizing cordierite from the double alkoxide aluminosilicate. The powder produced has not yet been characterized, but particles produced were irregularly shaped and much smaller than had been hoped for.

Narrow size distribution, submicron zirconia was prepared by controlled hydrolysis of zirconium n-propoxide. Surface area was found to be strongly affected by both the solvent used to rinse the powder and the length of time the powder remained in solution afterwards.

Narrow size distribution zirconia powders homogeneously doped with Y_2O_3 were prepared by coprecipitating $Zr^n(OPr)_4$ and $Y^i(OPr)_3$. Powder packing was reproducible, and grain size after sintering was uniform and submicron.

Uniformly coated, narrow size distribution zirconia-alumina composite powders were prepared by adding zirconia n-propoxide to a dispersion of size-fractionated, dried alumina, then hydrolyzing with an ethanol solution to precipitate zirconia as a coating on the alumina particles. Sintering produced largely submicron and nonuniform grain sizes.

BASIC RESEARCH ON PROCESSING OF CERAMICS FOR SPACE STRUCTURES

AFOSR-83-0192
Final Report

October 1984

H. Kent Bowen
Richard L. Pober

Massachusetts Institute of Technology
Materials Processing Center
77 Massachusetts Avenue
Cambridge, MA 02139

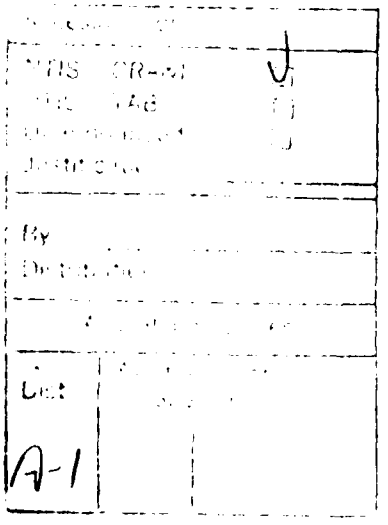

Table of Contents

I. INTRODUCTION

Materials for aerospace structures must be lightweight, rigid, and capable of withstanding wide temperature excursions. Composite ceramic materials can meet both these requirements and many more of importance to the aerospace industry. Present processing techniques, however, are unable to produce composite ceramic structures reliably and reproducibly because material composition and microstructure cannot yet be adequately controlled.

Control is a key concept in ceramics processing. A relatively recent finding has been the strong interdependence of all steps in the ceramics production sequence (e.g., particle synthesis or preparation, dispersion chemistry and powder handling, particle packing, fabrication, and sintering). Ceramic pieces can be fabricated reliably and reproducibly only if every step is performed properly; mistakes cannot be corrected through subsequent processing.

Over the last four years, the Ceramic Processing Research Laboratory has demonstrated the feasibility of a chemical science-based approach to ceramics powder processing — an approach that may be well suited to aerospace structural technology because of its applicability to a wide variety of complex materials. The approach requires a diverse team that includes not only experts in conventional sintering and grain growth, but also authorities on colloid, polymer, and organometallic chemistries, physics, and math, providing the broad base needed to explore the fundamentals of ceramics processing.

Controlled processing requires understanding of the physical and chemical forces governing ceramic particles' behavior during each processing step; rheological behavior, polymer chemistry, and binder burnout are also

considerations. Hundreds of billions of particles must be manipulated successfully to produce a single satisfactory component from ceramic powder, the particles of which may be crystalline or amorphous, single- or polyphase. The primary difficulty in handling all these particles is inhomogeneity in particle packing prior to densification; microstructure and property control are key to ceramic materials' reliability and reproducibility. Research in this area -- presintering science -- is vital, and has already attracted international attention.

Experimentation has shown it possible to prepare and control the size distribution, shape, and chemistry of ceramic particles in single-cation oxide systems. Specimens can be prepared with controlled particle packing (and therefore controlled microstructure) when colloid chemistry is understood and interparticle forces controlled. This year's research extends the current body of knowledge to include multi-cation and multiphase materials such as magnesium-aluminum-silicate (cordierite), alumina-zirconia, alumina-silica, and silicon carbide-zirconia.

Research done this year combined basic understanding of particle formation and surface chemistry with development of theoretical processing models. Critical experiments tested generalizations for controlling presintered structure and sintered microstructure. Research utilized novel chemical preparative concepts in colloid and ceramic sciences to produce reproducible and reliable microstructures. Sintered microstructure development was studied as a function of particle packing, pressure, and temperature, with experiments being performed in controlling size and distribution of pores and other minor phases, and in controlling composition for thermal, dielectric, and mechanical characteristics.

II. RESEARCH SUMMARY

A number of studies this year utilized a newly developed continuous flow reactor to reproducibly synthesize uniform composite ceramic powders: powders generally consisting of "core" particles coated with one or more other materials that influence the final product's properties. Composite processing's principal objective is to homogeneously and reproducibly distribute a ceramic's components so resulting ceramic pieces' structures are uniform and their properties predictable. This objective has not been met using conventional methods that typically employ mechanical mixing.

Particle coating in each synthesis using the continuous plug flow reactor configuration was done by metal alkoxide hydrolysis in an alcohol/core particle suspension. Experimental results indicate that coating particles bind to core particles via a chemisorption process in which alkoxide molecules are adsorbed at core particle surfaces, reacting with surface hydroxyl groups to form a core-metal alkoxide condensate. If this is true, water-wet core particle surfaces may be necessary for composite particle synthesis; when the tri-alkoxy-metal-core particle complex is mixed with water in the continuous reactor, the three alkoxy groups react to give a metal oxide core particle composite and three alcohol molecules.

$Al_2O_3 \cdot SiO_2$ ceramics are lightweight and have low densities, low dielectric constants, and firing temperatures lower than that of Al_2O_3. Submicronic, monosize alumina-silica composite particles were synthesized by heterocoagulating separate colloidal dispersions of alumina and silica. A dispersion of commercially available alumina size-fractionated to a narrow size distribution was slowly introduced into a dispersion containing excess commercially available colloidal silica with much smaller particle diameters.

Centrifuging for an hour yielded a composite powder consisting of alumina particles, each coated by two layers of silica particles. Sintering studies showed the composite's enhanced sintering behavior relative to commercial alumina; its firing temperature was significantly lower. Firing at 1400°C for 1 hour produced a sintered body with a relative density of 98% and no significant grain growth.

Experiments to prepare composite alumina-silica powder by hydrolyzing a silicon alkoxide in an aqueous alumina dispersion did not produce nonagglomerated particles with a significant amount (> 1 wt%) of silica. Attempts were also made unsuccessfully to introduce boron compounds into the alumina-silica matrix to reduce silica viscosity during firing. Hydrolyzing a silicon-boron alkoxide produced agglomerated particles; impregnating compacted alumina-silica composite powder with a boric acid solution damaged the green body's dense compaction, and introduced very little B_2O_3 into the matrix.

Two titanium-based ceramics — titania-coated alumina ($TiO_2 \cdot Al_2O_3$) and anatase (TiO_2) — were prepared from narrow size distribution powders, and their sintering behavior studied. Narrow size distribution, unagglomerated, rounded titania-coated alumina containing 30-60 mole % titania was prepared by stepwise hydrolysis of titanium alkoxide in a colloidal alumina dispersion. The amount of titania coated on alumina depended on the total amount of alkoxide hydrolized; powders with varying amounts of titania were reproducibly synthesized. Autoclaving was not found effective in producing a crystalline coating from the otherwise amorphous titania coating, because although autoclaving did crystallize the titania, much of the coating broke off during subsequent ultrasonic redispersion. The composite powder was

finally sintered to form aluminum titanate, a well-known ceramic with an apparent low thermal expansion coefficient and a high melting point. Fired specimens had high relative densities, but contained domain structures. Cracks tnat form around these structures reduce the final ceramic's strength, preventing its use in practical applications.

Fine size, narrow size distribution, spherical, nonagglomerated anatase (TiO_2), a high-temperature ceramic, was also synthesized, by controlled hydrolysis of titanium tetraethoxide in ethanolic solution. Some powder samples were autoclaved to transform the low-density amorphous product to anatase, reducing shrinkage during subsequent processing steps. It was found that anatase crystal size depends on hydrothermal conditions rather than apparent initial particle size. During sintering, autoclaved powders shrank homogeneously; their shrinkage behavior was less dependent on temperature and heating rate than that of unautoclaved powder. Isostatic pressure increased a pure anatase filtered compact's green and sintered densities; its sintered density was 99.2% of the theoretical density.

Many desired ceramic materials have multi-cation compositions. New research this year included preparation of two important multi-cation systems: alumina-zirconia oxides and cordierite ($2MgO \cdot 2Al_2O_3 \cdot 5SiO_2$), both of which have potential structural applications and diverse properties, determined by chemistry and microstructure. Research drew on our extensive experience preparing oxides by hydrolyzing alkoxides.

Alumina-zirconia composites are ideal high-temperature structural ceramics because of their strength and toughness, but their properties are critically dependent on sintered microstructure. Sintered pieces made from alumina-zirconia composite powders are expected to be more homogeneous than

those based on milled powder mixtures, and therefore should have more desirable mechanical properties. Alumina-zirconia composites containing 5-10% zirconia have optimum mechanical characteristics. Uniformly sized, chemically similar alumina-zirconia composite powder particles were produced this year in a continuous flow reactor, with zirconia contents as little as (nominally) 4 and 8 weight%. It was found that autoclaving significantly increased green density and largely eliminated sintering problems, producing better-defined, more closely adhering zirconia layers than could be obtained without autoclaving. Experimental results indicated that composite formation is based on liquid phase adsorption.

Studies on how slurry characteristics affect alumina consolidation in a colloid press revealed that 1) pH conditions far from a slurry's isoelectric point are preferable, 2) dispersant should not be used, 3) binders can strengthen powder compacts, and 4) blowing gas through specimens under load in the press does not seem to help.

Cordierite could not be synthesized from single alkoxides because hydrolysis proved too rapid and uncontrollable. Double alkoxide precursors were therefore tried since they 1) generally have more moderate reaction kinetics, 2) are often completely soluble in a given solvent (a requirement for synthesis), unlike single alkoxides, and 3) minimize system complexity by reducing the number of reactants.

One soluble double metal alkoxide, calcium aluminum ethoxide, was successfully synthesized in our laboratory this year, but in gel form rather than as the desired powder. Varying reactant concentrations should alter reaction kinetics enough that a powder of the desired composition will form.

Attempts will then be made to coat the powder particles on zirconia to produce stabilized $ZrO_2 \cdot CaO$, a high-strength ceramic.

A second double alkoxide, of magnesium and aluminum, was prepared and converted to spinel, $MgAl_2O_4$. This was used in a partially successful attempt to incorporate MgO and Al_2O_3 into silica to obtain cordierite: a gel formed, rather than a powder, consisting of 75% cordierite and 25% spinel. Future work will strive to produce solely cordierite powder particles by varying reactant concentrations, solution pH, and solvents.

Another study concentrated on synthesizing cordierite from the double alkoxide aluminosilicate. The powder product has not yet been characterized, but particles produced were irregularly shaped and much smaller than had been hoped for. IR spectroscopy will determine whether cordierite or another triple alkoxide has been synthesized. Kinetics of the hydrolysis reaction will then be studied, along with the solvent's effect on hydrolysis and final powder characteristics.

Progress was made in synthesizing narrow size distribution powders of ZrO_2 (which has important applications in sensing devices), and $Y_2O_3 \cdot ZrO_2$ and $ZrO_2 \cdot Al_2O_3$ (noted for their high strength). Narrow size distribution, submicron zirconia was prepared by controlled hydrolysis of zirconium n-propoxide. Surface area was found to be strongly affected by both the solvent used to rinse the powder and the length of time the powder remained in solution afterwards. Sintering at approximately 1160°C for about an hour produced samples with uniform submicron microstructures.

Narrow size distribution zirconia powders homogeneously doped with Y_2O_3 were prepared by coprecipitating $Zr^n(OPr)_4$ and $Y^i(OPr)_3$. The resulting alkoxide mixture was hydrolyzed, then heated. The powder product proved to

be amorphous, but calcining at 1100°C for about eight hours transformed the zirconia to cubic form. Powder packing was reproducible, and grain size after sintering was uniform and submicron.

Uniformly coated, narrow size distribution zirconia-alumina composite powders were prepared by adding zirconia n-propoxide to a dispersion of size-fractionated, dried alumina, then hydrolizing with an ethanol solution to precipitate zirconia as a coating on the alumina particles. Sintering produced largely submicron and nonuniform grain sizes.

III. RESEARCH RESULTS

Following are reports made by the nine researchers this year who took part in this project.

Bruce Novich

CONTINUOUS PROCESSING OF COMPOSITE CERAMICS

I. Introduction

"Composite ceramics" are multicomponent ceramic materials that form the basis of the structural ceramic and electronic ceramic industries. These materials generally consist of 1) core phases, which form the "ceramic matrix", and 2) coating phases, which act as modifiers for the substrate's chemical, physical, and/or electronic properties. For example, in the $Al_2O_3 \cdot ZrO_2 \cdot YO_2$ structural ceramic system, alumina is the core phase (typically 90% by weight), acting as substrate for the zirconia and yttria coating phases. Zirconia (typically 8% by weight) transformation-toughens the alumina matrix, and yttria (typically 2% by weight) stabilizes the zirconia.

Composite processing's principal objective is to produce a ceramic whose components are homogeneously and reproducibly distributed throughout the body so the resulting ceramic pieces have both uniform structure and predictable behavior. Conventional techniques, which typically employ mechanical mixing, fall grievously short of achieving this objective.

This report details a new continuous processing technique from which uniform composite ceramic powders can be reproducibly manufactured. Composite powder manufacture consisted of mixing a suspension of core particles in an alcohol/metal-alkoxide solution with water to produce a core-metal oxide composite. Continuous composite powder production was carried out in a plug flow reactor configuration. Particle coating was done by metal alkoxide hydrolysis in an alcohol/core particle suspension.

II. Experimental Procedure

Composite ceramic materials were manufactured using the continuous production method to be described here. The systems investigated were:

	Core	Coating
1.	Al_2O_3	ZrO_2
2.	Al_2O_3	TiO_2
3.	SiC	ZrO_2

The alumina was bulk XA-139 supplied by Alcoa, and the silicon carbide was Fujimi Lot 37223. Alkoxides used for coating and their manufacturers are listed in Table 1.

Nominal coating percentages ranged from 4% to 37% by weight. H_2O/alkoxide molar ratios in the reactor were 20:1 for the $Al_2O_3 \cdot ZrO_2$ and $SiC.ZrO_2$ composites and 10:1 for the $Al_2O_3 \cdot TiO_2$ composite. Deionized water ($\rho = 17 \times 10^6$ ohm-cm) at pH=6-6.5 was used for zirconia and titania synthesis. Punctilious 200-proof ethyl alcohol was used as the carrier fluid. All experiments were carried out within the 22-26°C temperature range.

The reactor configuration, consisting of six stages, is depicted in Figure 1a. The six stages are:

1. reactants
2. pumps
3. filters
4. mixers
5. reactor
6. products

There were two classes of reactants: wet and dry. The wet reactants were water (Stream 1) and bulk, 200-proof alcohol (Stream 2). These were stored at ambient conditions. The dry reactant stream (Stream 3) consisted of a suspension of core particles (alumina in these experiments), metal alkoxide, and 200-proof alcohol. Dry reactants were stored under dry

nitrogen. The system conduit and fittings were stainless steel, and the pumping system consisted of three Cole-Parmer paristaltic pumps (one for each reactant stream) plumbed with Masterflex-C tubing. Total flow rates were typically 200 ml/min, yielding approximately 300 grams of composite per hour using Figure 1's setup.

From the pumps, wet reactants proceeded through two filters -- first a 5-micron Ballastan filter and then a 0.22-micron Millipore filter. After filtration, both wet reactant streams were mixed as they flowed into a T-section and out through a turbulent flow Kenics Static Mixer (Stream 4).

The dry suspension was thoroughly mixed and ultrasonicated prior to use. During each experimental run, the suspension was stirred continuously and pumped through a turbulent-flow Kenics Static Mixer to prevent flow segregation. After emerging from the mixer, the dry stream (Stream 3) was mixed with the wet stream (Stream 4) in a T-section just prior to entering the reactor.

Products collected at the reactor outlet were subjected to a washing sequence of centrifugation -> decantation -> suspension -> ultrasonification, as shown in Figure 1b. This sequence was performed twice with bulk, 190-proof alcohol, and three times with deionized water. The washed powders were stored in water at pH=6.

III. Results and Discussion

Composite ceramic powder products were analyzed using scanning electron microscopy (SEM) and transmission electron microscopy (TEM) for visual analysis, energy dispersive X-ray analysis (EDX) and inductively coupled plasma analysis (ICP) for chemical composition determination, X-ray

diffraction analysis (XRD) for crystal structure determination, and nitrogen BET analysis for surface area determination.

As shown in Figures 2, 3, and 4, all three composite systems exhibited the same general powder structure: large core particles ~0.5μm alumina or silicon carbide) were coated by fine coating particles (ZrO_2 and TiO_2). XRD analysis indicated that coatings were amorphous and composed of approximately 100Å equiaxed particles, as viewed by TEM. BET analysis gave surface areas of approximately 200 m^2/g, which translates to a mean surface particle size of 100Å, based on a spherical morphology. Coating particle and composite powder characteristics appeared to be independent of reaction conditions (alkoxide and water concentrations, mean residence time in reactor, 10-degree temperature variation over the 20° to 30°C range, etc.) as long as the reaction coordinate, R, was greater than 100 and the alkoxide concentration was greater than 0.05M. The reaction coordinate is given as follows:

$$R = [H_2O]^3\ [\text{Alkoxide}]$$

Coating particles were produced under these constraints in the absence of core particles. As shown in Figure 5, the coating particles are equiaxed and fall within a narrow size distribution. These particles' physical properties have been determined to be virtually identical to the physical properties of the composite coating particles. This indicates that the presence of core particles during coating particle synthesis has no effect on the physical nature of the coating. Oguri (in another section of this report) has studied the hydrothermal, consolidation, and sintering behaviors of ultrafine titania particles.

In the presence of core particles, coating particles do not act as a discrete phase. When synthesized in core particles' presence, coating

particles become firmly attached to the core particles' surfaces. As shown in Figure 6, even after prolonged periods of high frequency ultrasonification followed by hydrothermal treatment at 250°C for 10 hours, coatings remain firmly attached to substrates. During hydrothermal treatment, the coating changes from a pointed gelatin to a well-defined crystalline phase. Moffatt (in another section of this report) has studied the hydrothermal, consolidation, and sintering behaviors of alumina-zirconia composite powders.

Several experiments were performed to understand how coating particles bind to the core. Results indicate a chemisorption process in which the alkoxide molecule is adsorbed at the core particle surface, then reacts with surface hydroxyl groups to form a core-metal alkoxide condensate. Mechanisms for the alumina and silicon carbide reactions might be as follows:

ALUMINA:

$$Al\text{-}OH + M(OR)_4 = Al\text{-}O\text{-}M(OR)_3 + ROH$$

SILICON CARBIDE:

$$Si\text{-}OH + M(OR)_4 = Si\text{-}O\text{-}M(OR)_3 + ROH$$

For both core particle types, one would expect the aluminum and silicon surface atoms to be hydroxylated, since initial starting powders were not treated to remove adsorbed water prior to the powder's introduction into the alcohol/alkoxide solution. Barringer's (1983) observations that the alkoxides react in a stepwise manner[1] is consistent with this mechanism. Parish (1984) has postulated and experimentally verified this mechanism for alkoxide-like polymer coupling agents as binders in ceramic systems.[2]

Further support is given the chemisorption hypothesis by the following experimental observations:

1. The metal alkoxide must be thoroughly mixed and equilibrated with core particle surface prior to hydrolysis, or the coating will not bind to the core. Figure 7 shows that the powder product consisted of discrete interstitial zirconia and "clean" alumina particles when alumina was introduced into the reactor while suspended in the water stream. Figure 6 shows a very different powder produced under reaction conditions that are identical except for the fact that only the alumina was preconditioned in the alcohol/metal alkoxide solution.

2. Metal alkoxide introduction into an alcoholic core particle suspension significantly affects suspension behavior. Prior to alkoxide introduction into an alumina or silicon carbide ethanol suspension, particles appeared to flocculate rapidly and sediment at a rate of approximately 10 cm/min. Once core particles were dispersed in a dilute alkoxide/ethanol solution, they remained dispersed and exhibited a sedimentation rate of less than 0.1 cm/min. This behavior indicates that alkoxides adsorb at the core particle/ethanol interface and act as dispersants, and is consistent with the similar chemical natures of the solvent and alkoxide ligand.

3. Quantitative chemical analysis of the alumina-zirconia composites show plateau coating regions above which no further coating occurs and zirconia forms interstitially. This is typical for an adsorption-controlled system. Using a modified multilayer BET analysis given by Novich (1984),[3] the average free energy of adsorption was calculated to be -4.5 kcal/mole and the threshold

adsorption density was 9.6×10^{-9} mole/cm^2, corresponding to 9.4% zirconia by weight. Figure 8 shows the same trend for BET surface area analysis of the dry powders.

If the surface hydroxyl mechanism is valid, a water-wet core particle surface may be necessary for composite particle synthesis. As the tri-alkoxy-metal-core particle complex is mixed with the water stream, the three alkoxy groups react to give a metal oxide core particle composite and three alcohol molecules.

IV. Conclusion

A continuous process for composite ceramic material production has been developed, consisting essentially of three steps:

1. adsorption of alkoxide onto a core particle,
2. chemical grafting of alkoxide molecules through a surface condensation reaction, and
3. hydrolysis of the remaining unreacted alkoxy groups.

Composite powders synthesized this way were produced uniformly and reproducibly on a continuous basis.

V. Future Work

Detailed alkoxide adsorption studies of alcohol/core particle suspensions should be performed, and spectroscopic methods (specifically FTIR) used to detect 1) chemisorption of the alkoxide onto the core surface, and 2) the subsequent condensation product, the tri-alkoxy-metal-oxygen-core particle complex.

VI. References

1. Barringer, E. A., "The Synthesis, Interfacial Electrochemistry, Ordering and Sintering of Monodisperse TiO_2 Powders," doctoral thesis, Mass. Inst. of Tech., Cambridge, MA (1983).

2. Parish, M. V., "Titanium-Coupled Dispersants for Barium Titanate Powders," CPRL Report Q1 (1984).

3. Novich, B. E., "A Predictive Flotation Model Based on Adsorption, Coagulation Kinetics Contact Angle and Micellization in the Alkylamine-Quartz Flotation System," doctoral thesis, Mass. Inst. of Tech., Cambridge, MA (1984).

TABLE I. Alkoxide Reagents Used for Coating Synthesis

Compound	Supplier	Resulting Oxide
Zirconium-n-tetrapropoxide	Kay Fries Inc.	ZrO_2
Titanium-n-tetraethoxide	Kay Fries Inc.	TiO_2
Tetraethyl orthosilicate	Aldrich Chemical Co.	SiO_2

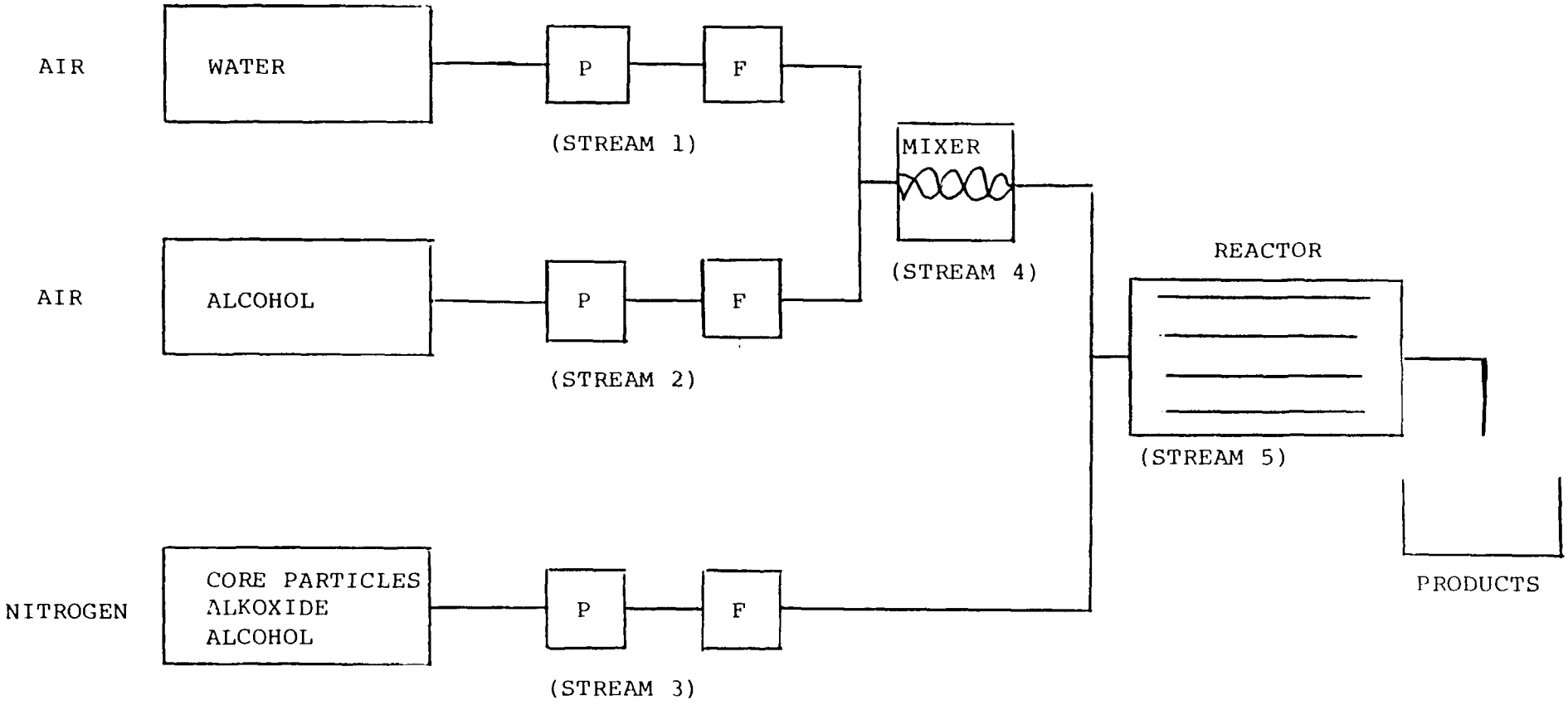

Figure 1a. Continuous Flow Reactor Configuration

PRODUCT STREAM

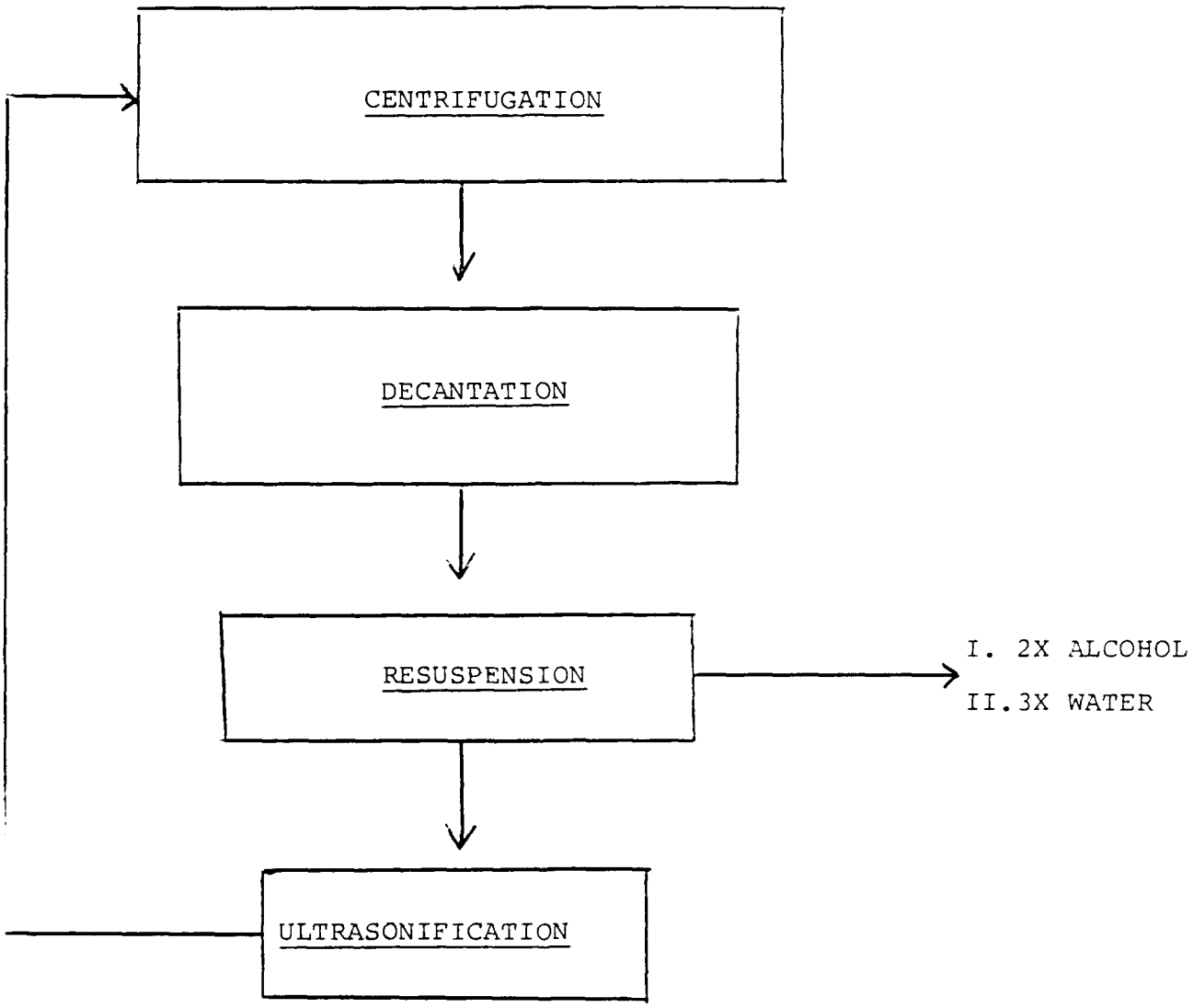

Figure 1b. Product Stream Washing Sequence

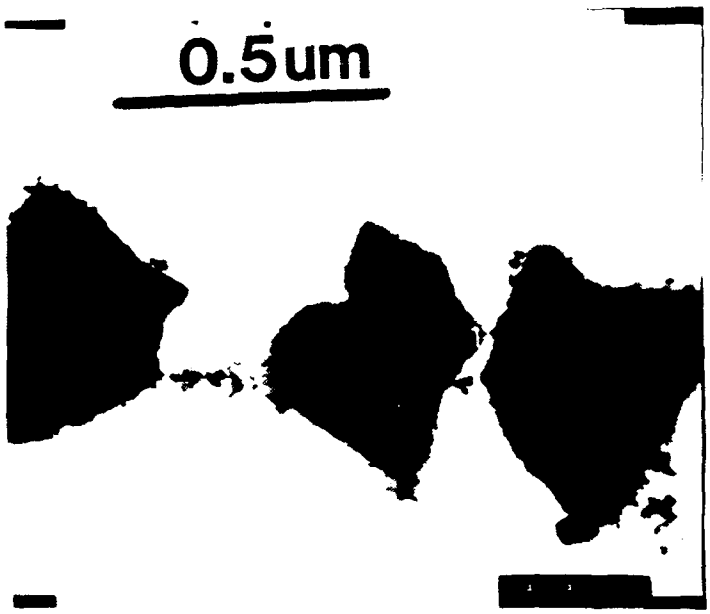

Figure 2. Alumina-zirconia composite powder.

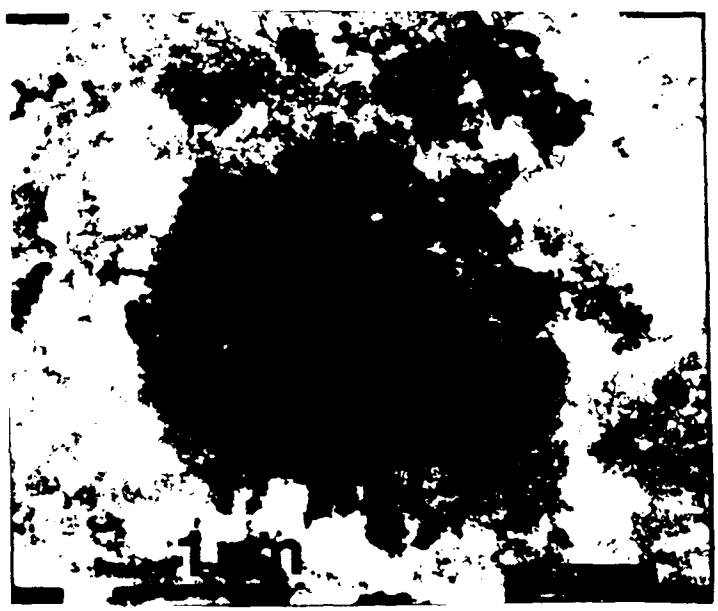

Figure 3. Alumina-titania composite powder.

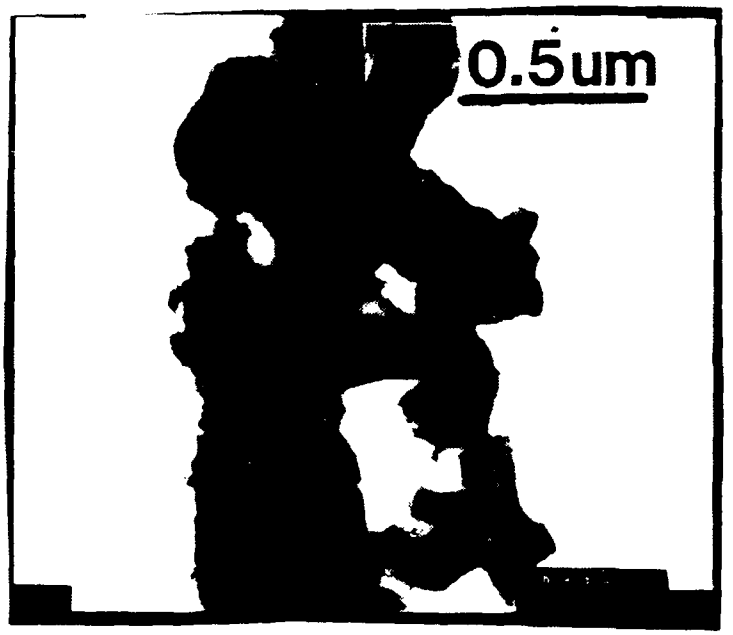

Figure 4. Silicon carbide-zirconia composite powder.

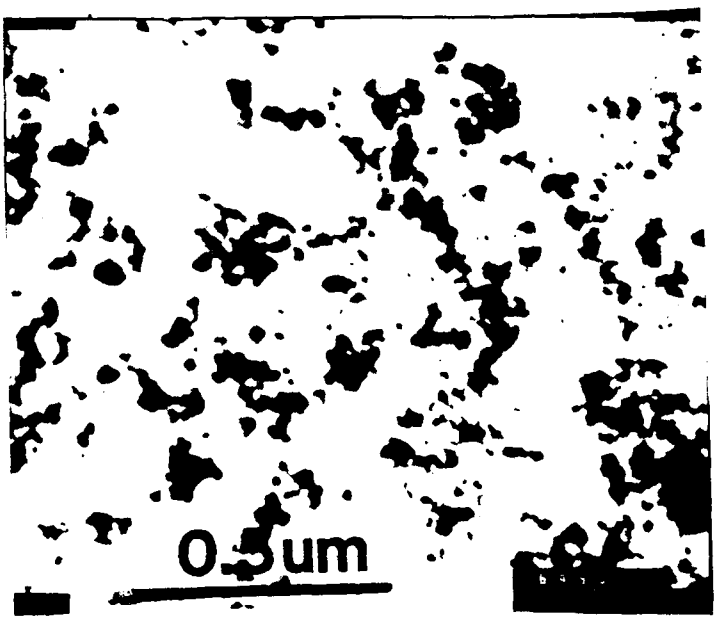

Figure 5. Zirconia coating particles.

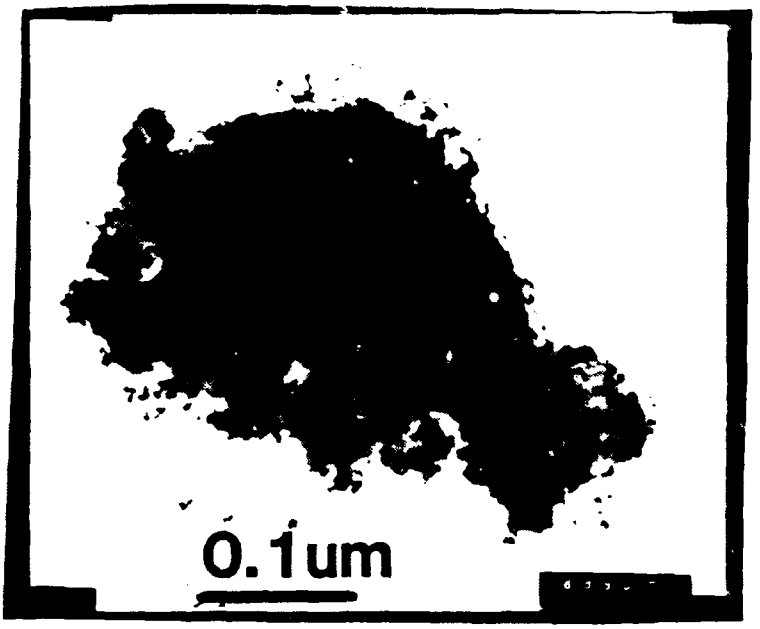

Figure 6. Autoclaved alumina-zirconia composite powder.

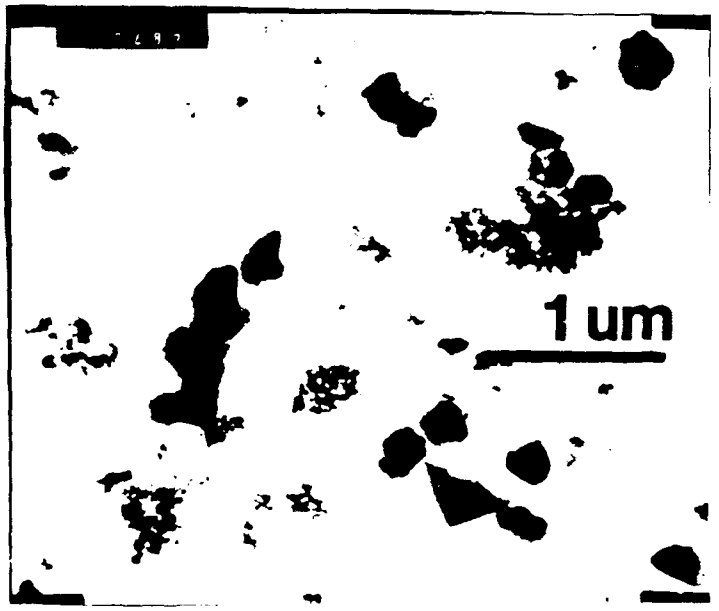

Figure 7. Alumina-zirconia product of non-equilibrated slurry of alumina core particles and alkoxide.

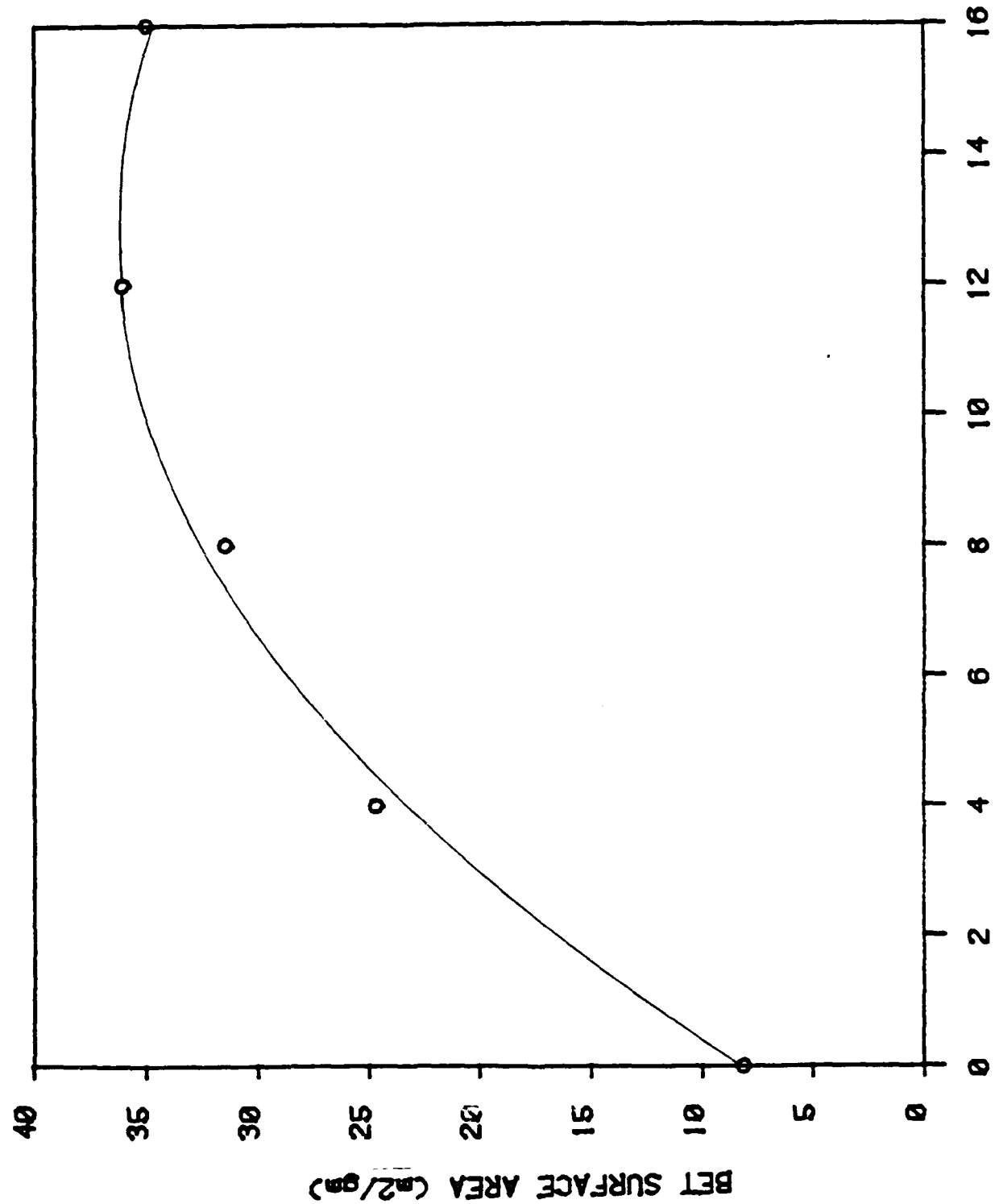

Figure 8. BET specific surface area vs. nominal weight percent zirconia for zirconia-alumina composites made in continuous flow reactor (unpublished results of Hyman).

Pierre E. Debély, Eric A. Barringer, and H. Kent Bowen

PREPARATION AND SINTERING BEHAVIOR OF FINE GRAIN $Al_2O_3 \cdot SiO_2$ COMPOSITE

I. Introduction

$Al_2O_3 \cdot SiO_2$ ceramics have the important properties of low density, light weight, low dielectric constant, and firing temperatures lower than that of Al_2O_3. To make a composite ceramic of Al_2O_3 and SiO_2, it is important to prepare a powder whose individual particles have the final ceramic's chemical composition; the powder should be composed of monosized composite particles. Submicronic, monosized, and uniformly packed particles provide maximum surface free energy to serve as the driving force for homogeneous sintering throughout a sample.[1,2] Optimum powder compaction reduces the probability of voids.

This report describes how separate colloidal dispersions of Al_2O_3 and SiO_2 can be heterocoagulated through mutual attraction by electrostatic forces to form a single dispersion of submicronic, monosize, composite $Al_2O_3 \cdot SiO_2$ particles.

Alumina particles dispersed in a solution of pH < 9 have a positive electrostatic charge and silica particles dispersed in a solution of pH > 2 have a negative charge, since the isoelectric points of alumina and silica are 9 and 2, respectively. Thus, at pH levels between 2 and 9, a mixed colloidal dispersion of Al_2O_3 and SiO_2 may heterocoagulate through mutual attraction by electrostatic forces to form a dispersion of composite particles.[3] If the silica particles are much smaller than the alumina particles, the latter will be covered with one or two layers of the former. The dispersion can then be sedimented, centrifuged, or filter pressed to obtain a uniform green compact for firing.

II. Experimental Procedure

A. Use of colloidal silica dispersion to make alumina-silica composite

There is no simple method for producing submicronic, monosized, unagglomerated α-Al_2O_3 particles. Spherical aluminum hydroxide particles can be produced,[4] but particle size control is lost during the phase transformation to α-Al_2O_3. In the present study, a commercially-available fine-grained alumina powder[+] was separated into narrow size fractions by centrifugal classification.[5] The average grain size of the fraction used, determined by photon correlation spectroscopy,[†] was 0.29 ± 0.05 μm (Figure 1). The commercially available colloidal SiO_2 used consisted of uniform, spherical particles having an average diameter of 0.020 ± 0.003 μm.[≠]

The alumina powder, at a concentration of 0.40 mole/liter, was ultrasonically dispersed in water to which acetic acid had been added to attain a pH of 3.5. The colloidal SiO_2 was diluted to a concentration of 1.2 moles/liter of solution in water and sufficient acetic acid added to match the alumina dispersion's pH. Equal volumes of the two dispersions were prepared.

The alumina dispersion was then introduced at a rate of 3.5 ml/min into the vigorously stirred silica dispersion, allowing the alumina particles to become completely covered with silica particles. The composite colloidal dispersion was then centrifuged at 2500 G for 1 hour, and the supernatant containing excess SiO_2 particles decanted. The remaining concentrated slurry

---

[+] Alcoa XA 139 SG, Alcoa, Alcoa Center, PA 15069
[†] Coulter N4D, Coulter Electronics, Inc., Hialeah, FL 33010
[≠] Nyacol 2034 DI colloidal silica, Nyacol Product Inc., Asland, MA 01721

was pressed at 5100 psi in a die set having two porous punches,[6] yielding a green compact having a relative density of 61%. A pellet of the commercial α-Al_2O_3 was pressed to the same relative density using this method.

Samples were fired in air at temperatures between 900 and 1580°C for 1 to 13 hours in air, and the relative linear shrinkage measured with a dilatometer.[§]

B. Use of silicon alkoxide to make alumina-silica composite

Instead of using a colloidal silica dispersion to prepare the composite powder, a silicon alkoxide can be hydrolyzed in an aqueous alumina dispersion to form an alumina-silica dispersion.

Tetraethylorthosilicate, $Si(OC_2H_5)_4$, can be hydrolyzed and condensed to produce silica as follows:

$$nSi(OC_2H_5)_4 + 4H_2O \longrightarrow nSi(OH)_4 + nC_2H_5OH \qquad (1)$$

and

$$nSi(OH)_4 \longrightarrow nSiO_2 + 2nH_2O \qquad (2)$$

or

$$\begin{array}{c} RO \\ | \\ RO\text{-}Si\text{-}RO \\ | \\ RO \end{array} + 4H_2O \longrightarrow \begin{array}{c} OH \\ | \\ OH\text{-}Si\text{-}OH \\ | \\ OH \end{array} + 4ROH \qquad (3)$$

If the silicon alkoxide has a low concentration, it should not polymerize with itself to form silica particles or nuclei on which silica will deposit.

---

§ Netzsch 40A E, Netzsch Geraetebau, GmbH D-8672 Selb, West Germany

Polymerization could take place, however, at alumina particle surfaces where OH groups are always present. Tests have been conducted for solutions ranging in pH from 2 to 14.

C. Use of boron alkoxide to make alumina-silica-boron oxide composite

Boron oxide in a significant amount (20 wt%) reduces silica viscosity considerably during firing. Boron oxide can be added to the alumina-silica dispersion by hydrolyzing a boron alkoxide. A silicon-boron alkoxide was made by mixing silicon and boron alkoxides. L. Janavicius' technique[7] was used to make borosilicate particles in the presence of alumina particles.

D. Impregnation of alumina-silica composite powder with boron oxide

A compacted composite powder made by mixing alumina and silica dispersions was impregnated with a H_3BO_3/H_2O solution in an attempt to disperse a boron compound homogeneously throughout the $Al_2O_3 \cdot SiO_2$ matrix to reduce silica viscosity during firing.

III. Results and Discussion

A. Use of colloidal silica dispersion to make alumina silica composite

The nonagglomerated composite powder obtained by the heterocoagulation technique is shown in Figure 2. Since the alumina dispersion was introduced slowly into the silica dispersion, each alumina particle could be entirely covered with silica before encountering another alumina particle not yet covered with silica. In addition, excess silica was used so that all alumina particles would be completely covered. These conditions were necessary to prevent extensive heterocoagulation that would result in large agglomerates

(> 1 μm) containing many Al_2O_3 particles. Specific surface areas, determined by single-point BET, were 37 m^2/g for the composite powder and 9 m^2/g for the Al_2O_3 powder. Heat treatment in air to 500°C for 1 hour removed all traces of water and organic compounds, as shown by differential thermal and thermogravimetric analyses.

A fracture surface of the compacted composite powder (Figure 3) shows the packing uniformity attained using the slurry pressing technique. Samples of the $Al_2O_3 \cdot SiO_2$ and commercial α-Al_2O_3 compacts were fired in air at a constant heating rate of 10°C/min; their respective relative linear shrinkages are shown in Figure 4. These data confirm the enhanced sintering behavior of the composite $Al_2O_3 \cdot SiO_2$ powder.

The chemical composition of the composite powder, 80 wt% Al_2O_3 and 20 wt% SiO_2, was determined with an electron microprobe. This value corresponds to about two layers of 0.020 μm spherical SiO_2 particles covering the surface of 0.3 μm Al_2O_3 particles.

The composite powder reached a full density of 3.4 after firing for one hour at 1550°C (Figure 5). As expected from the $Al_2O_3 \cdot SiO_2$ phase diagram,[8] the mullite phase ($3Al_2O_3:2SiO_2$) formed at this temperature, giving the overall phase composition of 29 wt% Al_2O_3 and 71 wt% mullite, as confirmed by X-ray diffraction analysis. When the mullite phase formed, the sample expanded due to mullite's slightly lower density compared to that of an equivalent mixture of alumina and silica (Figure 4). Differential thermal analysis indicated that the phase transformation began at 1490°C. The alumina grains are surrounded by a continuous mullite phase, as shown in Figure 6.

Figure 7 shows the relative densities obtained for the composite powder compact after firing for 1 and 13 hours at temperatures ranging from 900 to 1550°C. The composite material had a relative density of 69% after firing for 13 hours at 1080°C (Figure 8) and 74% after firing for one hour at 1200°C (Figure 9); no grain growth was observed. Figure 10 shows the same material fired at 1400°C for 1 hour; its relative density is 98% and no significant grain growth occurred. Firing temperatures of 1125°C and 1310°C, respectively, were required to give the same relative densities after 13 hours.

B. Use of silicon alkoxide to make alumina-silica composite

It has not yet been possible to obtain nonagglomerated alumina particles coated with a significant amount (> 1 wt%) of silica by hydrolyzing a silicon alkoxide in an aqueous alumina dispersion. Tests conducted for solutions ranging in pH from 2 to 14 showed that if pH exceeds ~11, all the silica is dissolved as silicate. If pH drops below 8, the deposition rate is very low.

C. Use of boron alkoxide to make alumina-silica-boron oxide composite

Alumina particle agglomeration could not be prevented when boron alkoxide was used in an attempt to make alumina-silica-boron oxide composite powder.

D. Impregnation of alumina-silica composite powder with boron oxide

The amount of B_2O_3 that infiltrated the porous compact was very low, and impregnation significantly damaged the starting green body's dense compaction. No offsetting positive effect was observed during sintering.

IV. Conclusions

The firing temperature of alumina-based ceramic is significantly reduced when monosized $Al_2O_3 \cdot SiO_2$ composite powder is used as the starting material.

V. Future Work

Firing temperature could be reduced further by increasing the green density to ~ 70% or by adding boron oxide to lower the silica phase viscosity. Increasing the relative amount of silica by using larger SiO_2 particles in the initial dispersions would also enhance sinterability.

Silicon alkoxide and an aqueous alumina dispersion will be mixed using the continuous flow reactor in a further attempt to hydrolyze silicon alkoxide at the alumina particle surface.

VI. References

1. H. K. Bowen, "Basic Research Needs on High Temperature Ceramics for Energy Applications," Mater. Sci. Eng., 44 [1] 1-56 (1980).

2. E. A. Barringer and H. K. Bowen, "Formation, Packing and Sintering of Monodisperse TiO_2 Powders," J. Am. Ceram. Soc., 65 [12], C199-201 (1982).

3. R. K. Iler, "Adsorption of Colloidal Silica on Alumina and of Colloidal Alumina on Silica," J. Am. Ceram. Soc., 47 [4], 194-198 (1964).

4. R. Brace, E. Matijevic, "Aluminum Hydrous Oxide Sols - 1. Spherical Particles of Narrow Size Distribution," J. Inorg. Nucl. Chem., 35, 3691-3705 (1973).

5. R. L. Pober, unpublished report, M.I.T.

6. B. Novich, W. Moffatt, unpublished results, M.I.T.

7. L. V. Janavicius, "Formation and Processing of Monosized Borosilicate Powder," M.S. thesis, Mass. Inst. of Tech., Cambridge, MA (1984).

8. I. Aksay and J. Pask, "The Silica-Alumina System: Stable and Metastable Equilibria at 1.0 Atmosphere," Science, 183, 70 (1974).

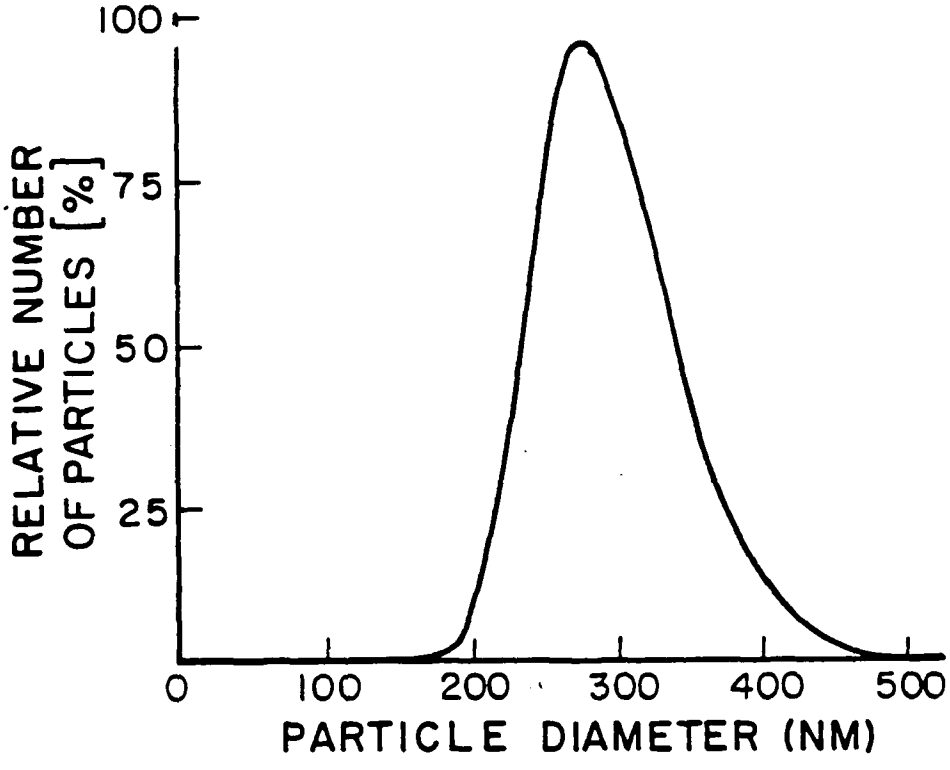

Figure 1. Particle size distribution of size-classified α-alumina powder, 0.2-0.3 μm grain size.

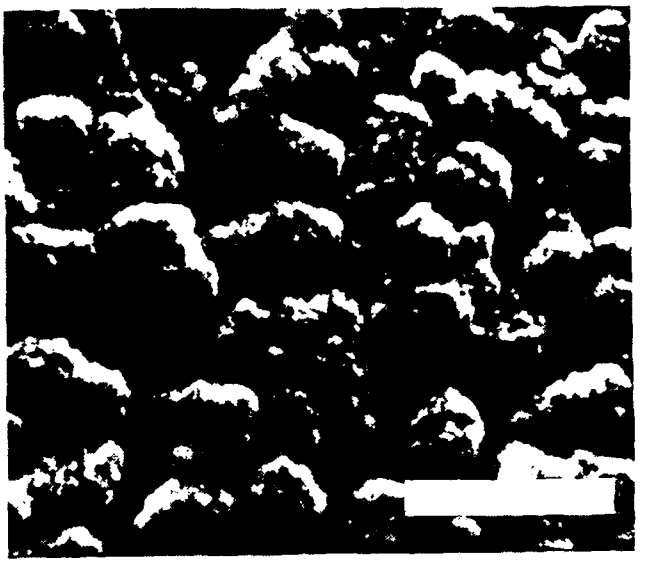

Figure 2. Nonagglomerated, compacted Al_2O_3 particles coated with ultrafine SiO_2 particles (bar = 0.5 μm).

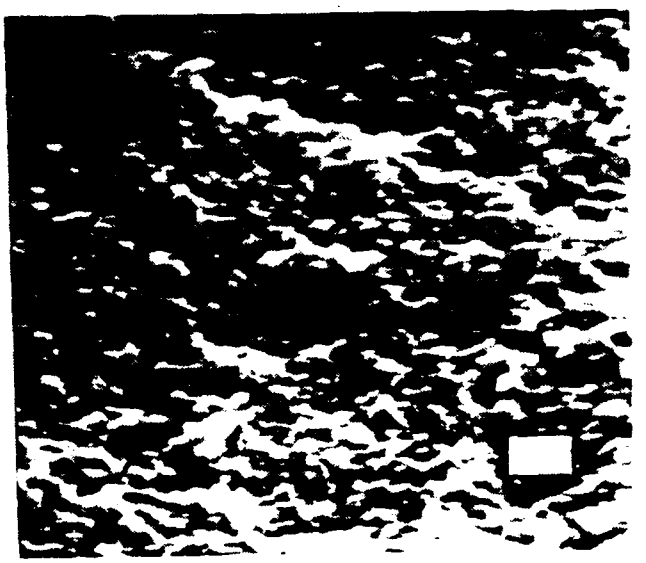

Figure 3. Fracture surface of green composite powder (bar = 1 μm).

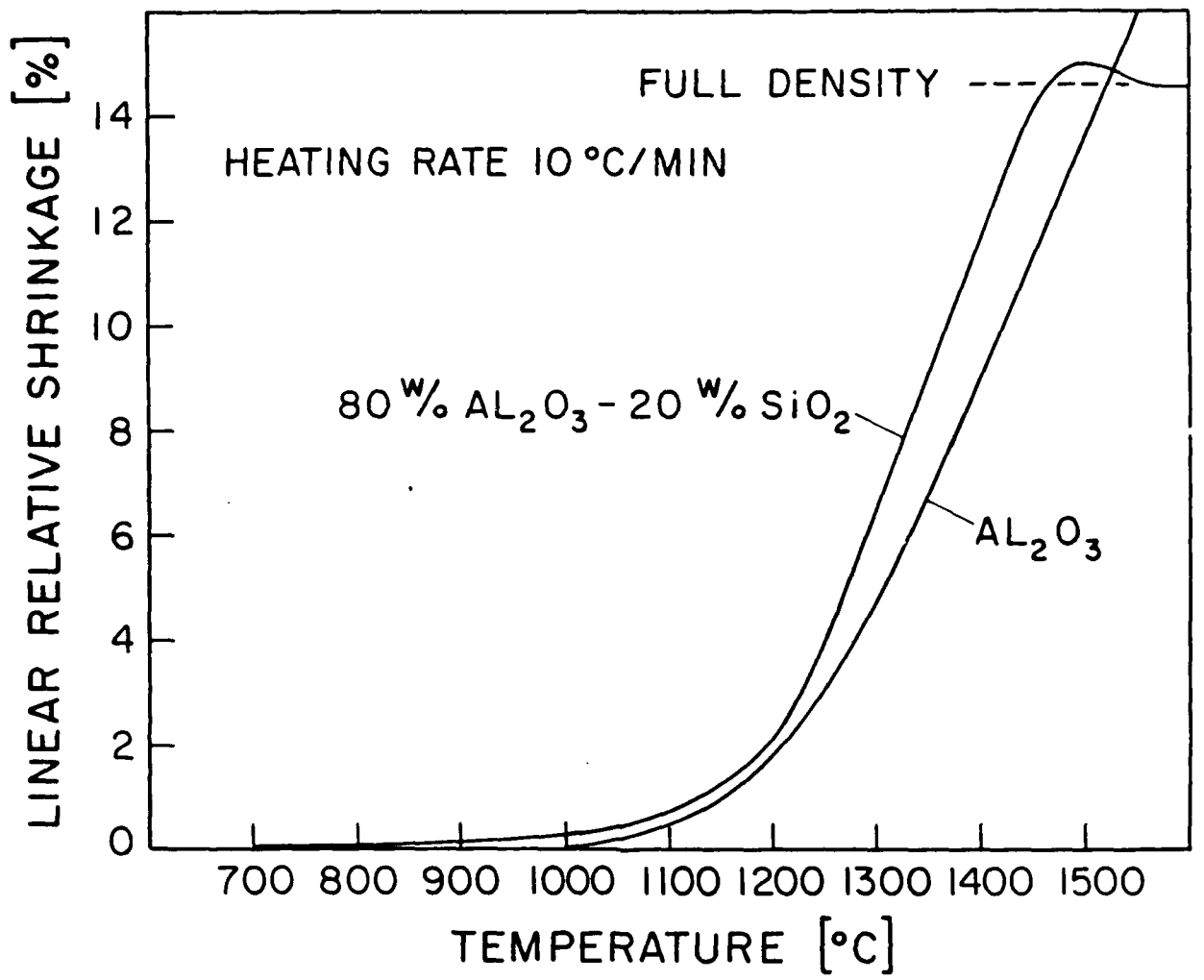

Figure 4. Sintering behavior of Al_2O_3-SiO_2 and Al_2O_3 compacted powder fired in air at a rate of 10°C/min.

Figure 5. Fracture surface of composite Al_2O_3-SiO_2 ceramic sintered in air at 1550°C for 1 hour (bar = 1 μm).

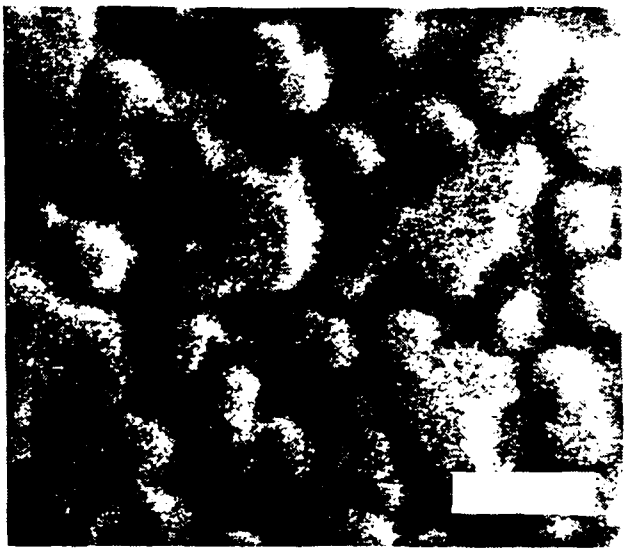

Figure 6. Composite Al_2O_3-SiO_2 ceramic sintered in air at 1550°C for 1 hour (bar = 0.5 μm). The polished surface shows the alumina phase (white) and mullite phase (dark).

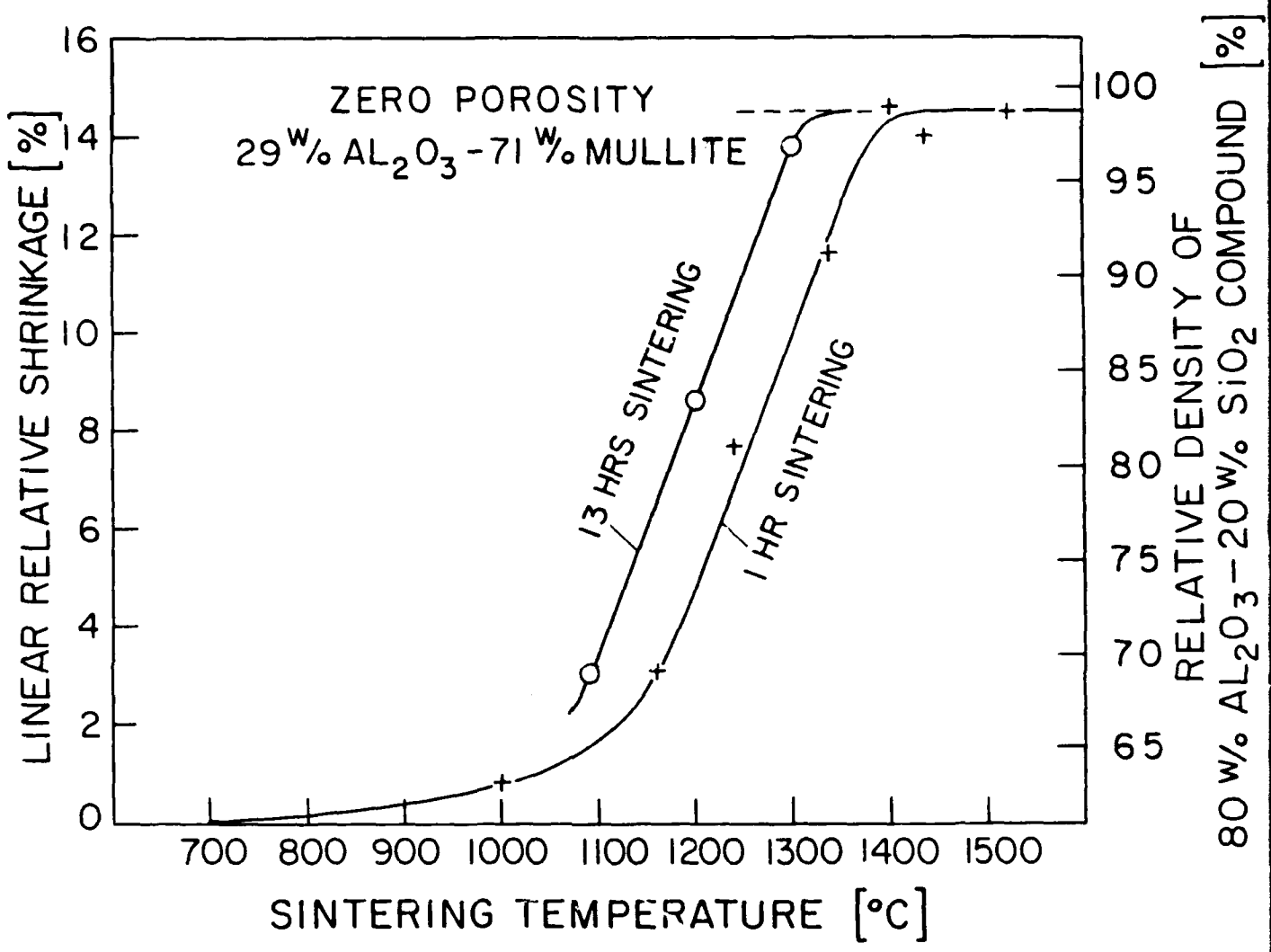

Figure 7. Sintering behavior of Al_2O_3-SiO_2 composite ceramic fired in air for 1 and 13 hours.

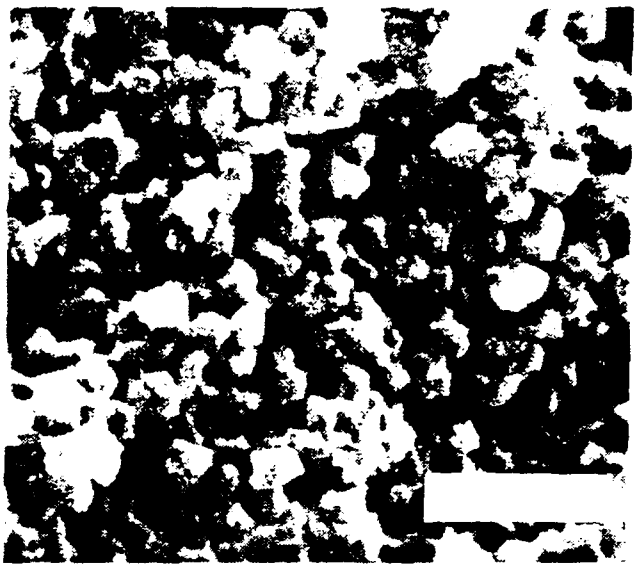

Figure 8. Fracture surface of composite Al_2O_3-SiO_2 ceramic (69% dense) sintered in air at 1080°C for 13 hours (bar = 1 μm).

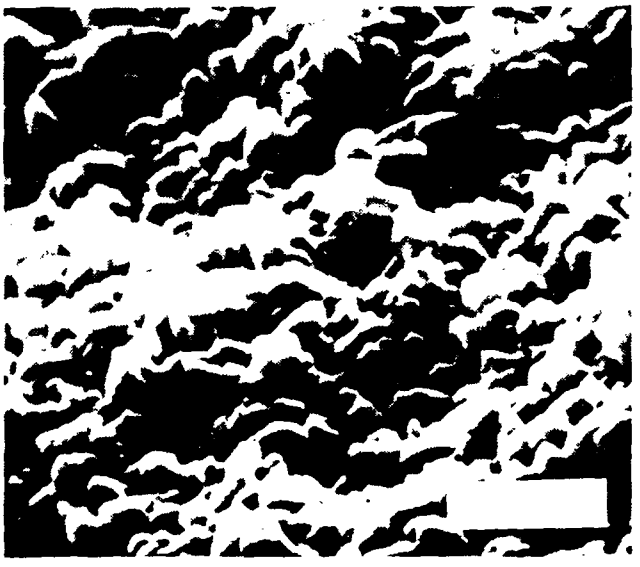

Figure 9. Fracture surface of composite Al_2O_3-SiO_2 ceramic (73% dense) sintered in air at 1200°C for 1 hour (bar = 1 μm).

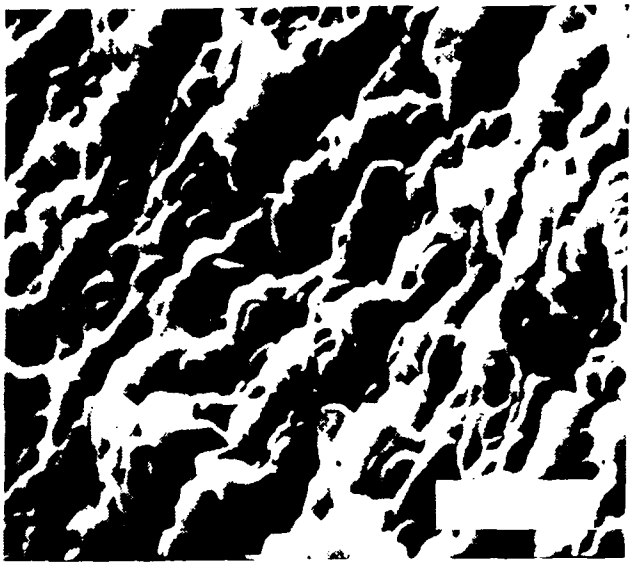

Figure 10. Fracture surface of composite Al_2O_3-SiO_2 ceramic (98% dense) sintered in air at 1400°C for 1 hour (bar = 1 μm).

Hiromichi Okamura

PREPARATION AND SINTERING OF $TiO_2 \cdot Al_2O_3$ POWDERS

I. Introduction

Aluminum titanate (Al_2TiO_5) is a well-known ceramic having the advantages of an apparent low thermal expansion coefficient (4×10^{-6}/°C at 1000°C) and a high melting point (1850°C).[1] Its poor mechanical strength, however, has prevented aluminum titanate from being used in practical applications. The poor mechanical strength unfortunately derives from the same source as the low thermal expansion coefficient: grain boundary cracks form during cooling after sintering because of aluminum titanate crystals' large thermal expansion anisotropy.

To begin improving this ceramic's mechanical properties, Hamano et al. investigated the relationship between its microstructure and mechanical strength, using fired specimens prepared from stoichiometric mixtures of alumina and rutile.[2] Their results imply that the formation reaction of aluminum titanate from corundum and rutile is determined by a nucleus formation mechanism, and that newly formed aluminum titanate grains orient strongly in the same crystalline direction as the initial grains. Also, aluminum titanate's reaction rate might be faster than each grain's growth rate, producing "domain structures" — grain aggregates, each 100-200μm in size, formed by the agglomeration of many 3-4μm grains. Domain structures behave like single crystals, but cracks around them reduce fired specimens' strength.

The same authors also investigated relationships between microstructure, mechanical strength, and thermal expansion behavior of aluminum titanate prepared from sintered and milled powders. They found that free corundum in aluminum titanate powders markedly reduces titanate grains' growth rate, increasing the final ceramic's mechanical strength and bulk density.[3]

Ceramics in that study were prepared by conventional processing methods such as ball-milling and isostatic pressing. Such methods, however, often do not yield powders mixed homogeneously on a microscopic scale, and do not allow control of particle size and shape. To obtain improved, reliable ceramic materials, macrostructures and microstructures must be controlled during fabrication.[4] Microstructures developed during sintering are largely determined by powder characteristics (e.g., particle size, size distribution, shape, state of agglomeration, and chemical composition) and particle packing in the green microstructure.[4,5]

In this laboratory, therefore, narrow size distributed TiO_2,[6] ZrO_2,[7] and doped TiO_2[8] powders have been reproducibly prepared by controlled hydrolysis or cohydrolysis of the corresponding metal alkoxide. Narrow size distribution powders demonstrate significantly reduced sintering time and temperature, and uniform density.[6] Although doped powders (0.1-1.0 wt% doped) have been prepared successfully from alkoxide mixtures, synthesis of composite powders having higher compositions (10-50%) of a second component with a narrow size distribution has been reported only for B-doped SiO_2.[9]

Cohydrolysis of alkoxide mixtures is more difficult to control than hydrolysis of single alkoxides, since the cohydrolysis reaction mechanism of mixed alkoxides has not yet been adequately studied. This study therefore concentrated on coating procedures, rather than cohydrolysis of alkoxides,

for preparing composite powder. Hydrolysis of the coating component's alkoxide in a colloidal dispersion of the substrate component proved effective in producing a composite powder for the $TiO_2 \cdot Al_2O_3$ system. Stepwise hydrolysis of alkoxides was also found to be effective in obtaining unagglomerated particles.

This report describes the synthesis and characterization of uniform-size TiO_2-coated Al_2O_3 powders (the amount of TiO_2 ranging from 30 to 60 mol%), and gives partial results of sintering studies made of these. Powders were synthesized using stepwise controlled hydrolysis of titanium alkoxide in Al_2O_3 dispersions. The basic synthesizing technique described might be applied to other systems, such as $ZrO_2 \cdot Al_2O_3$ and $SiO_2 \cdot Al_2O_3$.

II. Experimental Procedure

A. Powder preparation

TiO_2-coated Al_2O_3 powders varying in TiO_2 content (30-60 mol%) were prepared by stepwise controlled hydrolysis of titanium tetraisopropoxide, $Ti(OC_3H_7^i)_4$, in a dispersion of alumina in isopropyl alcohol.

The starting material used was high purity alumina (corundum) having a narrow size distribution (mean diameter: 0.2-0.3μm; standard deviation: 30% of the mean). This was prepared from a dispersion of commercial powder* by centrifugal separation of particles into size classifications. The alumina powders were dried at 140°C for 24 hours, then ultrasonically dispersed in dry isopropyl alcohol (alcohol dried over CaH_2, then distilled). A photon correlation particle analyser** was used before each coating

---

* Alcoa XA-139 S.G.

** Coulter N-4 Submicron Particle Analyser

procedure to confirm that alumina powders were adequately dispersed.

Water in the amount of 5 times the molar ratio to alumina was added to the alumina dispersion while this was being stirred, to partially saturate the Al_2O_3 powder surface with adsorbed water. Without this procedure, it was found that alkoxide hydrolysis reactions became extremely slow, since dried alumina powders adsorb water so strongly that the free water concentration was reduced below the necessary level (>3 molar ratio of H_2O to alkoxide). The hydrolysis reaction's number of steps was determined so the amount of alkoxide hydrolyzed per step could be kept at a level less than 15 mol% of the amount of dispersed Al_2O_3 powder; at higher levels, the coating procedure produced highly agglomerated powders.

In a typical experiment (molar ratio TiO_2:Al_2O_3 = 1), a 0.12M solution of $Ti(OC_3H_7^i)_4$ in isopropyl alcohol and an equal volume of a 1.8M water in isopropyl alcohol solution were prepared, and each divided into 4 portions. Twice the original (alcohol or water solution's) volume of a 6.12 g/l (0.06M) Al_2O_3/isopropyl alcohol dispersion was prepared separately, as described in the previous two paragraphs.

As the synthesis' first step, a 1/4 portion of the water solution was added to the Al_2O_3 dispersion, followed by a 1/4 portion of the alkoxide solution. The resulting solution was slowly mixed by magnetic stirrer for 15 minutes. After redispersing slightly flocculated powders ultrasonically, powder particle size and distribution were measured by photon correlation particle analyser to confirm that the powder was adequately dispersed. After each hydrolysis step, the solution was redispersed ultrasonically to break slight flocculations.

As the second step, another 1/4 portion each of the water and alkoxide solutions were added to the Al_2O_3 solution, as in step one. The last two 1/4 portions of the water and alkoxide solutions were then added for steps three and four, respectively — again, as described for step one. Final mixing (after step four) gave a solution with a concentration of 0.03M alkoxide and 0.45M water, with 0.03M alumina.

By controlling the total amount of alkoxide hydrolyzed, the amount of TiO_2 coated on Al_2O_3 powder could be controlled. The molar ratio of water (not including water added to partially saturate the alumina surface) to alkoxide was always 15 or greater to achieve rapid hydrolysis.

For comparison, composite powder was also produced using a single-step procedure, in which both the water and alkoxide solutions were added all at once to the Al_2O_3 dispersion. The powder was centrifuged to remove the alcohol solution, redispersed in deionized water, then centrifuged and redispersed in slightly basic aqueous solution (pH=10). Powder compacts prepared by centrifugal settling of the dispersion were vacuum-dried, first at room temperature and then at 80°C.

The powder's physical and chemical properties were then measured. Assessments of particle shape, state of agglomeration, and size distribution were obtained from scanning electron micrographs and photon correlation particle analyses. Specific surface area was determined by a single point BET method. The powder was also studied by X-ray diffraction and differential thermal-thermogravimetric analysis (DTA-TGA). The molar ratio of TiO_2 to Al_2O_3 was determined by quantitative X-ray diffraction analysis after calcining the powder at 1000°C for 3 hours.

B. Sintering

Cakes (bulk density 55%) were prepared by centrifuge casting from a dispersion of TiO_2-coated Al_2O_3 powder (molar ratio TiO_2:Al_2O_3 = 1) and sintered under various conditions using a dilatometer. Specimens were fired at 1500°C for 10 min; 1400°C for 30 min; 1350°C for 30 min; 1320°C for 2 hr; 1300°C for 3 hr; and 1280°C for 4.5 hr, all at a rapid heating rate (50°C/min). The fired specimens' microstructures were observed by scanning electron microscope, and their densities measured by the Archimedes method.

C. Hydrothermal Treatment

To obtain TiO_2-coated Al_2O_3 powder in crystalline form, two batches of coated powders, one containing 50M% TiO_2 and the other 60M% TiO_2, were treated hydrothermally. The powders, each dispersed in its own basic (pH=10) aqueous solution, were heated separately in an autoclave (the 50M% TiO_2 powder at 250°C for 4 hours, and the 60M% TiO_2 powder at 300°C for 3 hours) without stirring. The treated powders were then analyzed by photon correlation particle analyser to determine particle size distributions. Particle surface conditions were observed by scanning electron microscope.

III. Results and Discussion

Figure 1 shows TiO_2-coated Al_2O_3 (TiO_2:Al_2O_3 = 1) powder made by the stepwise hydrolysis of $Ti(OPr^i)_4$ in an alumina dispersion. Figure 2 shows the size-classified Al_2O_3 powder, and TiO_2-coated Al_2O_3 powder made by single-step hydrolysis. These photographs are representative of the size, shape, and state of agglomeration of the initial powder and TiO_2-coated Al_2O_3

powder (made by both the stepwise and single-step methods) in a number of important ways.

First, initial Al_2O_3 powder particles have irregular, polyhedric (sharp-edged) shapes, whereas TiO_2-coated Al_2O_3 powders are more rounded (smooth-surfaced).

Second, TiO_2-coated powder particles, when washed with water, are coated with a fine (10-20nm) precipitate, clearly shown in Figure 2B. TiO_2 powder made by controlled hydrolysis of alkoxide has the same fine-grain coating.

Third, TiO_2-coated powder particles made by stepwise alkoxide hydrolysis have narrower size distributions than powder particles made by the single-step method. Figure 3 shows particle size distributions of coated powder measured by photon correlation particle analyser after each hydrolysis step, along with particle size distributions of initial Al_2O_3 powder and washed, coated powder. Although the mean diameter of final washed, coated powder particles was larger than the expected value because of slight flocculations, the standard deviation was still within the range (30% of the mean) of the initial powder particles.

Fourth, TiO_2-coated powder particles made by the stepwise method are generally discrete, while powder particles made by the single-step reaction are highly agglomerated.

Fifth, the coating process yields Al_2O_3 particles coated with TiO_2, rather than mixed with TiO_2 particles. Furthermore, scanning electron microscopy X-ray maps (Ti) of coated Al_2O_3 powder show uniform TiO_2 distributions that match the respective Al X-ray maps. Thus, TiO_2 is not

concentrated in large clumps, but appears to cover Al_2O_3 particles uniformly.

Particle size reproducibility of the stepwise coating method is illustrated in the two plots of particle size versus hydrolyzed alkoxide amount in Figures 4 and 5. Figure 4 shows the mean diameter change of particles after each hydrolysis reaction step for two batches that used Al_2O_3 powders having different mean diameters. The difference in mean diameter between the initial powders was maintained in the final coated powders. Figure 5 shows the mean particle diameter change for four different batches, in which the amount of alkoxide hydrolyzed was changed from 30 mol% to 60 mol % in six steps for the same starting alumina powder. In each batch, almost the same rate of increase in mean diameter was observed for all hydrolysis reaction steps. Thus, the size of the coated powder could be controlled by selecting the size of starting powder.

Table I summarizes measured physical properties for TiO_2-coated Al_2O_3 powders having different amounts (30-60 mol%) of TiO_2. X-ray diffraction showed the TiO_2 coating phase to be amorphous for all powders. As mentioned previously, particle size changes with the amount of TiO_2 coating, but particle shape and structure are not affected. Density measurements obtained with a stereopycnometer gave values inversely proportional to TiO_2 level. A single point BET method gave surface areas for coated powder (washed with deionized water) in the same range as those for pure TiO_2 powder prepared by Barringer.[10] The high surface area of water-washed TiO_2-coated Al_2O_3 powder was attributed to a surface coating of fine spherical precipitate, which resulted from the rapid hydrolysis of residual (unreacted) alkoxide on contact with water.

Figure 6 shows the results of simultaneous differential thermal-thermogravimetric analyses (DTA-TGA) conducted on TiO_2-coated Al_2O_3 (TiO_2: 50 mol%) powders. The observed weight loss correlates with powder treatment after synthesis: powders that were not washed, or that had previously been heated, lost the most weight (15%); powders washed and then calcined at 450°C for 30 min lost the least weight (2%). Most weight loss was due to water loss between 90° and 250°C; the remainder resulted from burnoff of organics between 370° and 480°C. The DTA curve shows an endothermic peak in the temperature range where water was lost, and an exothermic peak in the region where organics were burned off. Another endothermic peak was observed between 1350° and 1410°C; this is assumed to be due to aluminum titanate formation.

X-ray diffraction analyses were made of TiO_2-coated Al_2O_3 powder (TiO_2: 50 mol%) calcined under different conditions. The results are shown in Table II. TiO_2's crystal phase changed from amorphous to anatase, then to rutile, and finally to aluminum titanate with the increasing temperature of calcination. Formation reaction of aluminum titanate occurred above 1320°C, as expected from the DTA results; this temperature is higher than would be expected from the phase diagram.[11]

Figure 7 shows results of quantitative X-ray diffraction analyses for coated powders' TiO_2 content. Amounts of TiO_2 detected were directly proportional to the amounts of alkoxide hydrolyzed. The conversion factor of $Ti(OR)_4$ to TiO_2 was 0.98.

Results of sintering studies are summarized in Table III. Specimens fired at and above 1320°C showed high relative densities (95-99%), but domain formations were observed in all specimens, as shown in Figure 8. For

sintered specimens fired between 1300 and 1350°C, a mixture phase of aluminum titanate, rutile, and corundum was found, and partial domain formations were observed. Specimens fired at 1280°C for 4.5 hours or at 1300°C for 3 hours, however, showed no domain formation (Figure 9), a relative density of 85-90%, and primary crystal phases of rutile and corundum with no Al_2TiO_5. These results confirm that the domain formation reaction ($TiO_2 + Al_2O_3 \Rightarrow Al_2TiO_5$) occurs above 1300°C, as expected from the results of DTA and X-ray diffraction analysis for calcined TiO_2-coated powders. Sintering studies for specimens having different ratios of TiO_2 to Al_2O_3 are currently being done.

Hydrothermally treated powder particles have rough surfaces, as shown in Figure 10. After ultrasonic redispersion, powder was separated into finer particles (mean diameter: 90nm) and particles of almost original size (mean diameter: 600nm). The finer particles' crystal phase was found to be anatase; original-size particles were corundum with anatase. From these results, it was assumed that the TiO_2 coating crystallized from amorphous to anatase form during hydrothermal treatment, but during ultrasonic redispersion, much of the TiO_2 broke off from the coating in fine particles. Hydrothermal treatment therefore was not effective in the production of crystallized TiO_2-coated Al_2O_3 powder.

IV. Conclusions

1. TiO_2-coated Al_2O_3 powders composed of narrow size distributed, rounded, unagglomerated particles can be prepared by stepwise hydrolysis of a titanium alkoxide in an alumina (size-classified) dispersion.

2. Powders having different amounts of TiO_2 can be reproducibly synthesized by controlling the total amount of alkoxide hydrolyzed.
3. TiO_2-coated Al_2O_3 powders were converted to Al_2TiO_5 powders having high relative densities (95-99%) by firing above 1320°C. Domain structures were observed in the fired specimens, however.
4. Hydrothermal treatment was not effective in the production of crystallized TiO_2-coated powders.

V. Future Work

Sintering studies for TiO_2-coated powders containing different amounts of TiO_2 will be performed. Relationships between microstructures and mechanical properties of fired specimens will be studied simultaneously.

VI. References

1. W. R. Buessem, N. R. Thielke, and R. V. Sarakauskas, "The Expansion Hysteresis of Aluminum Titanate," Ceramic Age 60:38-40 (1952).

2. K. Hamano, Y. Ohya, and Z. Nakagawa, "Microstructure and Mechanical Strength of Aluminum Titanate Ceramic Prepared from Mixture of Alumina and Titania," J. Ceram. Soc. Japan 91:2, 94-101 (1983).

3. Y. Ohya, K. Hamano, and Z. Nakagawa, "Microstructure and Mechanical Strength of Aluminum Titanate Ceramics Prepared from Synthesized Powders," J. Ceram. Soc. Japan 91:6, 289-297 (1983).

4. H. K. Bowen, et al., "Basic Research Needs on High Temperature Ceramics for Energy Applications," Mat. Sci. and Eng., 44:1-56 (1980).

5. G. Y. Onoda, Jr. and L. L. Hench, Eds., Ceramic Processing Before Firing, John Wiley and Sons, NY, 1978.

6. E. A. Barringer and H. K. Bowen, "Formation, Packing, and Sintering of Monodisperse TiO_2 Powders," J. Am. Ceram. Soc. 65:C113 (1982).

7. B. Fegley, Jr., "Synthesis, Characterization, and Processing of Monosized Ceramic Powders," Mat. Res. Soc. Spring Meeting, Albuquerque, NM, 1984.

8. B. Fegley, Jr., E. A. Barringer, and H. K. Bowen, "Synthesis and Characterization of Monosized Doped TiO_2 Powders," J. Am. Ceram. Soc. 67:C113 (1984).

9. L. V. Janavicius, "Formation and Processing of Monosized Borosilicate Powders," M.S. thesis, Mass. Inst. of Tech., Cambridge, MA (1984).

10. E. A. Barringer, "The Synthesis, Interfacial Electrochemistry, Ordering, and Sintering of Monodispersed TiO_2 Powders," Ph.D. Thesis, Mass. Inst. of Tech., Cambridge, MA (1983).

11. A. M. Lejus, D. Goldberg, and A. Revcolevschi, C. R. Acad. Sci., Ser. C 263:20, 1223 (1966).

Table I. Physical Properties of TiO_2-coated Al_2O_3 Powders

	Powder*				
	Initial	30M%-TiO_2	40M%-TiO_2	50M%-TiO_2	60M%-TiO_2
Precursor		$Ti(OC_3H_7^i)_4$	$Ti(OC_3H_7^i)_4$	$Ti(OC_3H_7^i)_4$	$Ti(OC_3H_7^i)_4$
Crystal Form	Corundum	Amorphous + Corundum	Amorphous + Corundum	Amorphous + Corundum	Amorphous + Corundum
Average particle size range (μm)	0.2-0.3	0.3-0.4	0.4-0.5	0.4-0.6	0.5-0.7
Density (g/cm^3)	3.9	3.6-3.8	3.5-3.7	3.4-3.6	3.3-3.5
Surface Area (m^2/g)	10-15	35-45	110-120	190-210	240-260
Shape	Irregular Polyhedric¶	Round†	Round†	Round†	Round†
Structure	Singlet	Singlet	Singlet	Mostly Singlet	Mostly Singlet

* washed with deionized water

¶ sharp-edged shape

† smooth surface

Table II. X-ray Diffraction Results of TiO_2-coated Al_2O_3 Powders (TiO_2: 50 mol%) Calcined

Calcining Condition	Crystal Form	
	TiO_2	Al_2O_3
140°C - 5 hours	Amorphous	Corundum
500°C - 3 hours	Anatase	Corundum
1000°C - 3 hours	Rutile	Corundum
1280°C - 5 hours	Rutile	Corundum
1280°C - 20 hours	Rutile	Corundum
1300°C - 2 hours	Rutile	Corundum
1320°C - 2 hours	Rutile + Aluminum Titanate	Corundum + Aluminum Titanate
1350°C - 30 minutes	Aluminum Titanate	Aluminum Titanate
1400°C - 30 minutes	Aluminum Titanate	Aluminum Titanate

Table III. Sintering Results of TiO_2-coated Al_2O_3 Specimens (TiO_2: 50 mol%)

Sintering Condition	Sintering Specimen		
	Crystal Form	Domain Formation	Relative Density
1280°C - 4.5 hours	Rutile + Corundum	No	85%
1300°C - 3 hours	Rutile + Corundum	No	90%
1320°C - 2 hours	Rutile + Corundum + AT*	Yes (partially)	95%
1350°C - 30 min.	AT	Yes	98%
1400°C - 30 min.	AT	Yes	99%
1500°C - 10 min.	AT	Yes	98%

* AT: Aluminum Titanate

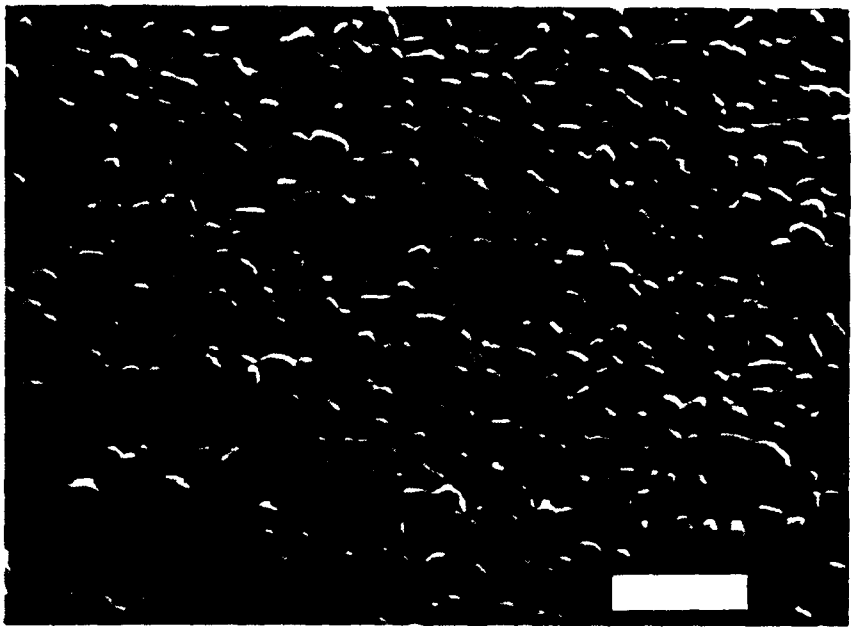

(A)

(B)

Figure 1. Scanning electron micrograph of (A) top surface and (B) fracture surface of TiO_2-coated Al_2O_3 (TiO_2:50 mol%) compact made by centrifuge casting (bar = 1um).

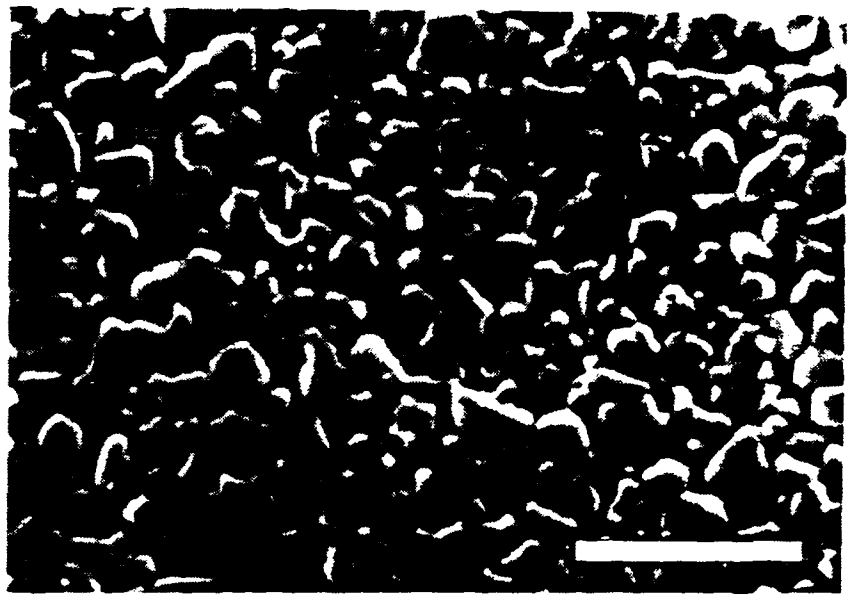

(A)

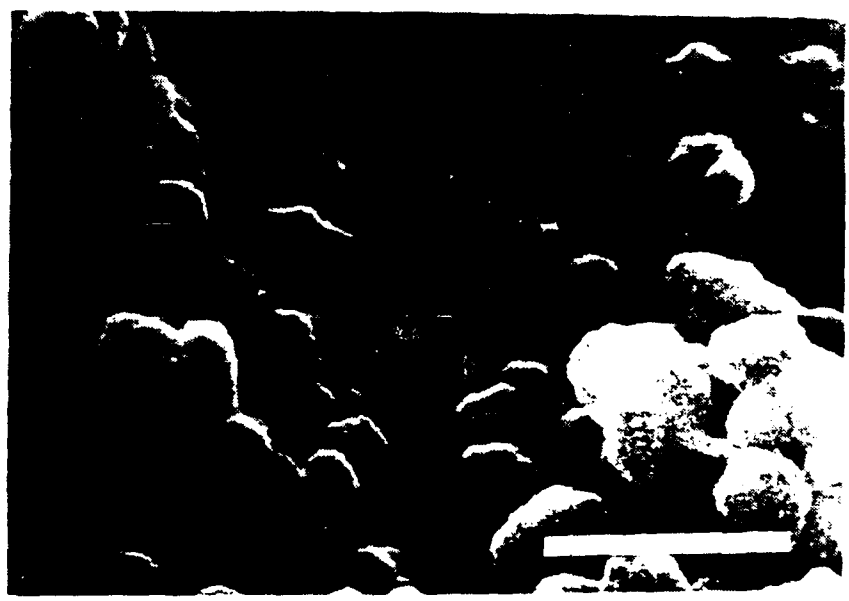

(B)

Figure 2. Scanning electron micrograph of (A) Al_2O_3 powder before coating and (B) TiO_2-coated Al_2O_3 powder (TiO_2:50 mol%) made by single-step hydrolysis of $Ti(OR)_4$ (bar = 1um).

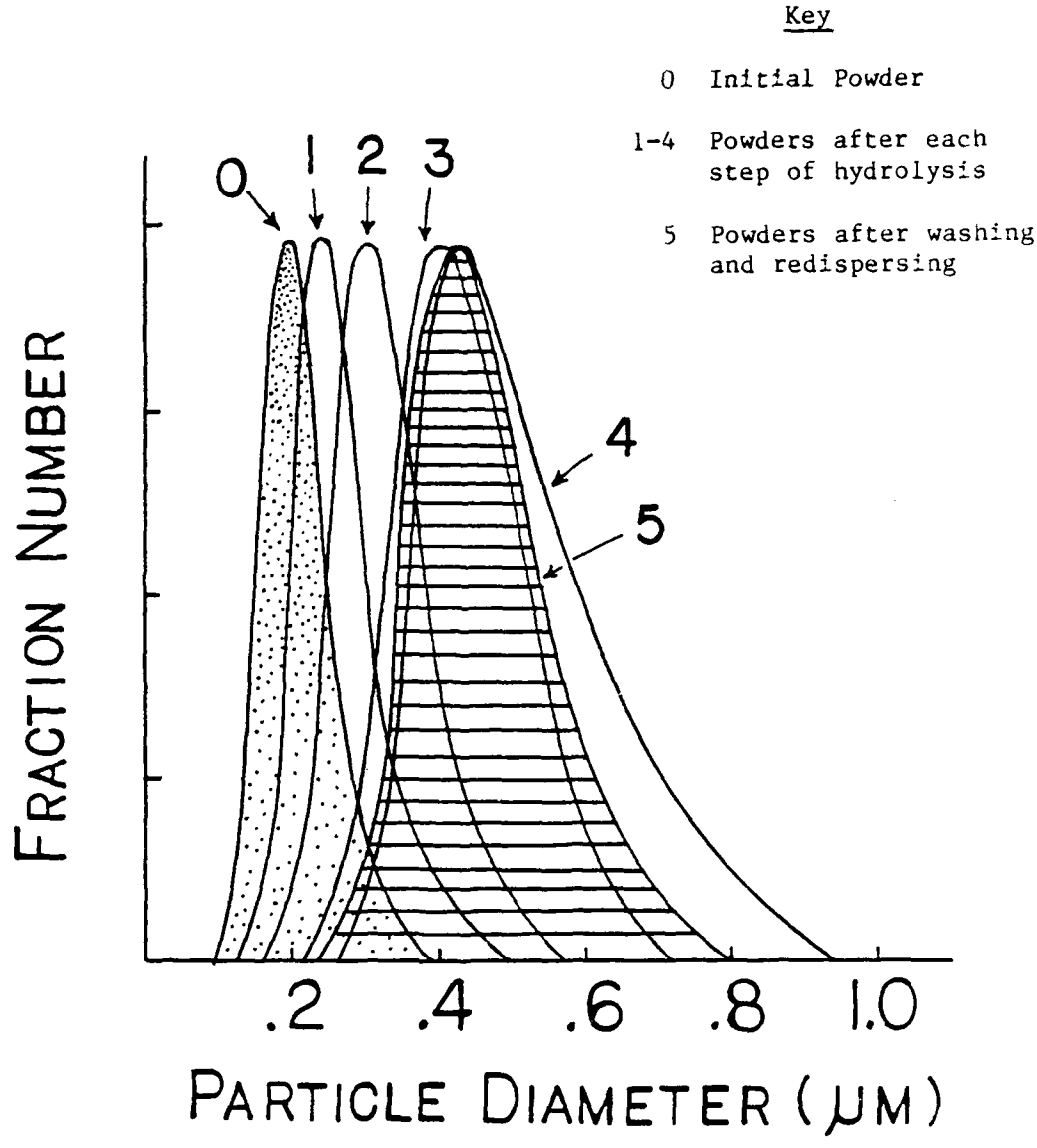

Figure 3. Particle size distributions for coated powder after each hydrolysis reaction step (Total TiO_2 amount: 50 mol%).

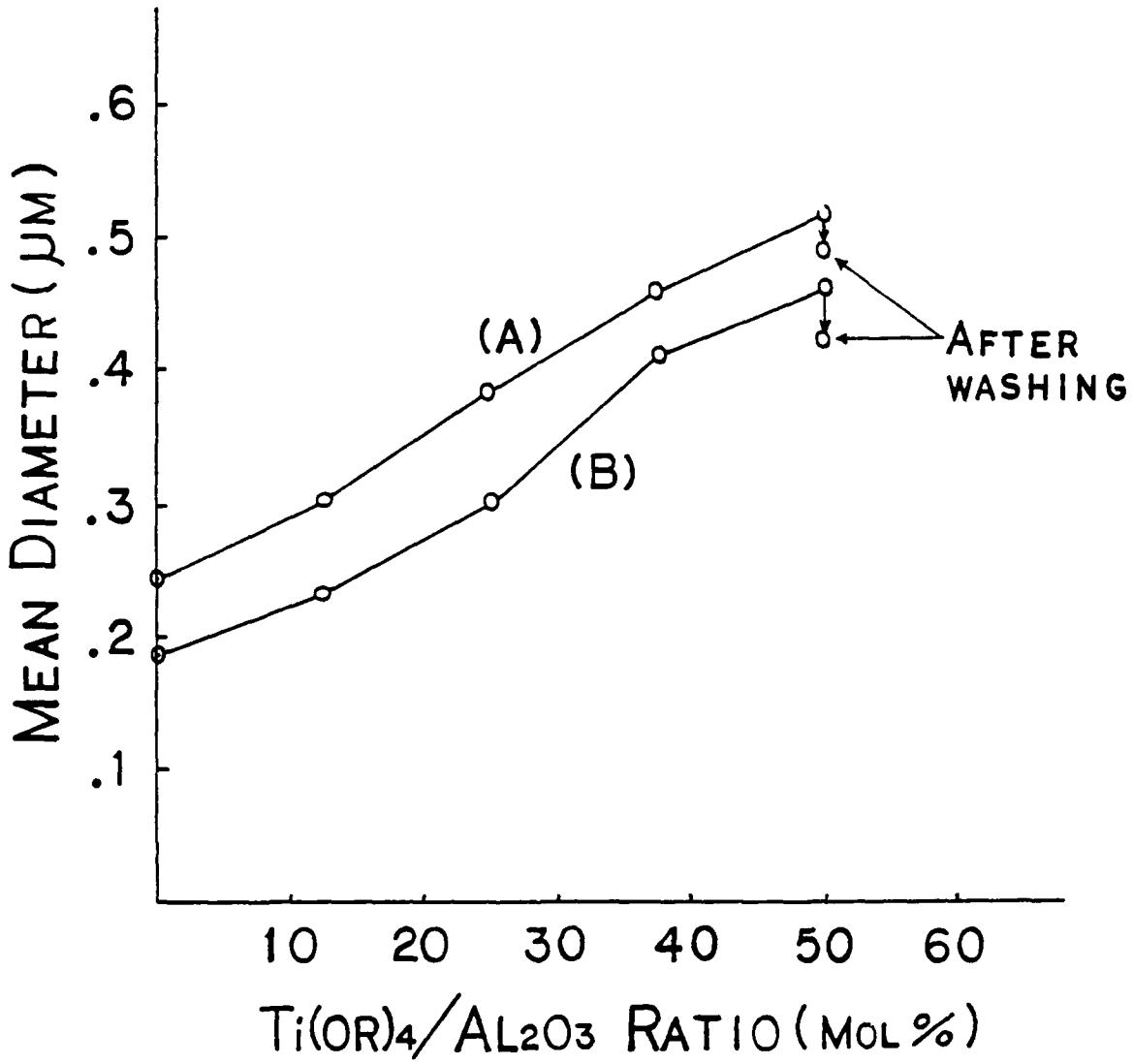

Figure 4. Mean diameter changes of particles after each hydrolysis step for two different batches that used alumina powders having different mean diameters: (A) 0.25 um, (B) 0.19 um.

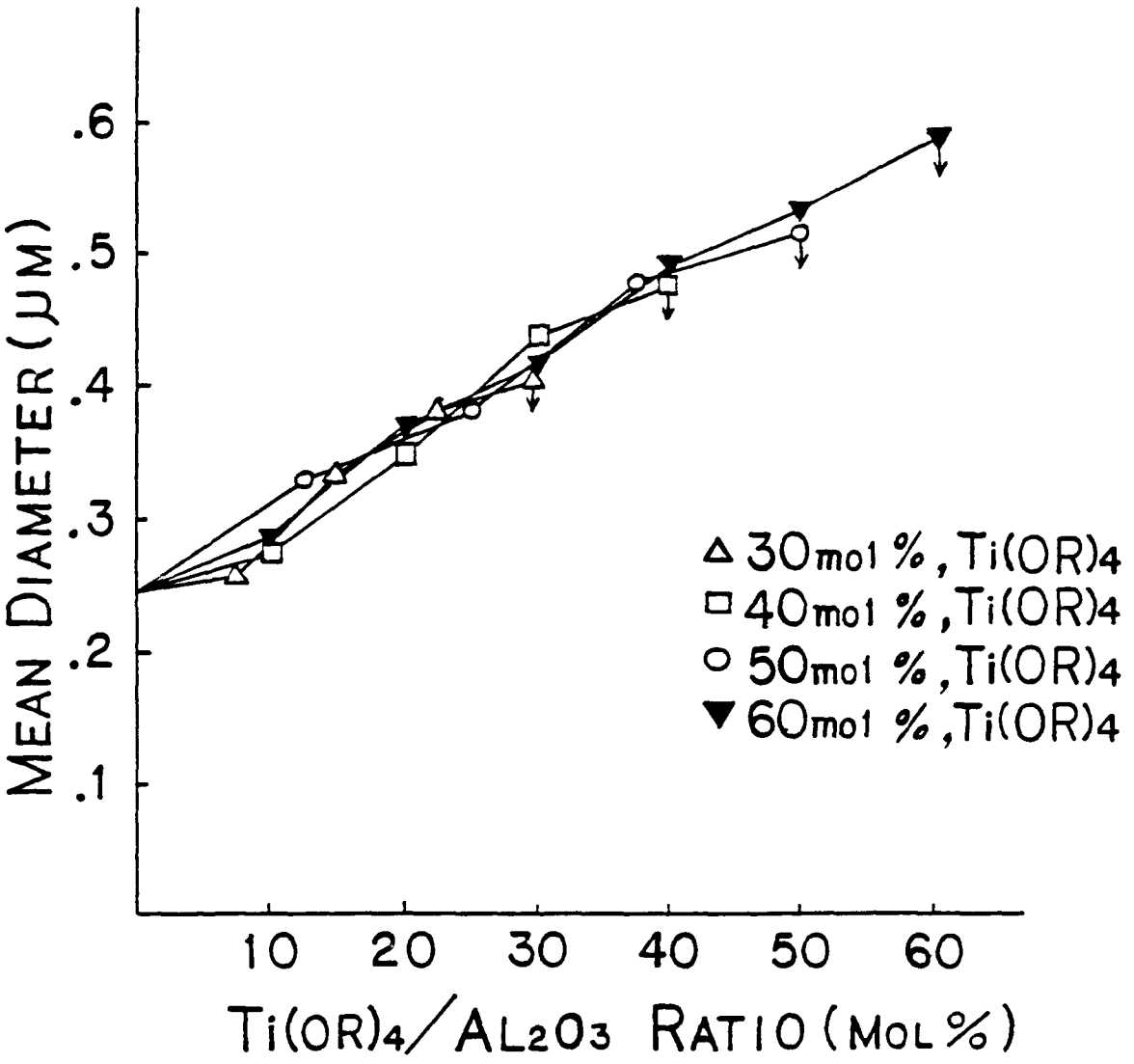

Figure 5. Mean diameter of particles after each step of hydrolysis for four different batches in which total amount of alkoxide was changed from 30 mol% to 60 mol%.

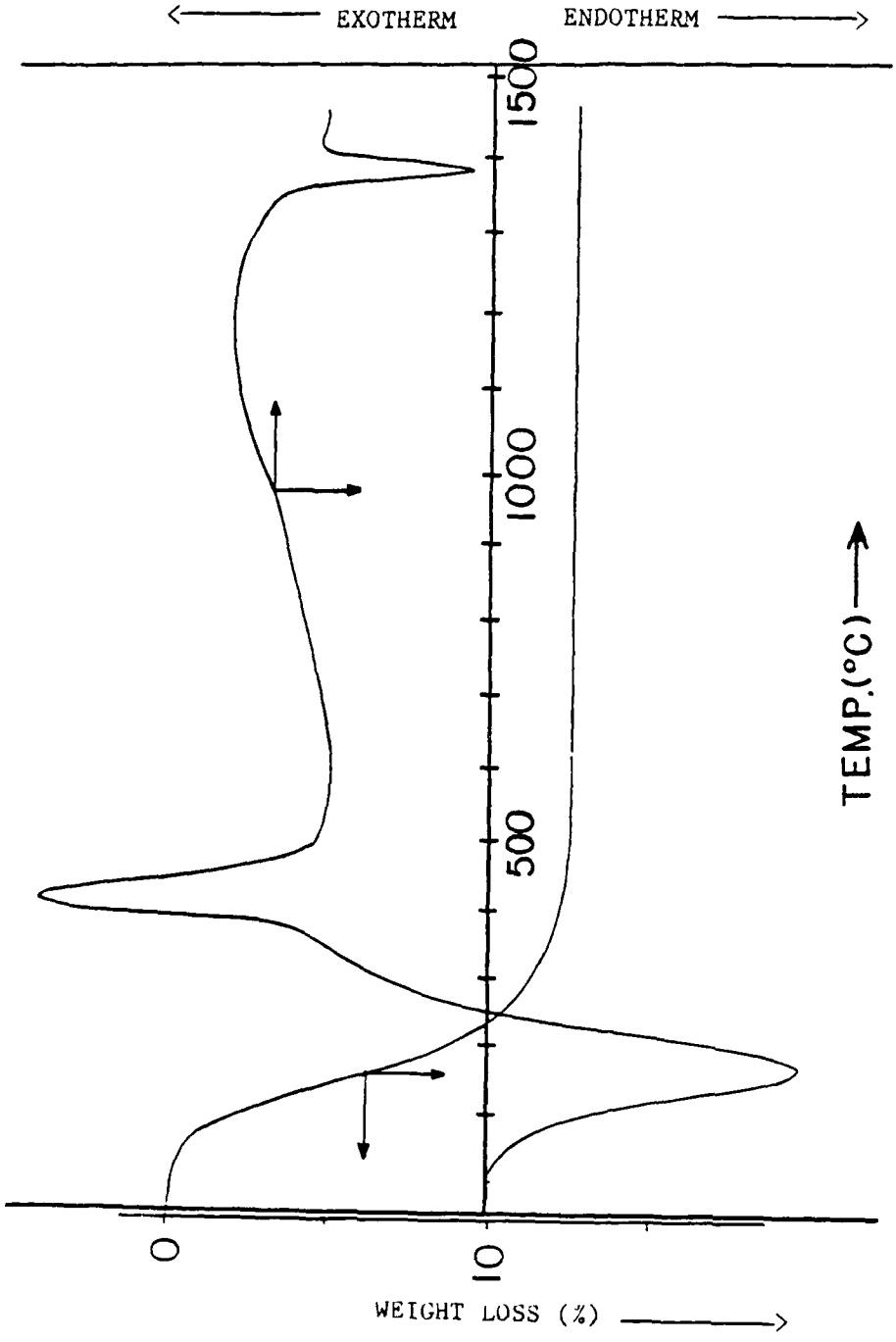

Figure 6. DTA and TGA curves for TiO_2-coated Al_2O_3 powders (TiO_2:50 mol%).

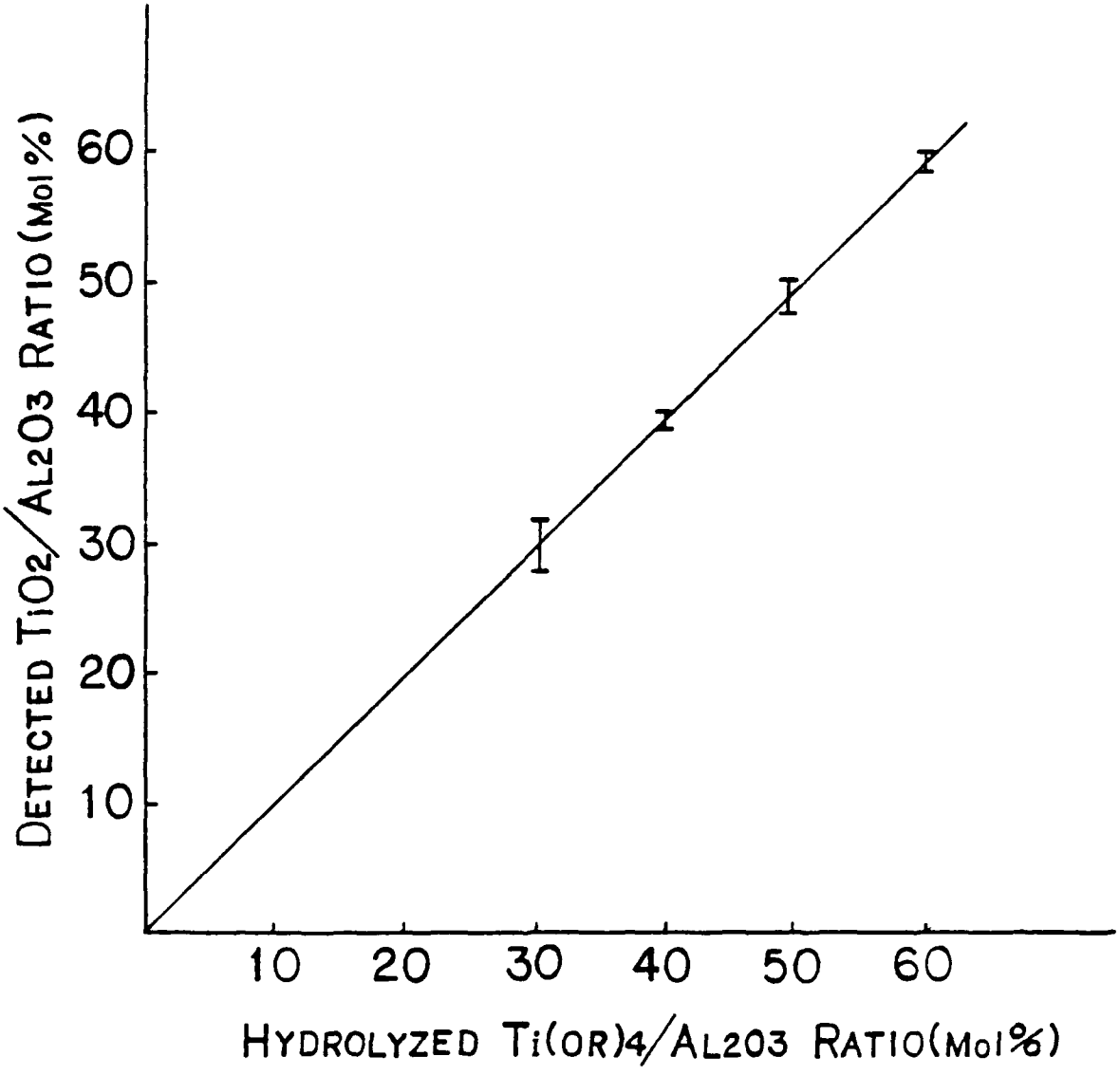

Figure 7. Detected TiO_2 amount versus hydrolyzed $Ti(OR)_4$ content. All powders were calcined at 1000°C for 3 hours before X-ray diffraction analysis.

(A) (B) (C)

Figure 8. Scanning electron micrographs of (A) top surface at a magnification of 9600X and fracture surface of TiO_2-coated Al_2O_3 (TiO_2:50 mol%) specimen fired at 1350°C for 30 min, at magnifications of (B) 9500X and (C) 190X.

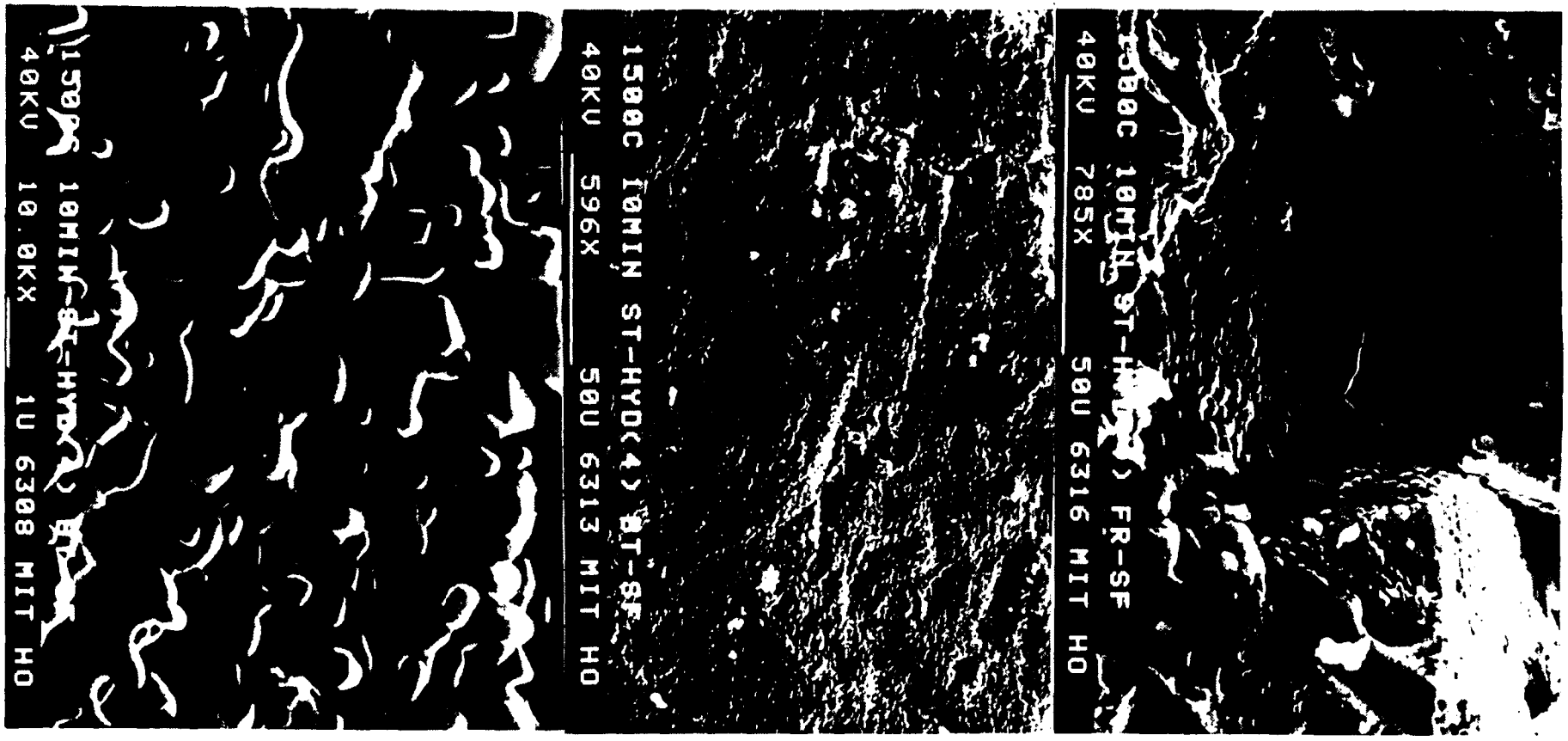

(D) (E) (F)

Figure 8. (cont'd) Scanning electron micrographs of top surface at magnifications of (D) 10,000X and (E) 596X, and (F) fracture surface of TiO_2-coated Al_2O_3 (TiO_2:50 mol%) specimen fired at 1500°C for 10 min, at a magnification of 785X.

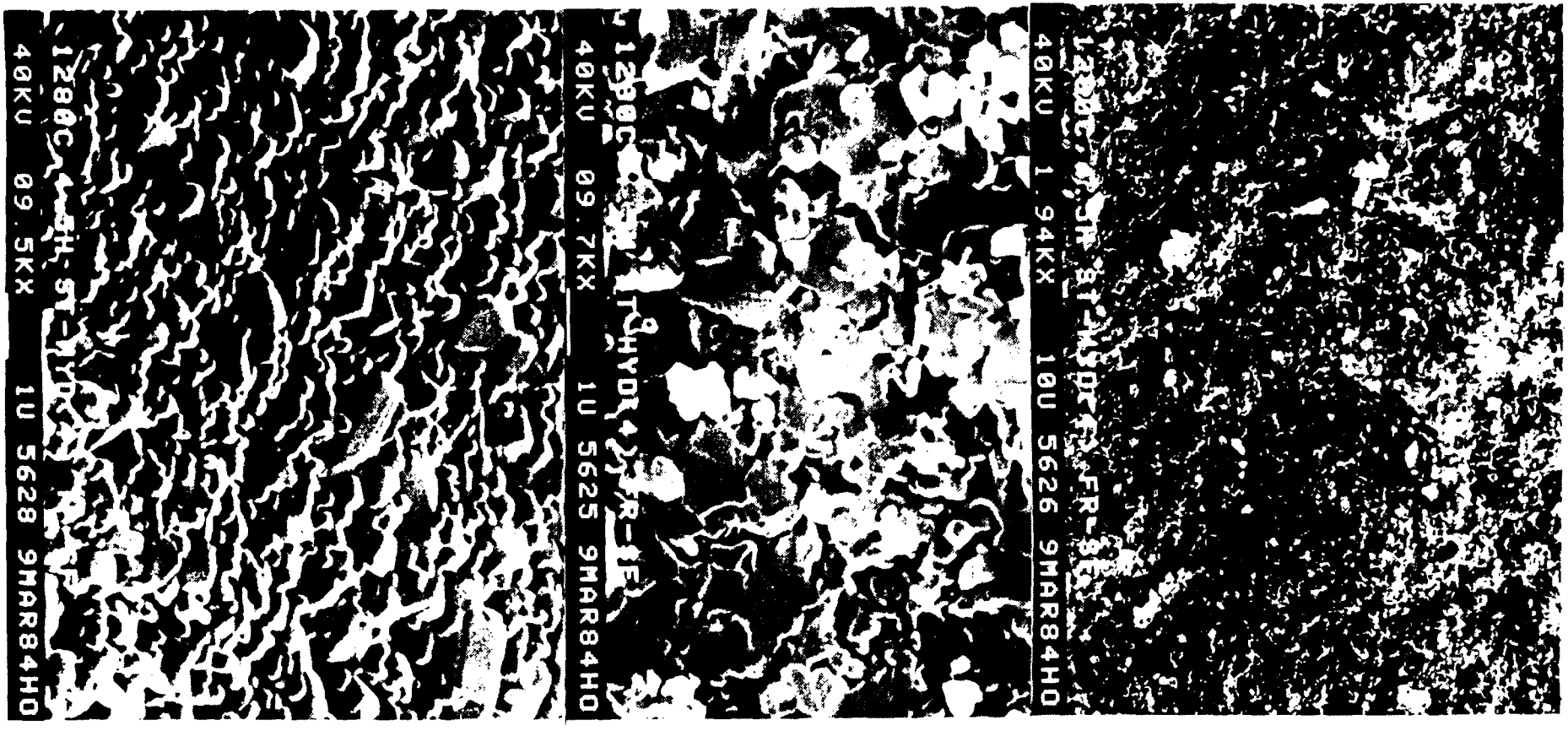

(A) (B) (C)

Figure 9. Scanning electron micrographs of (A) top surface at a magnification of 9500X, and fracture surface of TiO_2-coated Al_2O_3 (TiO_2:50 mol%) specimen fired at 1280°C for 5 hours, at magnifications of (B) 9700X and (C) 1940X.

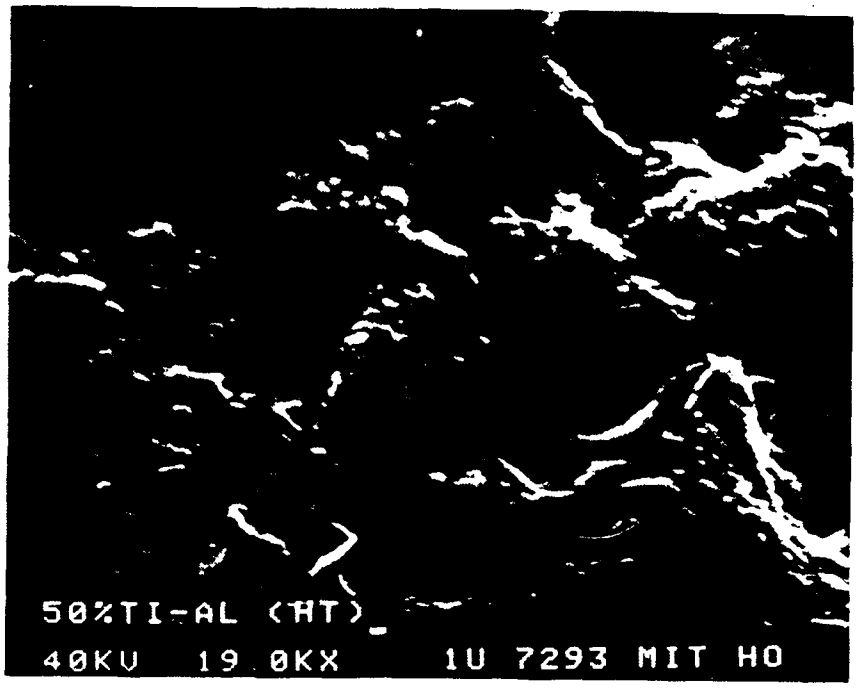

(A)

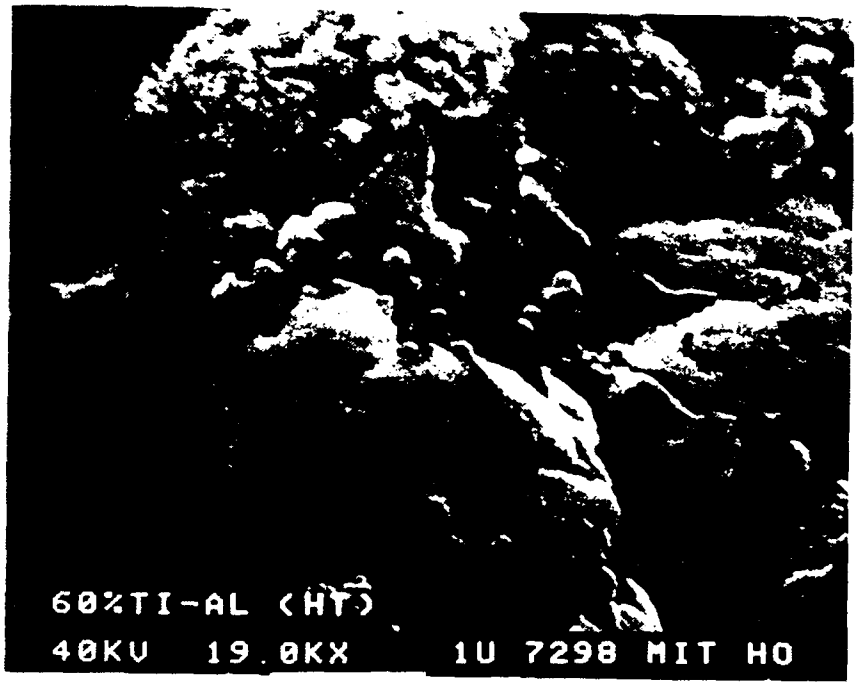

(B)

Figure 10. Scanning electron micrograph of hydrothermally treated (A) 50 mol% TiO_2-coated Al_2O_3 and (B) 60 mol% TiO_2-coated Al_2O_3.

Yasuo Oguri

PREPARATION AND SINTERING OF ANATASE TiO_2

I. Introduction

Anatase (TiO_2) ceramics, because of their ability to withstand high temperatures, are applicable for use in such devices as oxygen sensors and collecting electrodes in NaS batteries.

Fine size, narrow size distribution, spherical, nonagglomerated TiO_2 particles were synthesized in this study by controlled hydrolysis of titanium tetraethoxide in ethanolic solution. The amorphous product formed this way had a density (3.1 g/cm^3) lower than that of either of TiO_2's common crystalline forms, anatase (3.89 g/cm^3) and rutile (4.25 g/cm^3), and would therefore shrink more during subsequent ceramics processing. A denser crystalline product would be preferable, because it would shrink less.

Amorphous TiO_2 is easily converted to anatase and rutile by calcination, but the crystals are difficult to re-disperse in liquid, and particle agglomeration during calcination seems unavoidable. A well-known alternative method for obtaining the crystalline form is to use an autoclave: hydrothermal reactions at high temperature and pressure can produce crystalline oxides directly in aqueous dispersions.[1]

This report describes the synthesis, dispersion, and packing of uniform-size crystalline TiO_2 powders using hydrothermal reactions. It also demonstrates that densification can be controlled without the use of sintering aids when dense, uniformly packed bodies are sintered.

II. Experimental Procedure

Two kinds of amorphous TiO_2, designated Samples I and II and

characterized in Table 1, were produced from titanium tetraethoxide by Novich's continuous flow reaction method (described in his section of this report), for which reaction conditions are summarized in Table 2. The amorphous, hydrated TiO_2 precipitate was washed with deionized water three times, then dispersed in slightly basic (pH = 10) aqueous solution. The resulting slurry's solid content was adjusted to 5 weight%, and the slurry was then poured into an autoclave, illustrated in Figure 1.

The top of Table 3 summarizes hydrothermal conditions for each experimental run. In each case, autoclaving temperature was measured by a chromel-alumel thermocouple, and pressure was determined by a Bourdon tube pressure gauge.

Portions of Samples I and II were treated ultrasonically to disperse particles and break them down into individual crystals. Powder compacts were then prepared from dispersed and undispersed samples separately, using the following method: A millipore filter (0.3 μm) was set in the bottom of a glass tube (ID = 14.5 mm), and a 5 weight% slurry poured through. The tube was then evacuated until water could no longer be observed on the resulting filter cake's surface. The cake was dried at 25°C ± 1°C, then sintered.

Product particle shape, size, and agglomeration were observed by scanning electron microscopy (SEM); particle size and crystalline structure were also checked by X-ray diffraction. Qualitative size distributions were obtained by photon correlator,* and specific surface area was determined by the BET method.**

---

* Coulter N-4 equipment was used

** Quantachrome Corp. equipment was used

III. Results and Discussion

A. Powder Characterization

Results of subjecting the synthesized amorphous TiO_2 to hydrothermal treatment are summarized in the lower portion of Table 3. Amorphous TiO_2 was in all cases changed to anatase during autoclaving: X-ray diffraction showed larger anatase peaks, indicating more anatase in the sample, and particles' surface area decreased.

Particle sizes were checked by observing SEM photographs, which showed anatase's crystal size to be 0.01-0.05μm (100-500Å), independent of apparent particle size:

- Sample II's submicron (0.3-0.8 μm) particles had smooth surfaces before autoclaving (Figure 2). After autoclaving, surfaces were rough with 0.01-0.05μm grains, which gave particles a raspberry-like appearance (Figures 3a and 3b). (Ultrasonic treatment dramatically altered these particles. Figure 4 shows the surface of a compact made from a slurry that was not treated ultrasonically; Figure 5 shows the surface of a compact made from a slurry that was. Note that raspberry-like particles do not appear in the ultrasonically treated sample.)
- Sample I's particles (Figure 6) were 0.1-0.2μm in size. During autoclaving, their surfaces changed, too, with the appearance of numerous 0.01-0.05μm grains (Figure 7). Particle grains cannot be distinguished as easily on Sample I as on Sample II, however, because Sample I's initial particles were so small.

Particle sizes calculated from specific surface area and X-ray line broadening had the same order of magnitude as those determined from SEM micrographs. Together, these results indicate that when amorphous TiO_2 changes to the anatase crystal form, crystal size does not depend on apparent initial particle size; rather, it depends on hydrothermal conditions.

B. Differential Thermal Analysis and Thermogravimetric Analysis

Differential thermal analysis (DTA) of both autoclaved powder and powder that was air dried at 25°C showed a small endothermic peak under 100°C, corresponding to water evaporation. An intense exothermic peak, typical of ignition, indicated that unreacted alkoxy groups were oxidized at about 400°C. Thermogravimetric analysis (TGA) of both powders showed that all weight was lost below 450°C. Total weight losses were 5.6% and 38.8% for autoclaved and unautoclaved Sample II powders, respectively.

The overall TiO_2 precipitation reaction during hydrothermal treatment consists of hydrolysis and condensation,

$$\text{HYDROLYSIS:} \qquad Ti(OR)_4 + 4H_2O \xleftrightarrow{ROH} Ti(OH)_4 + 4ROH \qquad (1)$$

$$\text{CONDENSATION:} \qquad Ti(OH)_4 \longleftrightarrow TiO_2(s) + 2H_2O \qquad (2)$$

where $R = C_2H_5$. The hydrolyzed species polymerize to form higher molecular weight products during condensation, which proceeds either through a water elimination reaction,

$$Ti\text{-}OH + HO\text{-}Ti \longrightarrow Ti\text{-}O\text{-}Ti + H_2O \qquad (3)$$

or through alcohol elimination,

$$Ti\text{-}OR + HO\text{-}Ti \longrightarrow Ti\text{-}O\text{-}Ti + ROH \qquad (4)$$

In a high-temperature water dispersion, the rate for Reaction (4) is expected to increase. This is one reason why surface area decreased and crystal size increased during hydrothermal treatment. When powder (washed by ethyl alcohol) was heated at 200°C in ethyl alcohol, however, the anatase X-ray diffraction peaks were very broad, indicating small crystal size. SEM photographs also did not differ before and after treatment (Figure 8). In this case, the rate for Reaction (4) evidently did not increase.

C. Powder Compaction

Filtering rate was dependent on particle size distribution. About three hours were required for unautoclaved and autoclaved TiO_2 (Sample II) to form a 4-mm thick filter compact from 15 ml of slurry when particles were not dispersed by ultrasonic probe. Unautoclaved TiO_2 (Sample I) and autoclaved TiO_2 (Sample II) dispersed by ultrasonic probe took 48 hours to form the same sized filter compact.

Filtered compacts made from hydrothermally treated powder had lustrous surfaces. They shrank greatly during drying ($\Delta L/L \simeq 24\%$), but did not crack. During sintering, they shrank homogeneously.

Compacts prepared from unautoclaved large-particle (0.3-0.8μm) amorphous TiO_2 (Sample II) shrank 18% during air drying. They did not have lustrous

surfaces, and sometimes disintegrated while drying. During firing, these compacts always disintegrated.

Compacts prepared from unautoclaved small-particle (0.1-0.2μm) amorphous TiO_2 (Sample I) shrank 32% during air drying, did not crack, showed surface luster like the autoclaved compacts, and sintered well.

D. Sintering

Autoclaved and air-dried powders differed greatly in shrinkage behavior, as shown in Figure 9. Autoclaved powder shrank 10% up to about 590°C, then shrank at a constant rate until 900°C. The rate then decreased until, above 1000°C, it again became nearly constant. Amorphous powder, on the other hand, shrank 10% up to 780°C; over 1000°C, shrinkage rate decreased abruptly.

Figure 10 shows the relationship between 1/T and $\Delta L/L$. The shrinkage behavior of amorphous powder proved to be strongly dependent on sintering temperature; shrinkage behavior of autoclaved powder, on the other hand, was not as dependent. Autoclaved powder's shrinkage was also independent of heating rate (10°-50°C/min), unlike amorphous powder.

Activation energy for a constant heating rate process can sometimes be determined by plotting the temperature required to achieve a specific relative shrinkage as a function of heating rate, for several different heating rates.[2] This procedure can be used only if the resulting line plots are significantly different, however; in this case, data for the three heating rates used fell along the same line (Figure 11), so activation energy could not be determined.

Table 4 summarizes results of the investigation on sintered bodies. Density measurement, X-ray diffraction, and SEM observations were made under various sintering conditions.

The sample heated to 900°C at 10°C/min and then cooled had no trace of rutile; it showed only well-crystallized anatase. An SEM micrograph shows that sintering was almost completed (Figure 12).

This sample's density was 3.78 g/cm^3 (97.2% theoretical density (TD)). Green density can be calculated by using the relation:

$$\frac{\rho}{\rho_{th}} = \frac{\rho_o}{\rho_{th}} \left(1 - \frac{\Delta L}{L_o}\right)^{-3}$$

Substituting $\frac{\Delta L}{L_o} = 0.200$ and $\frac{\rho}{\rho_{th}} = 0.972$, the value of $\frac{\rho_o}{\rho_{th}}$ can be calculated to show that the green density was 50% TD.

SEM micrographs show great differences between samples heated for half an hour above 1000°C and samples heated to below 1000°C, as is evident from a comparison of Figures 12 and 13. These differences correspond with the amount of rutile in the sintered bodies. By roughly assuming that X-ray diffraction peak heights indicate the amounts of anatase and rutile in a sample, the theoretical density can be calculated.

In the case of Sample A in Table 4, theoretical density was calculated to be 4.11 g/cm^3, a value extremely close to that actually measured, 4.10 g/cm^3. This result also corresponds closely to findings made by dilatometry: Near 900°C, shrinkage rate decreased. From this point to the next turning point (approximately 1050°C), total shrinkage (about 10%) can be attributed

to phase transition from anatase to rutile. Heating at 1000°C for an hour yielded a density close to theoretical; heating above 1000°C for more than an hour did not further increase density.

SEM micrographs show the effects of heating: After heating at 1000°C for an hour, grain growth began to occur in the compact's top surface, and small pores appeared in the fracture surface (Figures 14a and 14b). Heating to 1240°C at a rate of 10°C/min caused grain boundaries to become clearly apparent, and small pores were found to have joined in forming large pores in the fracture surface (Figures 15a and 15b).

When the filtered compact made from Run No. 4's slurry (Table 3) was subjected to isostatic pressure of 40,000 psi and sintered at 900°C after being heated at a rate of 10°C/min, total shrinkage during sintering decreased from 20.0% (without isostatic pressure) to 17.6%. This shows that the filtered compact's calculated green density was increased by isostatic pressure, from 50% to 55% TD. Even with isostatic pressure, however, filtered compacts made from unautoclaved TiO_2 (Sample II) disintegrated during sintering. Sintered body density also increased from 3.78 to 3.86 g/cm^3. X-ray diffraction showed that this compact never changed to rutile.

Much data is currently being published on the densities of rutile and anatase. The Handbook of Chemistry and Physics (Weast, 63rd edition, 1982-1983, pp. B222, 223) gives the theoretical (X-ray) densities of these crystals to be 4.2453 ± 0.0017 g/cm^3 for rutile and 3.893 ± 0.005 g/cm^3 for anatase. Using these data to recalculate ρ/ρ_{th}, it can be seen that applying isostatic pressure to the filtered compact of pure anatase increased the value of ρ/ρ_{th} from 97.2% to 99.2%.

IV. Conclusions

Hydrothermal treatment above 200°C converted amorphous TiO_2 particles to small anatase crystal aggregates. These were broken down into individual crystals (100-500Å) by ultrasonic dispersion. A 50% TD green body made from this slurry by filtration began to sinter at 600°C, reaching 97% TD of anatase at 900°C. The green body's density increased to 55% when isostatic pressure was applied, yielding a sintered body with a 99.2% TD (of pure anatase). This anatase sintered body completely changed to rutile and densified to 4.21 g/cm^3 after being heated one hour at 1000°C.

V. References

1. A. N. Lobachev, ed., Crystallization Processes Under Hydrothermal Conditions, p. 3, Consultant Bureau, NY, 1973.

2. E. A. Barringer, "The Synthesis, Interfacial Electrochemistry, Ordering, and Sintering of Monodisperse TiO_2 Powders," Vol. 2, pp. 198-200, doctoral thesis, Mass. Inst. of Tech., Cambridge, MA, 1983.

Table 1 Physical Properties of TiO_2 Synthesized from $Ti(OC_2H_5)_4$

Sample #	Crystal Form	Specific Surface Area (m^2/g)	Mean Diameter (micron)	Shape and Size Distribution
I	amorphous	198	0.26	equiaxed 0.1 - 0.2μm
II	amorphous	323	0.69	spheroidal 0.3 - 0.8μm

Table 2 Conditions for Continuous Flow Reaction in Synthesis of TiO_2 from $Ti(OC_2H_5)_4$

	$[H_2O]$ (M)	$[Ti(OC_2H_5)_4]$ (M)	Residence Time in Reactor (sec)
TiO_2 (I)	9.4	0.6	1.6
TiO_2 (II)	0.98	0.26	11.9

Table 3 Hydrothermal Treatment of Synthesized TiO_2

Run No.	1	2	3	4	5
Sample #	I	I	II	II	II
Hydrothermal treatment conditions					
Temperature (°C)	253	282	200	253	282
pH	10	10	10	10	10
Time (hr)	5	4	5	5	5
Resultant crystal form	anatase	anatase	anatase	anatase	anatase
Crystallite size (Å)	120	290	120	140	180
Surface area (m^2/g)	103	67	110	90	71
Particle size (Å)	150	230	140	170	220
Structure and particle size distribution (Å)	100 to 500	100 to 500	100* to 500	100* to 500	100* to 500

* Crystals coagulated to 0.3 - 0.5μm (300-500Å) particles.

Crystallite size calculated by X-ray diffraction line broadening.

Particle size calculated by specific surface area.

Table 4 Density and X-Ray Diffraction (XD) Analyses of Sintered Bodies under Various Sintering Conditions

Sintered Sample*	Condition: Heating Rate (°C/min)	Condition: Final Temp(°C)	Condition: Holding Time (hr)	Density (g/cm^3)	XD Rutile:Anatase
A	3	1000	0.5	4.10	68:32
B	3	1000	1.0	4.21	92:8
C	3	1060	2.0	4.21	100:0
D	10	900	0	3.78	0:100
E	10	1240	0	4.22	100:0
F	10	900	0	3.86	0:100
G	3	1000	0.5	4.01	
H	10	1240	0	4.19	

* Sample type:

A-F - autoclaved powder

G-H - amorphous powder

F - subjected to 40,000 psi

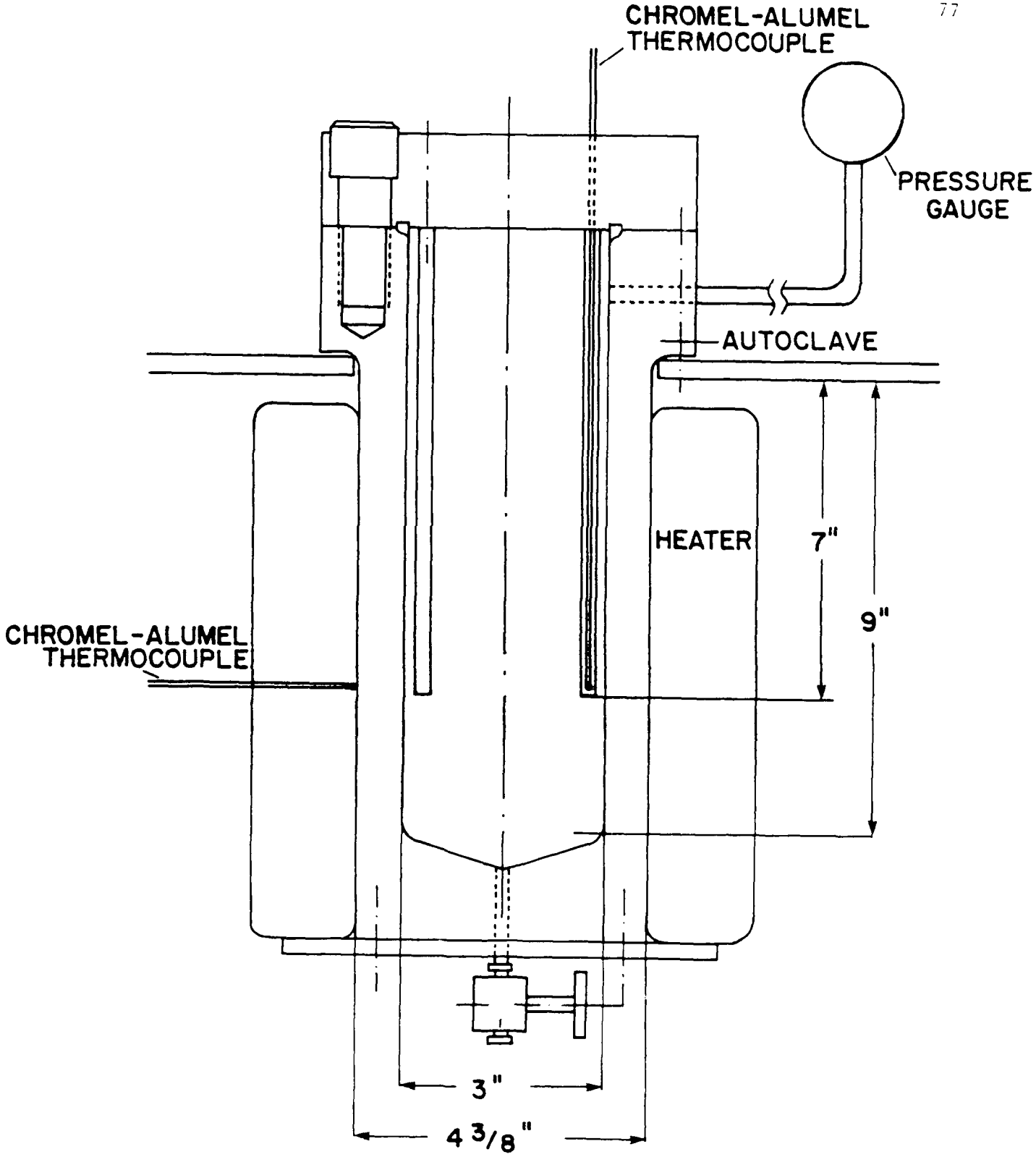

Figure 1. 1-liter autoclave.

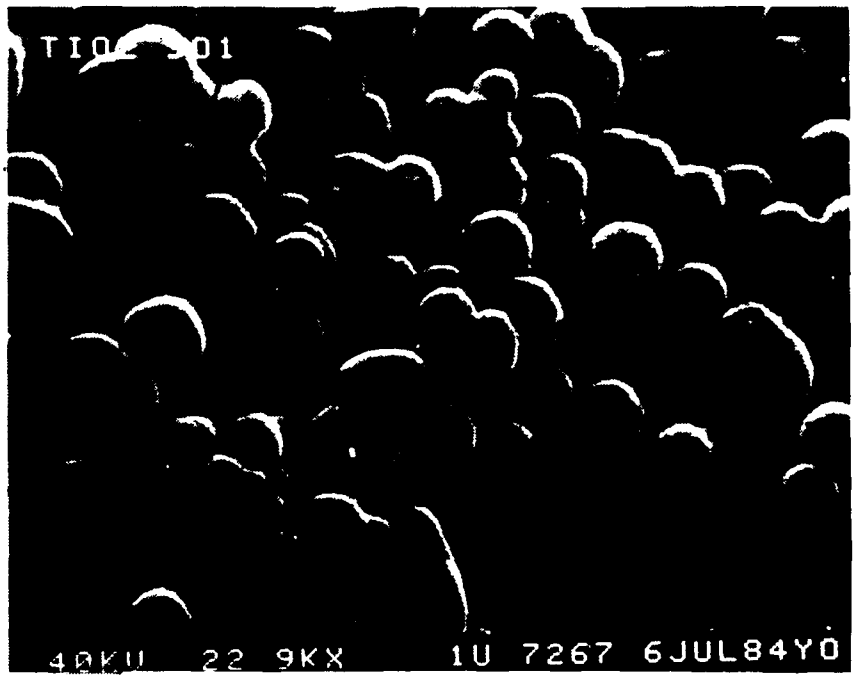

Figure 2. Scanning electron micrograph of TiO_2 (Sample II) powder.

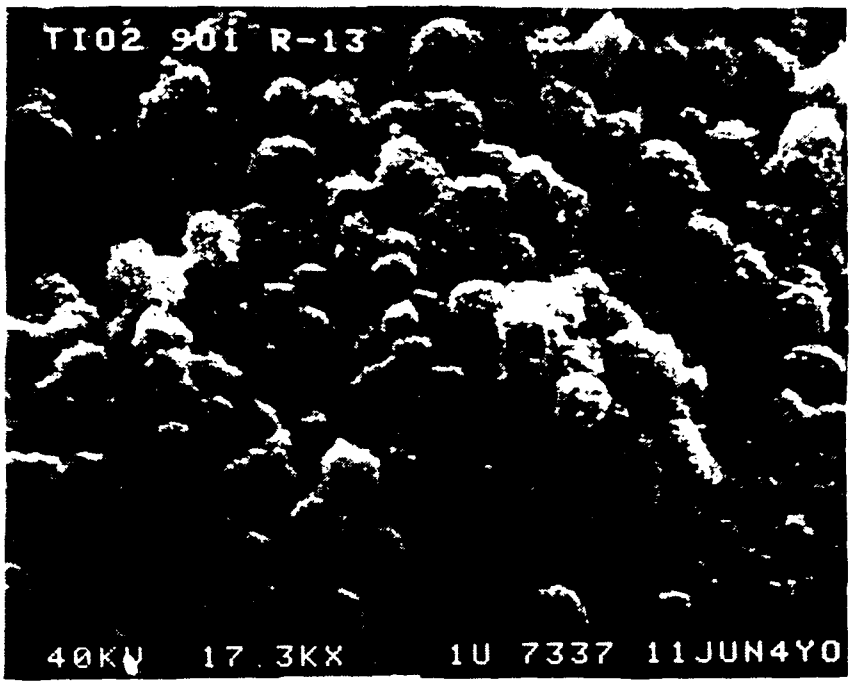

(A)

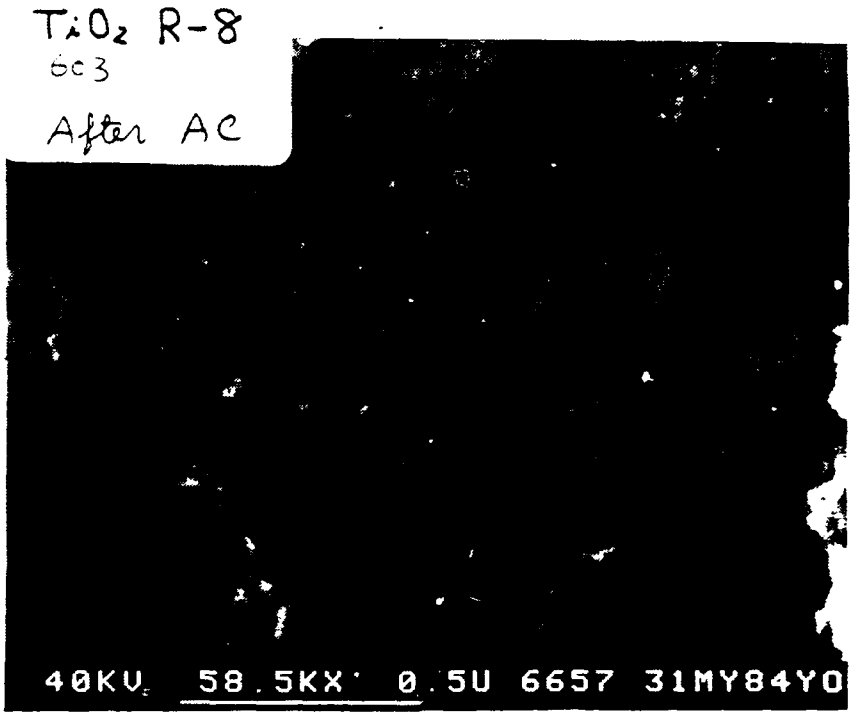

(B)

Figure 1. Scanning electron micrograph of TiO_2 (Sample II) powder after autoclaving (250°C for 5 hr) at magnifications of (a) 17500X, (b) 58500X

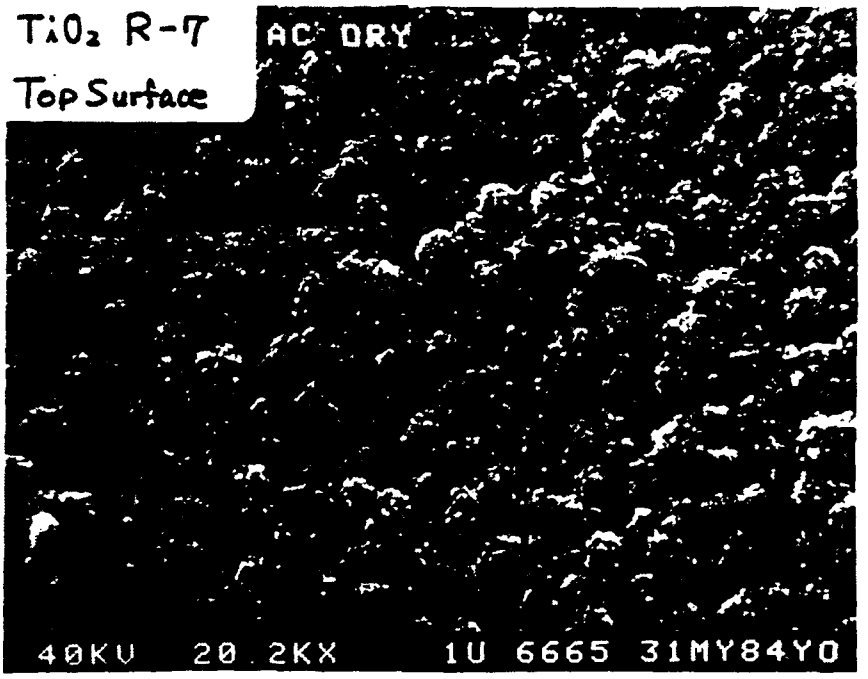

Figure 4. Scanning electron micrograph of the top surface of a filtered compact formed from an autoclaved slurry that was not treated ultrasonically.

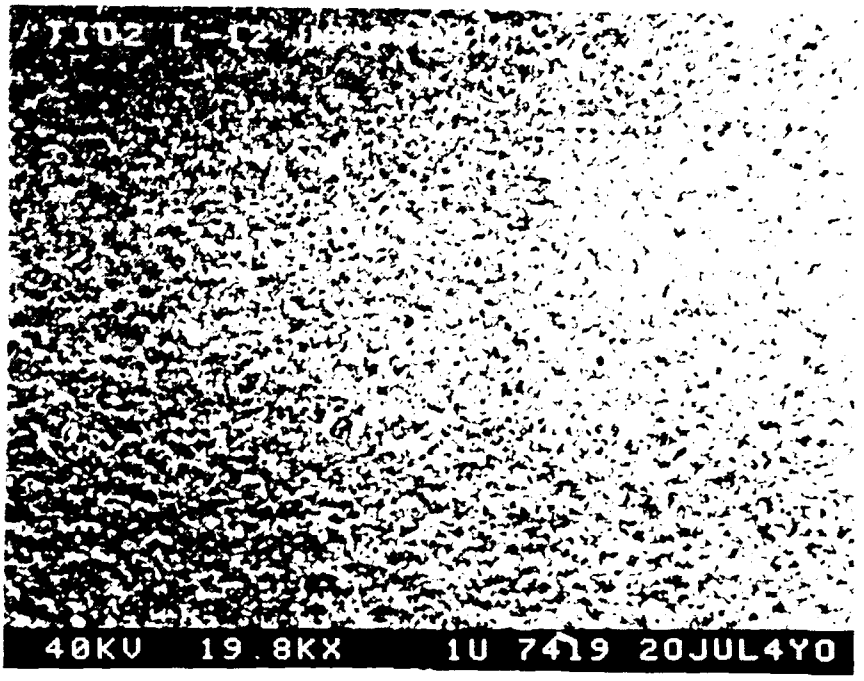

Figure 5. Scanning electron micrograph of the top surface of a filtered compact formed from an autoclaved slurry that was treated ultrasonically.

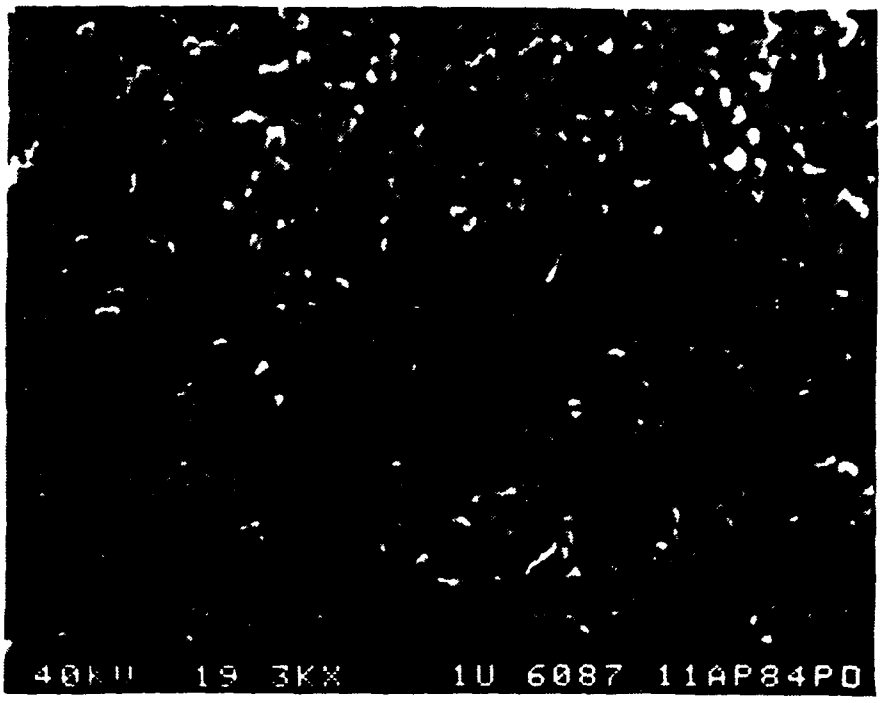

Figure 6. Scanning electron micrograph of TiO_2 (Sample I) powder.

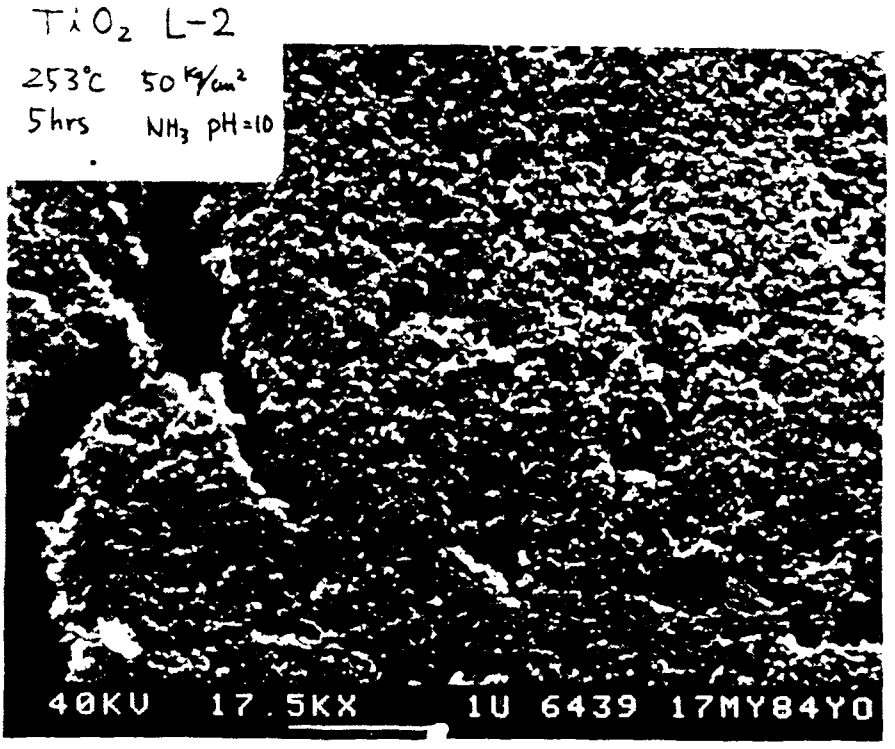

Figure 7. Scanning electron micrograph of TiO_2 (Sample I) powder after autoclaving.

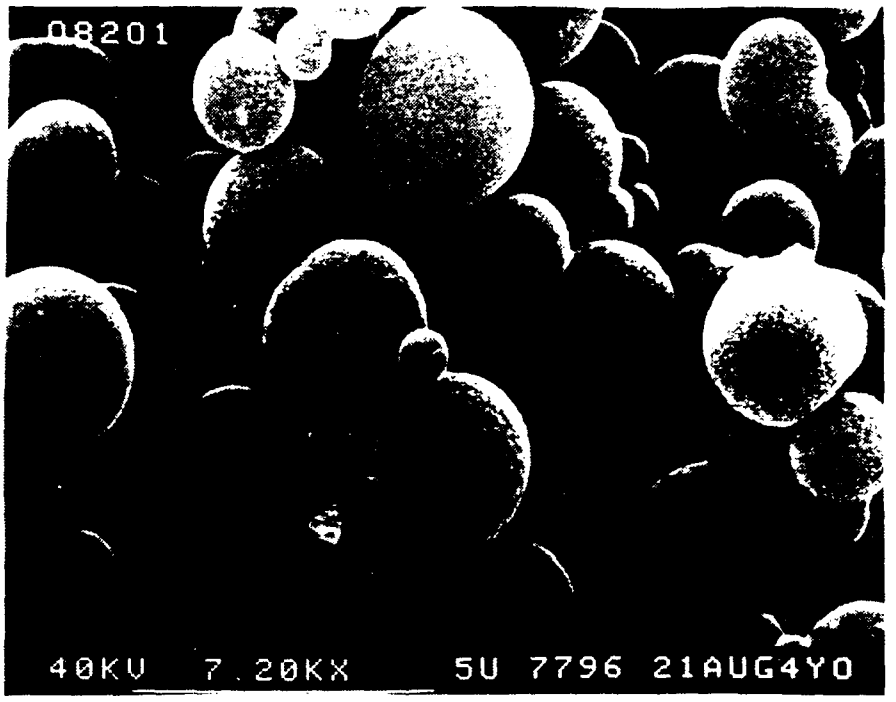

Figure 8. Scanning electron micrograph of TiO_2 washed with ethanol and heated in ethanol at 200°C for 5 hr.

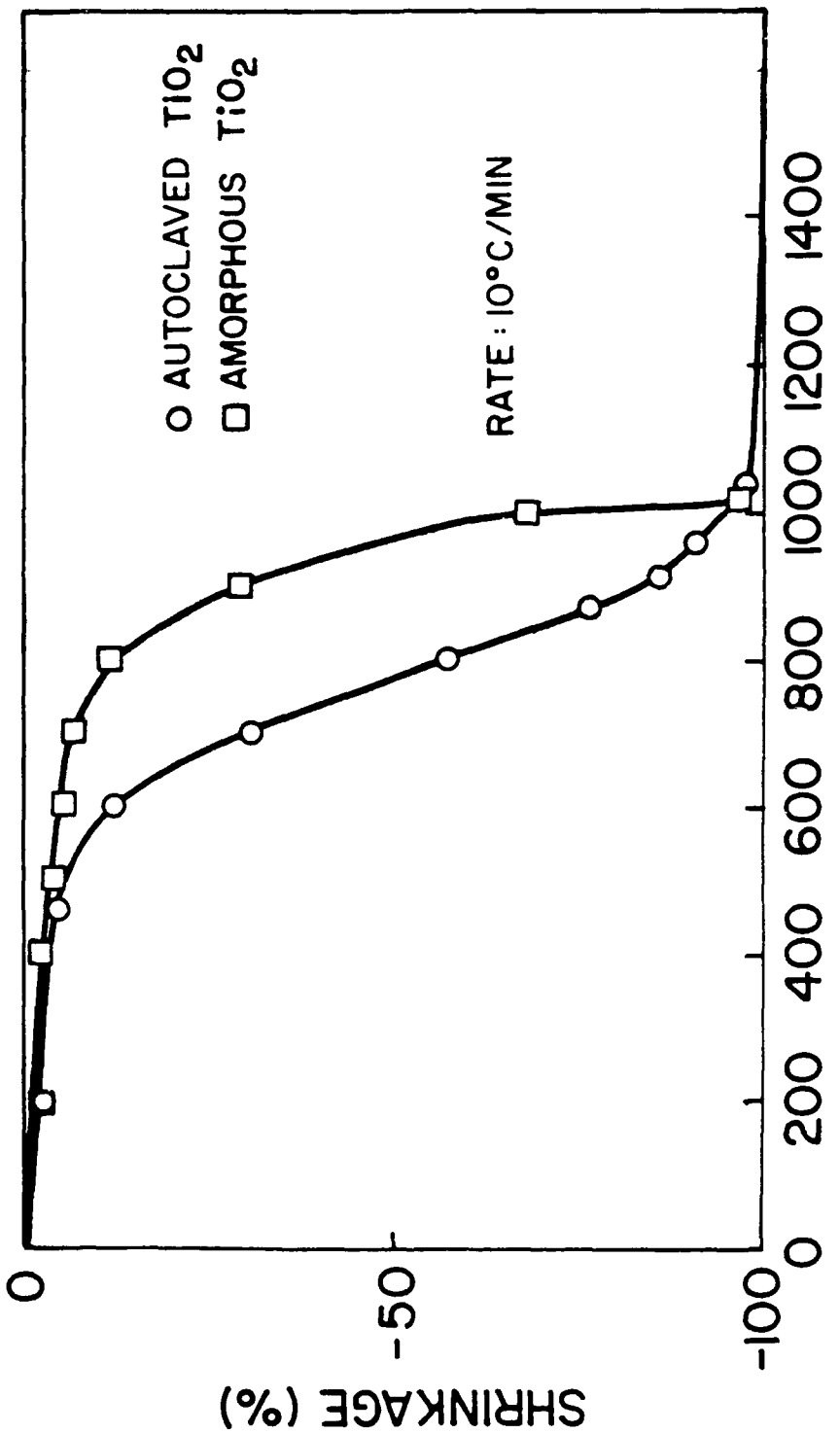

Figure 9. Normalized shrinkage as a function of temperature for constant heating rate.

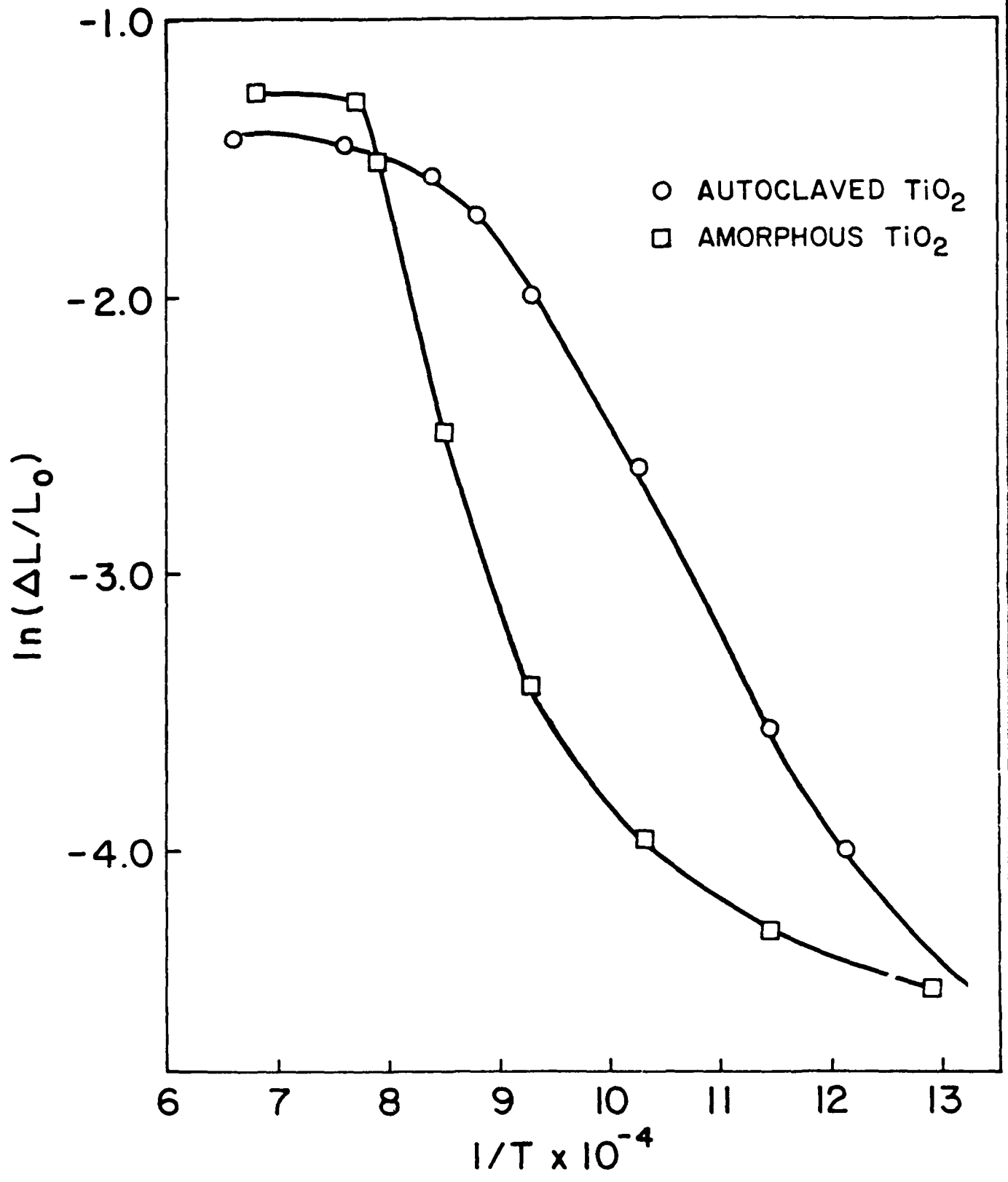

Figure 10. Relative shrinkage as a function of inverse temperature.

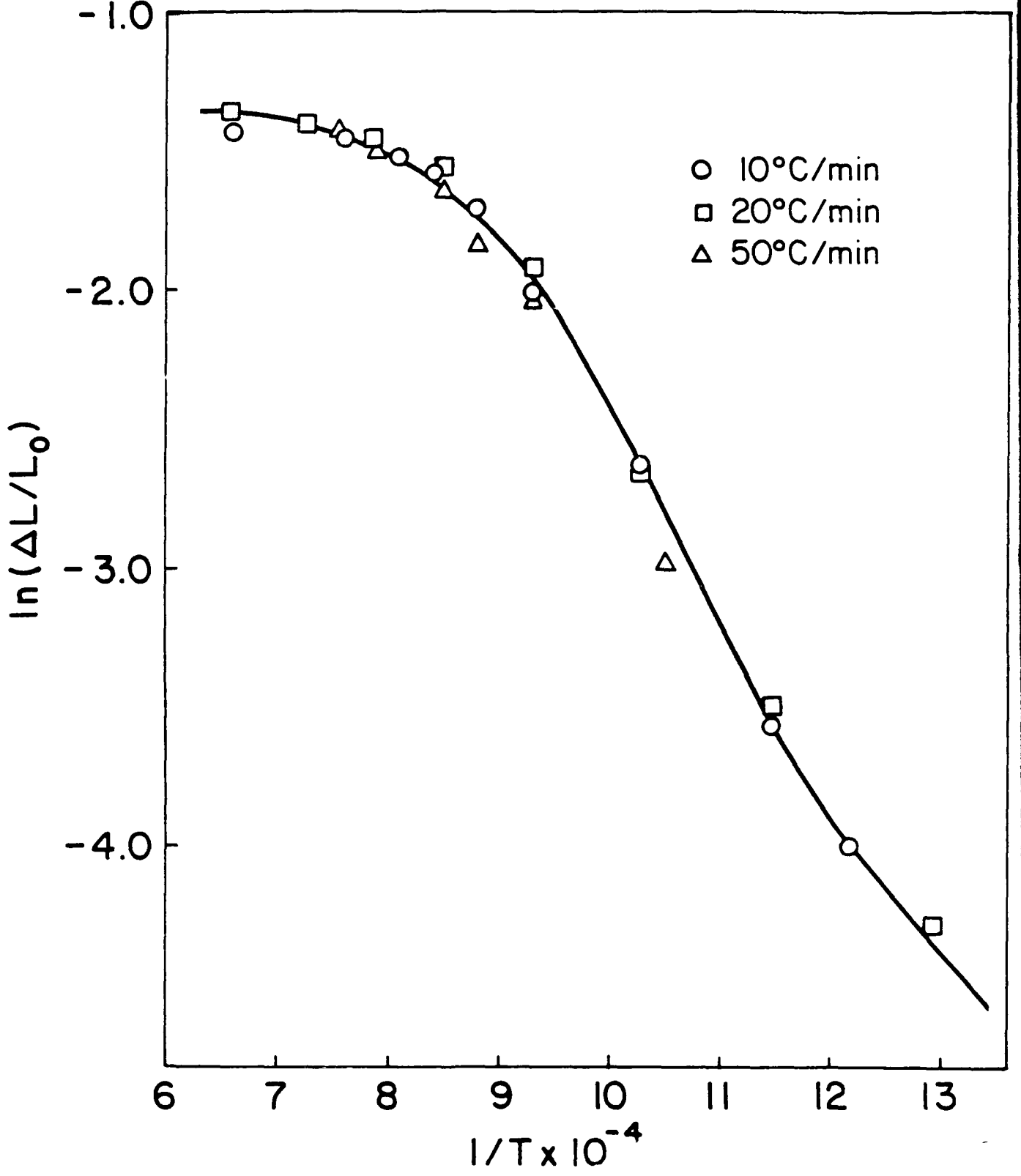

Figure 11. Relative shrinkage ($\Delta l/L_o$) as a function of inverse temperature for constant heating rates of 10°, 20°, and 50°C/min.

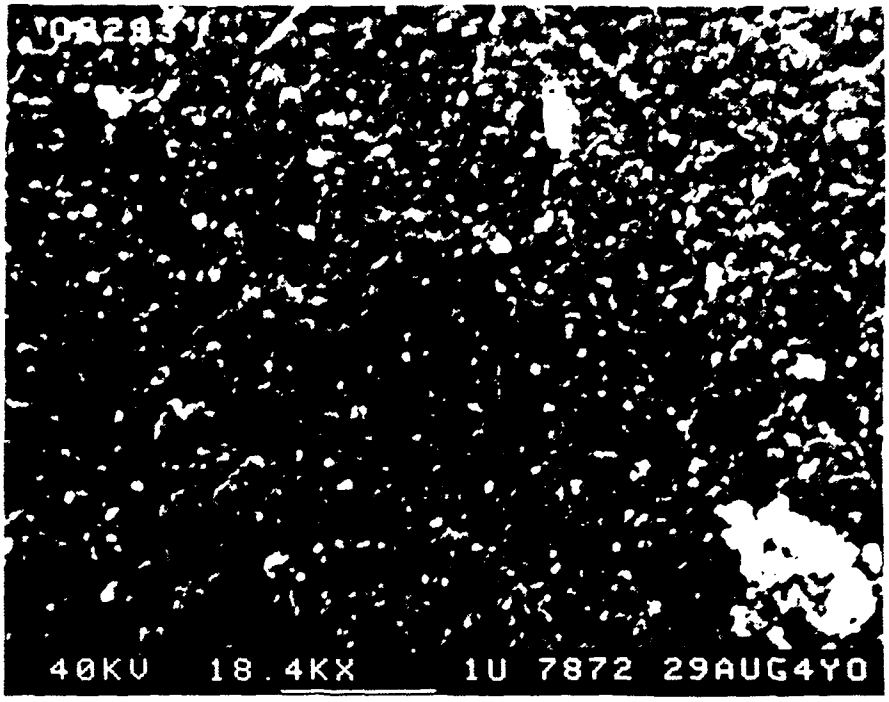

(A)

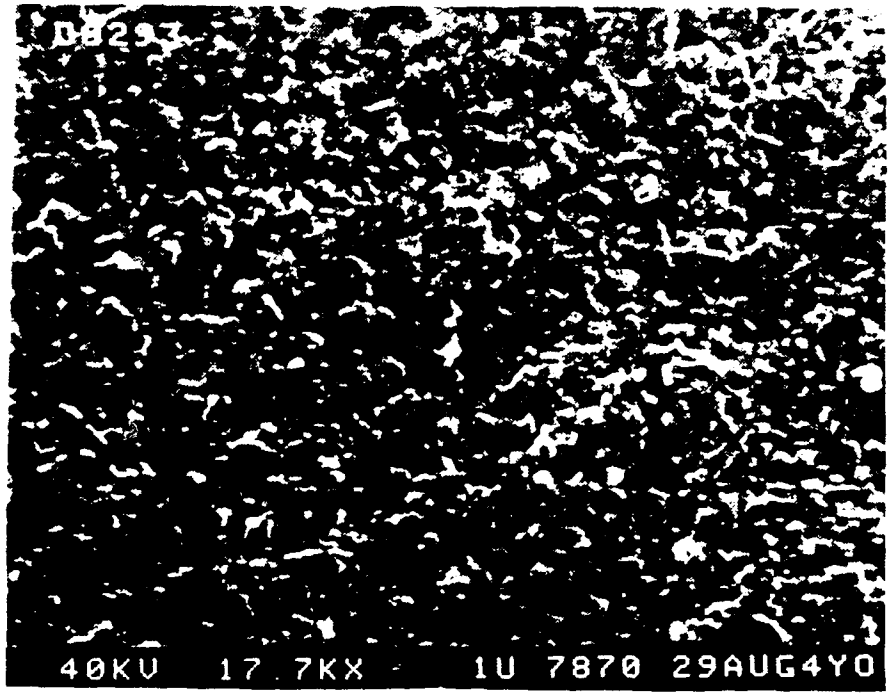

(B)

Figure 12. Microstructure of compact's a) outer surface, and b) fracture surface after heating at a rate of 10°C/min to 900°C. X-ray diffraction showed crystal form to be anatase.

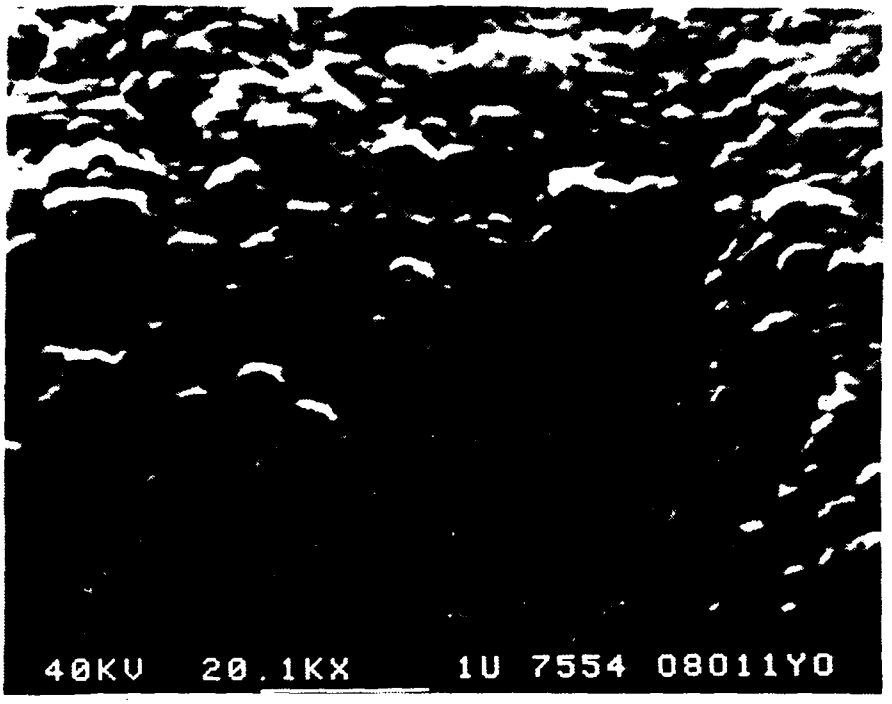

(A)

(B)

Figure 13. Microstructure of compact's a) outer surface, and b) fracture surface after heating at a rate of 3°C/min to 1000°C and maintenance at that temperature 0.5 hr. X-ray diffraction showed the crystal form to be a mixture of rutile and anatase.

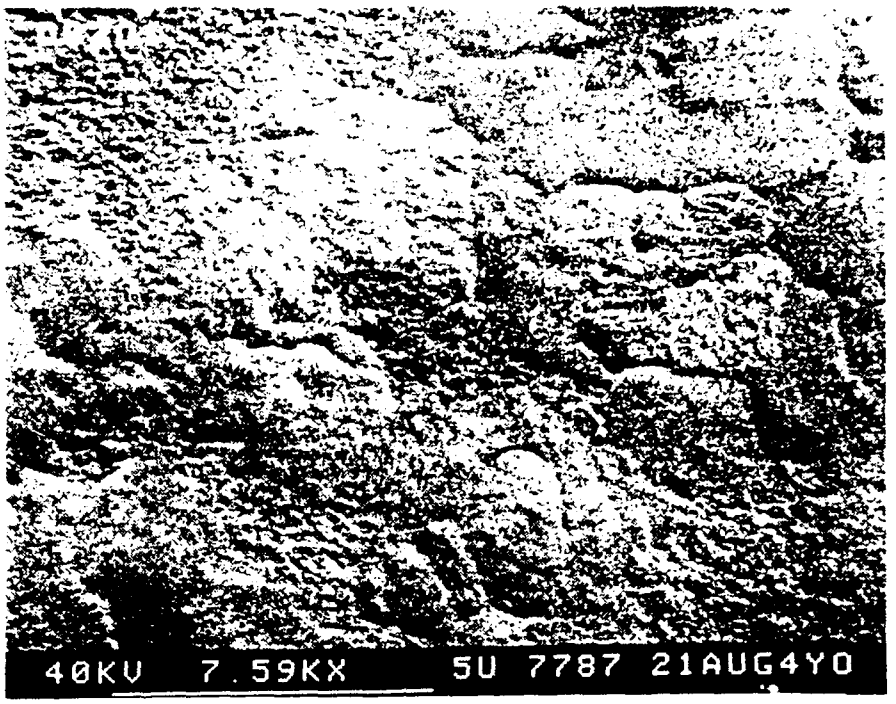

(A)

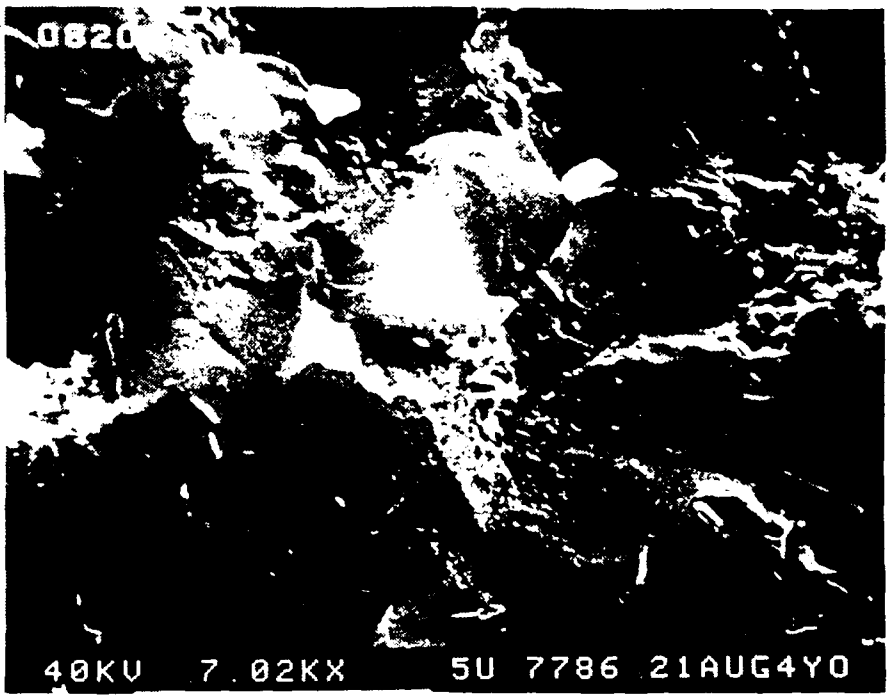

(B)

Figure 14. Microstructure of compact's a) outer surface, and b) fracture surface after heating at a rate of 3°C/min to 1000°C and maintenance at that temperature 1.0 hr.

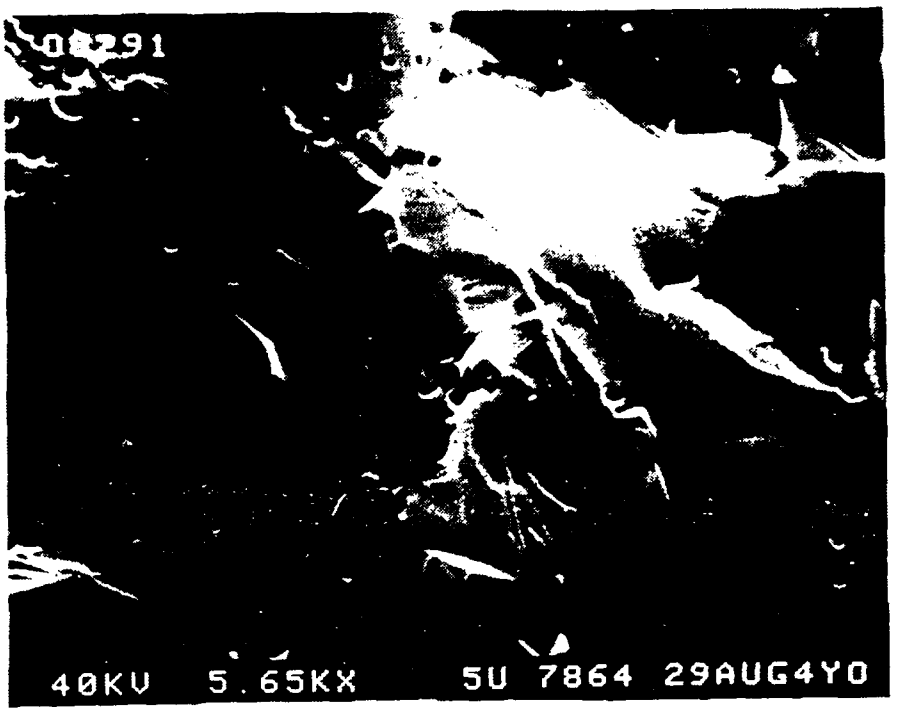

(A)

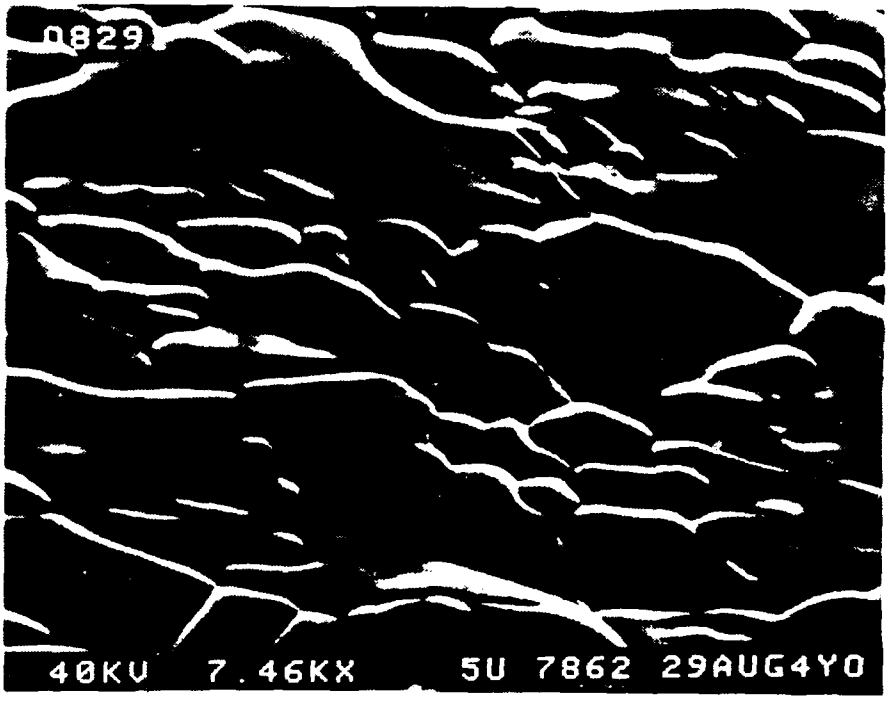

(B)

Figure 15. Microstructure of compact's a) outer surface, and b) fracture surface after heating at a rate of 10°C/min to 1240°C.

William Moffatt

PREPARATION OF $ZrO_2 \cdot Al_2O_3$ COMPOSITE POWDERS AND CONSOLIDATION OF CERAMIC POWDERS

I. Introduction

This report describes progress made in 1) producing alumina-zirconia composite powders, important for their strength and toughness, and 2) consolidating ceramic powders in general, and alumina powders specifically.

A colloid press was designed for powder consolidation in both studies, based on the concept that powder particles dispersed in a liquid solvent experience substantial repulsive forces due to coulombic or steric particle-particle interactions. Fegley and Barringer (1984) had already demonstrated that these forces can be used to create dense green bodies.[1] The colloid press as designed (Figure 1) is intended for use at 6000 psi, a pressure sufficient to cause direct interparticle contact and allow consolidation of concentrated powder slurries.

Experimentation showed that covering the press's porous metal frits with fine filter paper allowed simultaneous powder particle retention and water expulsion when sample was under load. Dissipation of pore pressure (load carried by water in the slurry) increased the powder-powder interaction forces. Hertzian contact between powder particles gives rise to local forces great enough to exceed the ~50,000 psi stress required to expel the last water layer from between particles. The porous metal frits were generally blown free of water with low-pressure nitrogen to prevent water from being drawn back into the specimen upon pressure release.

A second press has also been constructed, similar to the first in concept and design. This press has a rectangular cross-section, however, that is better able to produce modulus of rupture (mechanical test) specimens: because the samples produced are long and thin, less material is wasted. Preliminary tests have already been made with this press, which will be used more extensively as the focus of this project shifts to mechanical properties testing.

II. Experimental Procedure

A. $ZrO_2 \cdot Al_2O_3$

1. Introduction

One segment of this study involved the production, characterization, and consolidation of zirconia-alumina composite powders. These consist of particles having alumina cores and zirconia coatings. Sintered bodies based on such powders are expected to be more homogeneous than those based on milled powder mixtures.

Composite powders have been produced in the past by controlled hydrolysis of zirconium alkoxide molecules on colloidal alumina particle surfaces.[2] Most experiments have been performed in "batch" mode, in which dilute solutions of reactants are prepared, mixed in a large container, and allowed to react with stirring.

More specifically, a heated suspension of alumina in an ethanol/zirconium tetra-n-propoxide solution is reacted with a heated hyperstoichiometric water/ethanol solution. No foreseeable laboratory scaleup of this process is likely to provide the quantities of powder required for production of mechanical test specimens. This technique is,

however, well suited to producing the small powder quantities required for scientific studies.

Transmission electron microscopy (TEM) of these alumina-zirconia composite powders clearly shows a zirconia surface coating tightly adhering to the alumina particles. TEM also suggests that the surface layer is not monolithic. This has been confirmed by White's and Weisenberg's surface area determinations (Figure 2), which show a surface area rapidly increasing with increasing weight fraction of zirconia. The surface area/unit mass would be expected to decrease with increasing weight fraction of zirconia if the coating were impervious to gas. Actual observations are consistent only with a porous, convoluted zirconia layer.

Novich's continuous flow reaction method (described in his section of this report) eliminates some problems with the batch method:

- Since mixing is rapid in the high shear rate reactor* used, higher reactant concentrations may be used than with the batch method, yielding higher product concentrations in the output stream.
- Since the process is continuous, the total amount of powder produced in a run is limited only by reactant availability and the investigator's patience.

2. Procedure

Initial attempts in this study to produce alumina-zirconia composites using the continuous flow process had the alumina, zirconium alkoxide, and water streams meeting just before injection into the reactor. Powder

---

* Chemineer Kenics Model 3/4 KFC 6 Mixer; Cole Palmer Model 7520-20 peristaltic pumps

produced this way was not satisfactory, however, since it consisted of isolated alumina particles and zirconia clumps (Figure 3). This is probably because zirconium alkoxide molecules reacted with water before they were able to diffuse to alumina particle surfaces.

Further experiments, in which a premixed alumina/zirconium alkoxide stream was injected into the reactor along with a water/ethanol solution, gave far better results, with zirconia bonded to alumina particles (Figure 4). In these experiments, the alumina/alkoxide/ethanol solution was kept under constant stirring (magnetic stirrer) as it was being withdrawn for reaction.

As shown in Table 1, each starting slurry's alkoxide concentration was the same, as was the concentration of water with which it was reacted. Different zirconia weight fractions were targeted by changing the slurry's alumina concentration. Alkoxide hydrolysis would thus be expected to occur under almost identical conditions in each slurry.

After each synthesis, the slurry was centrifuged down* (3000 RPM, 0.5 hr) and the supernatant poured off. Powder was then washed, once in ethanol and once in deionized water (both washing procedures including high-power ultrasonic agitation and centrifugation), and finally redispersed in deionized water.

3. Results

Alumina-zirconia composites with nominally 4, 8, 12, and 16 weight percent zirconia were produced in the continuous flow reactor, using a

---

* IEC DPR-6000 centrifuge

premixed alumina/zirconium alkoxide stream reacting with a water/ethanol solution. Proton activation analysis of the nominally 8 and 16 weight percent composites gave actual values of 7.1% and 9.1%, respectively. Similarly, the BET surface area/unit mass leveled off at about 8 weight percent zirconia (Figure 5).

Alumina-zirconia composites had low green densities upon consolidation, and tended to crack on drying. (Similarly, alkoxide-derived titania powder compacts disintegrated during drying. All results of attempts to consolidate alkoxide-derived powders in the colloid press varied, at first, from mediocre to poor). Alumina-zirconia green bodies also became substantially distorted during sintering.

Autoclaving alumina-zirconia composite powders significantly increased compact green density and largely eliminated sintering problems. Comparison of Figure 6, a TEM of an autoclaved alumina-zirconia composite material, with Figure 4, a TEM of the same material before autoclaving, shows that autoclaving results in a better-defined, more closely adhering zirconia layer. This is consistent with the property improvements just mentioned.

4. Conclusions

This experiment's observations suggest a conceptually sound picture of a composite formation prccess based on liquid phase adsorption. Whereas separate alumina, zirconium alkoxide, and water streams had produced only isolated alumina particles and zirconia clumps, the premixed alumina/zirconium alkoxide stream reacting with a water/ethanol solution yielded zirconia bonded to alumina particles, as was hoped. It therefore seems necessary to allow the alkoxide sufficient time to adsorb onto and,

perhaps, chemically bind to the alumina substrate, if a composite powder is to be formed.

Other evidence supports this. Ethanol/alumina slurries are stabilized to an extraordinary degree by adding zirconium tetra-n-propoxide, decreasing the settling rate by more than two orders of magnitude, in some cases. This seems consistent with the notion that alkoxide molecules are adsorbed onto alumina particle surfaces, sterically stabilizing them.

The proton activation analysis and BET results suggest that an adsorption isotherm for zirconium tetra-n-propoxide may exist, and that unadsorbed alkoxide forms, on hydrolysis, very fine zirconia particles that are lost in powder washing.

B. Al_2O_3 Consolidation

1. Introduction

A second segment of this work systematically studied the influence of slurry characteristics on alumina consolidation in the colloid press. This study was done to better understand the physical processes that lead to dense green bodies.

2. Procedure

Powder consolidation tests were performed on XA139SG alumina (Alcoa) under a variety of slurry conditions:

- pH levels of 3, 7, and 11 were used to ascertain the effect on powder consolidation of varying surface charge levels. Slurries were made acid or basic, as required, with concentrated HNO_3 and NH_4OH, respectively.

- Half of the tests were performed with 3 weight % Darvan-C, a polymethacrylic acid dispersant, and half without, to determine the effect of steric stabilization on green density.
- Half of each specimen type was air dried to prevent cracking, which sometimes occurs during oven drying.

In each case, slurry components (1 gram Al_2O_3/ml deionized H_2O, and, in half the cases, 3 weight % (based on alumina weight) Darvan-C) were mixed using high-power ultrasonic agitation to ensure a good dispersion. The dispersion was then centrifuged, the supernatant poured off, and the remaining paste used as the basis for consolidation tests.

Auxiliary experiments were also performed on the use of:

1. binders to strengthen green bodies, and
2. high pressure gas to blow water out of specimens under load. It was hoped that this technique would allow drying in situ of very fine particle (<0.1μm) compacts, preventing the compact disintegration observed when drying is done under room pressure.

3. Results

Relative green densities ($\rho_{actual}/\rho_{Al_2O_3}$) found from the powder consolidation experiments are shown in Table 2. As green densities of both air-dried and oven-dried specimens were usually equal to within a 1% error range in these calculations, averages of air- and oven-dried sample values are given.

While Darvan-C produced very fluid and stable suspensions, consolidated specimens made from these did not have the highest green densities. Under basic or neutral conditions (i.e., near alumina's isoelectric point), the

dispersant seemed to have little effect on experimental results. Under acidic conditions, slurries containing Darvan-C behaved far more poorly than slurries containing acid alone. This is most likely the result of 1) acid neutralization of charged groups on the dispersant chain, diminishing steric stabilization, and 2) the high viscosity of the polymer-containing water, diminishing particle rearrangement rate.

Binders were found to strengthen compacts, but blowing gas through specimens under load resulted in no significant improvement.

4. Conclusions

Conclusions drawn from the powder consolidation experiments are that:

1. pH conditions far from the isoelectric point are best for slurry consolidation,
2. dispersant worsens the situation rather than improves it, and
3. binders can be used to strengthen powder compacts, but blowing gas through specimens under load does not help.

Because adsorption phenomena were shown to be so significant in ZrO_2/Al_2O_3 composite powder formation, the use of steric stabilizers in centrifugal separation of alumina powder particles into size classifications has been abandoned, as these dispersants are difficult to displace during later processing. Powder dispersions are now stabilized coulombically by acidifying slurries with nitric acid before particle separation into size classifications.

III. Future Work

The sintering of fine, narrow size distribution ceramic powders in general is of great scientific and technological interest. The sintering behavior of alumina powder in the ~.2-.3μm particle range is currently being investigated at MIT. Size-classified alumina powder will be used as the basis for synthesizing narrow size distribution alumina-zirconia composite powders. These powders' sintering behavior will then be determined, and their composition and thermal treatment adjusted to optimize their strength and toughness.

IV. References

1. B. Fegley, E. A. Barringer, "Synthesis, Characterization, and Processing of Monosized Ceramic Powders," paper presented at Materials Research Society, Albuquerque, NM, 1984.

2. E. A. Barringer, "The Synthesis, Interfacial Electrochemistry, Ordering, and Sintering of Monodisperse TiO_2 Powders," Ph.D. thesis, Mass. Inst. of Tech., Cambridge, MA, 1983.

Table 1. Reactant Stream Concentrations and Reactor Conditions for Alumina-Zirconia Composite Manufacture*

Stream #	Composition	Flow Rate
1	26.8 M solution H_2O in ethanol	56 cm^3/min
2	ethanol-based slurry: 0.0519 M zirconium tetra-n-propoxide and either 1.57 M, 0.785 M, 0.523 M, or 0.392 M alumina Final reactant concentrations in mixer: $[H_2O]$ = 13.8 M [alkoxide] = 0.0252 M $[Al_2O_3]$ = 0.762 M, 0.381 M, 0.254 M, or 0.191 M	53 cm^3/min

* All experiments performed at room temperature.

Table 2. Relative Green Densities (± ~ 1%) of Alumina Samples Consolidated in the Colloid Press

pH of Slurry	Dispersant	Relative Green Density
3	none	67.4%
7	none	56.0%
11	none	60.1%
3	3 wt% Darvan-C	54.0%
7	3 wt% Darvan-C	58.9%
11	3 wt% Darvan-C	60.1%

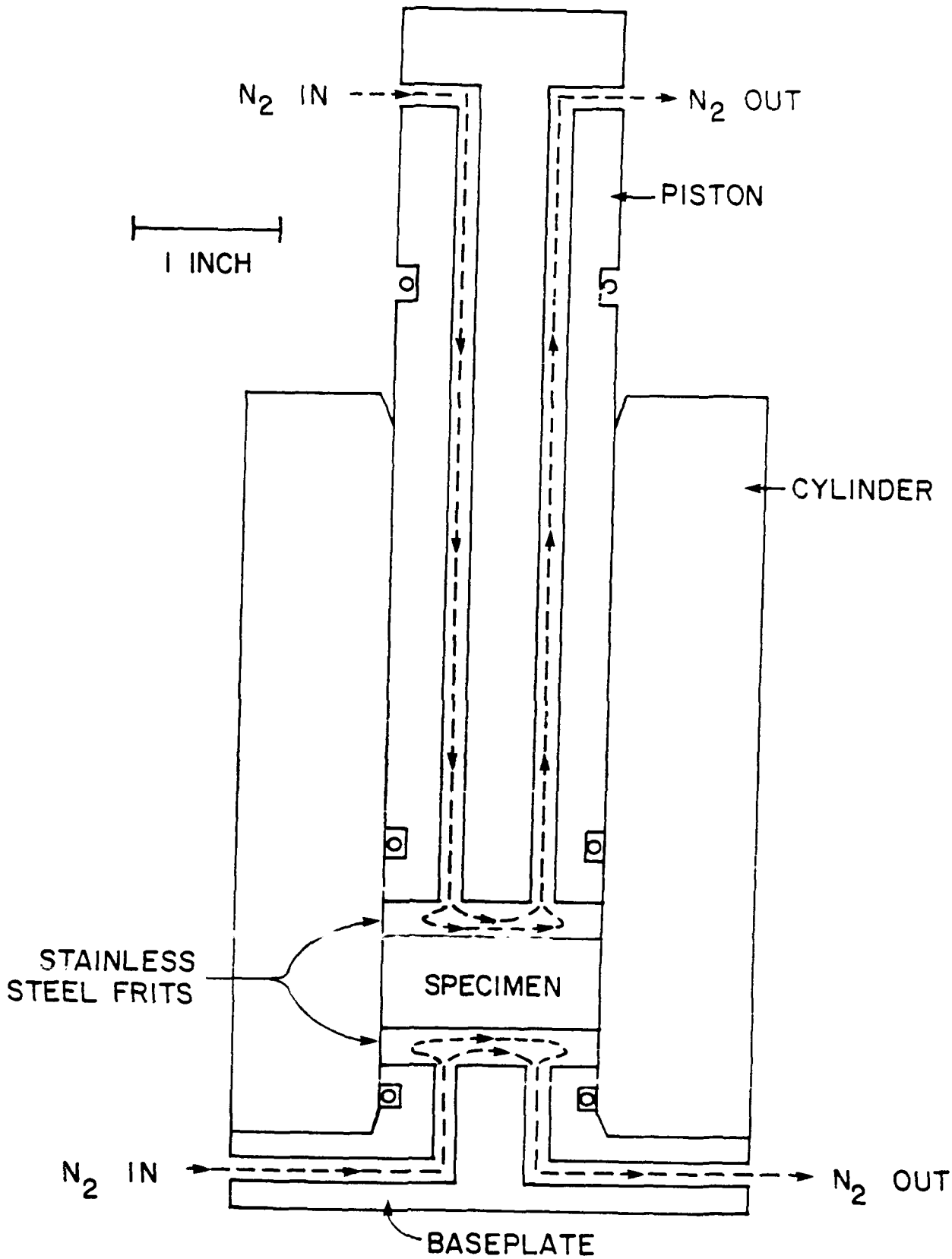

Figure 1. Cross-section of brass colloid press.

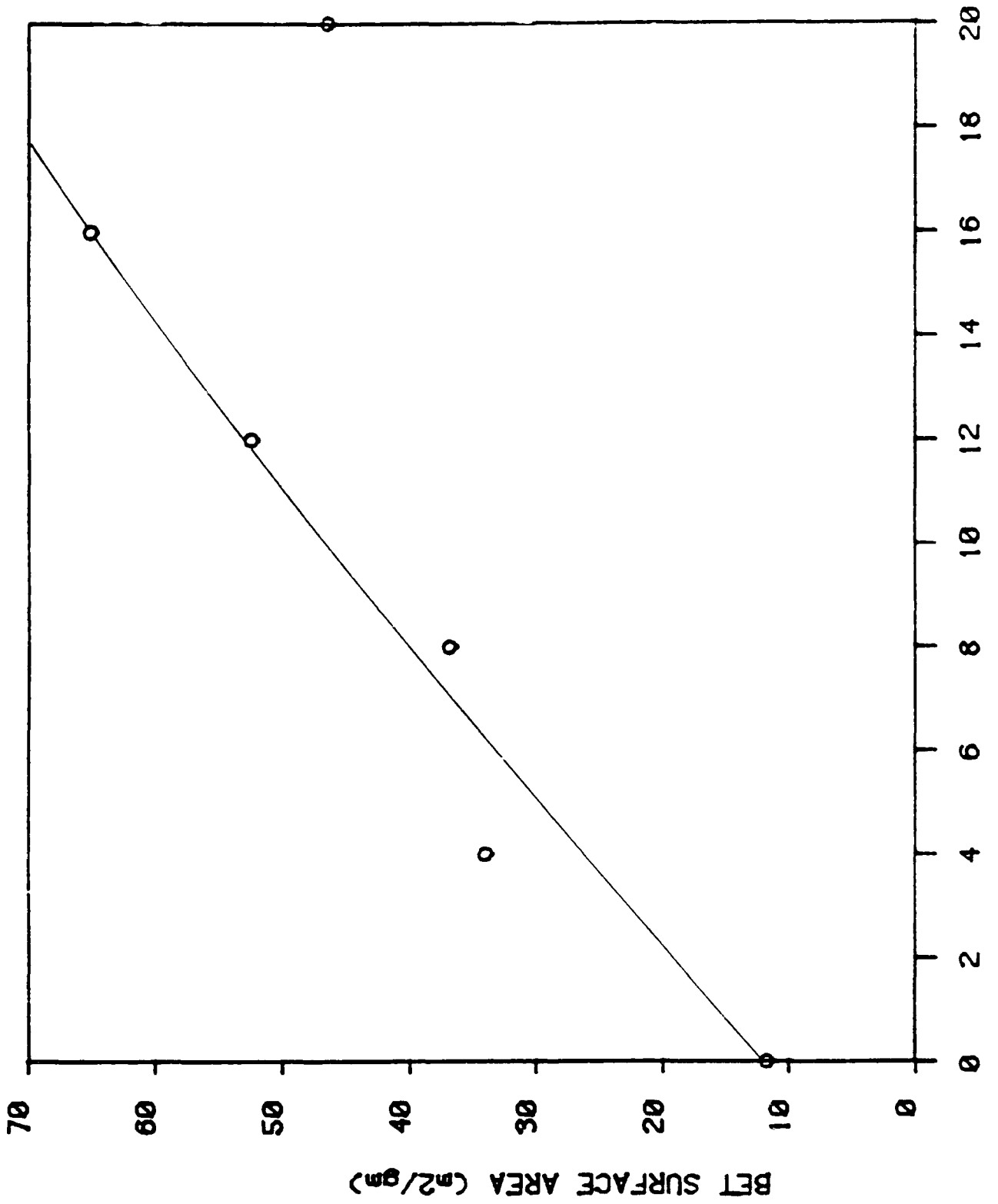

Figure 2. Bet specific surface area vs. nominal weight percent zirconia for zirconia-alumina composites (unpublished results of Matsoukas)

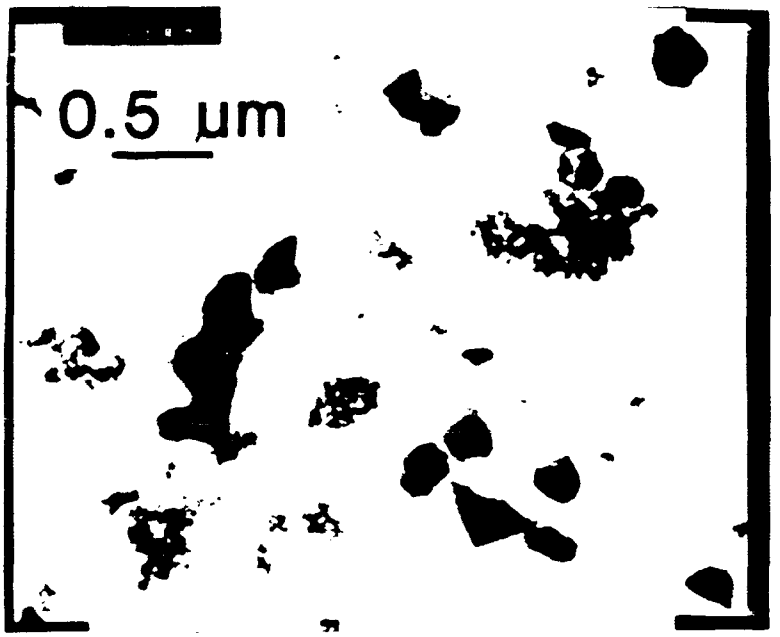

Figure 3. Zirconia-alumina composite synthesized with no reactant premixing.

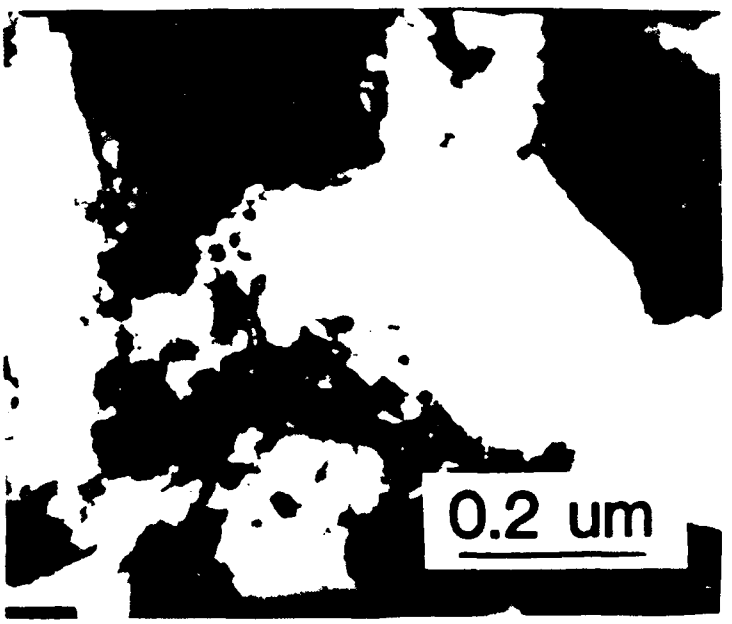

Figure 4. Zirconia-alumina composite synthesized with alumina and zirconium alkoxide premixed.

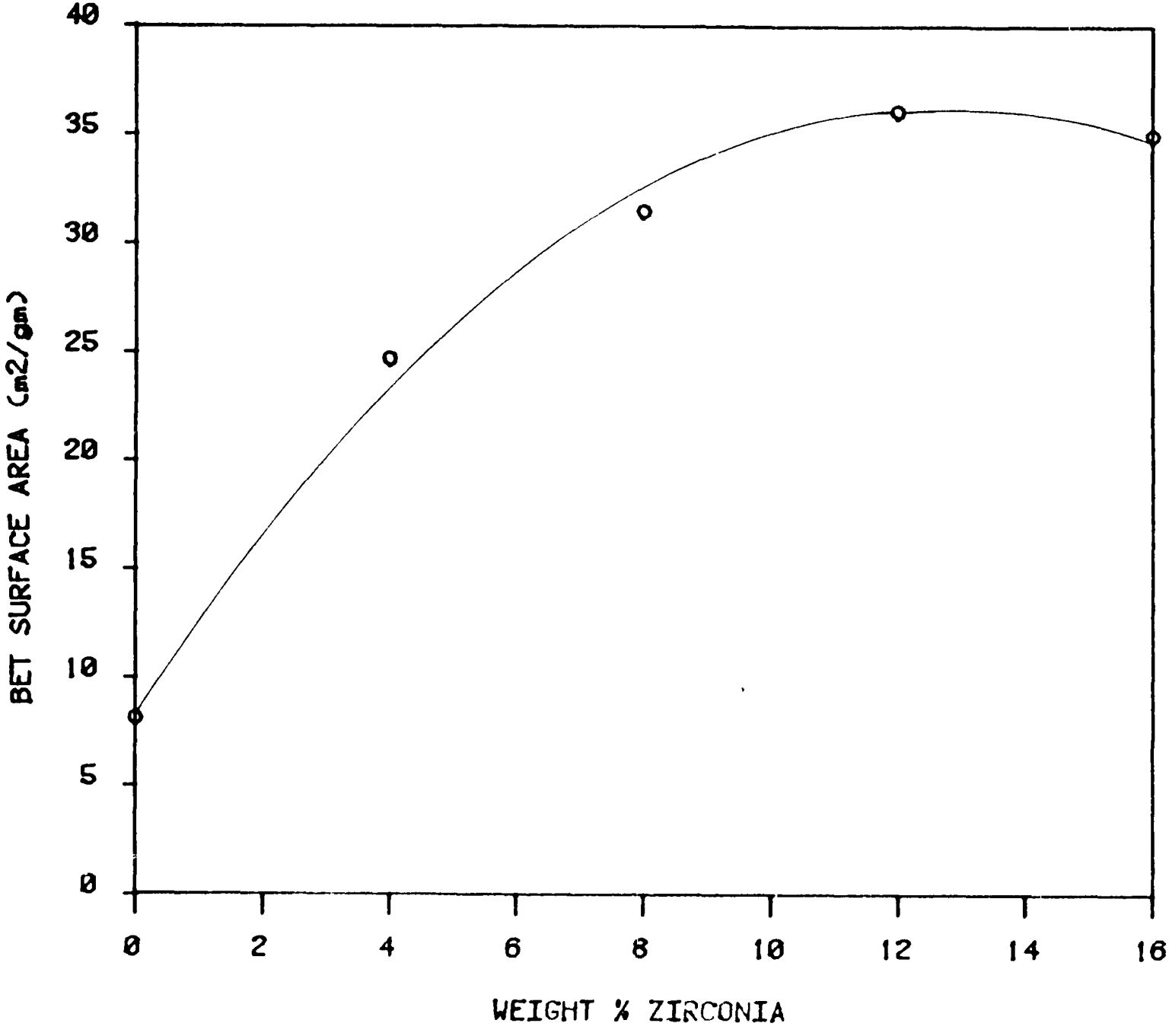

Figure 5. BET specific surface area vs. nominal weight percent zirconia for zirconia-alumina composites made in continuous flow reactor (unpublished results of Human)

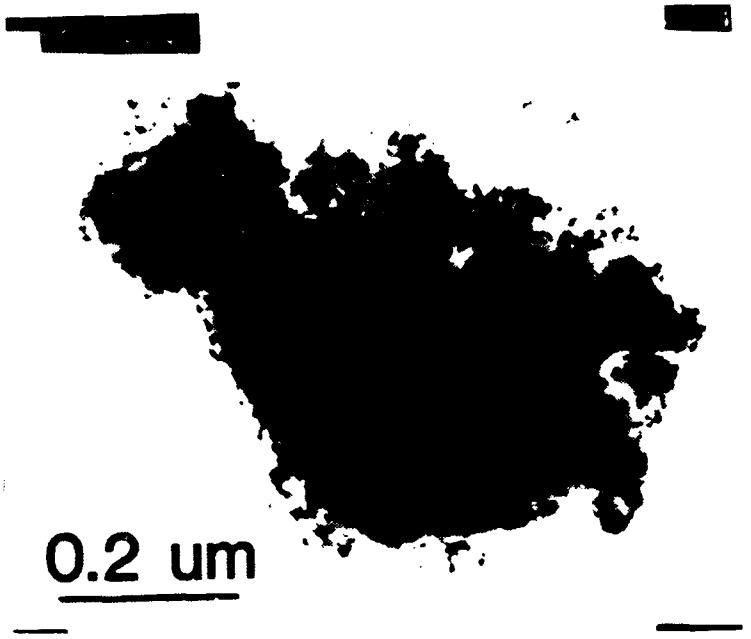

Figure 6. Zirconia-alumina composite synthesized with alumina and zirconium alkoxide premixed. Powder autoclaved for 4 hours at 250°C after synthesis.

Christine Sobon

SYNTHESIS OF SOLUBLE ALKOXIDES

I. Introduction

Synthesis of soluble alkoxide precursors to metal oxides is an important first step in ceramic powder formation. Soluble alkoxides provide a foundation for oxide materials like stabilized zirconia, important in high-strength applications.

Previous work[1] indicates that metal oxides of desired shape and size can be formed by controlled hydrolysis of dilute alkoxide and water solutions in alcohol. This process requires alkoxides that are soluble in alcohol. Unfortunately, a number of metal alkoxide precursors are alcohol-insoluble, making it necessary to find different compounds. Adding a second metal o a metal alkoxide results in a covalently-bonded species possessing unique solubility characteristics that can be utilized in hydrolysis reactions.

One example of a double metal alkoxide, calcium aluminum ethoxide, was reported by Govil and Mehrotra.[2] Experimentation done for the current study shows that this compound, cohydrolyzed with zirconium tetraethoxide, could potentially produce stabilized $ZrO_2 \cdot CaO$ for high-strength material applications. The composition desired is 8.0% CaO and 92% ZrO_2 (mole percents), with the option of altering levels by increasing or decreasing reactant amounts.

II. Experimental Procedure

A. Synthesis of $CaO.Al_2O_3$

Synthesis of calcium aluminum ethoxide involved a two-step procedure, with optional isolation of the intermediate (best results were obtained with EtOH rather than i-PrOH systems):

Step I

$$Al(metal) + 3EtOH \text{ ----> } Al(OEt)_3 + 3/2H_2$$

Step II

$$Ca(metal) + 3Al(OEt)_3 + 2EtOH \text{ ----> } Ca[Al(OEt)_4]_2 + H_2$$

Since ethanol is extremely hygroscopic and the desired product extremely sensitive to air and moisture, special precautions must be taken. These include performing all reactions in an inert atmosphere, and drying ethanol with magnesium turnings and iodine immediately before use.

In a typical procedure, 0.540 g (0.20 mole) Al metal*, 150 ml dry ethanol, and a trace of mercuric chloride# were refluxed overnight, allowing a white precipitate (believed to be aluminum ethoxide) to form. Next, 0.401 g (0.10 mole) Ca metal† and more catalyst (mercuric chloride) were added. Upon refluxing for 25 hours, the mixture turned clear as anticipated, indicating the double metal alkoxide's presence. The solution was condensed by rotary evaporation or vacuum distillation to form a white powder. Crude yields of several experiments were 93.4%, 89.7%, and 84.7%.

---

* MCB Manufacturing Chemists, Inc.
\# Fluka AG
† J. T. Baker Chemical Co.

Products were characterized by IR spectral analysis, done with KBr salt plates and Nujol mull. The IR spectrum is described in Table 1.

Controlled hydrolysis of a 1.00 g sample of Ca-Al alkoxide led to gel formation. Upon evaporation of ethanol, a white powder resulted, which was then calcined at ~1000°C. Qualitative analysis by X-ray diffraction indicated that the sample was still amorphous after 6 hours of calcination. After 15 hours, a binary phase emerged, with $CaO.Al_2O_3$ as the major component and $5CaO \cdot 3Al_2O_3$ as the minor. Perhaps if the sample were heated longer than 15 hours, there would be a total phase transformation to $CaO.Al_2O_3$.

B. Zirconia Coating

Since the objective was to coat zirconia, co-precipitation of zirconium and calcium aluminum alkoxides was attempted, using a procedure developed for zirconium hydrolysis by Fegley and co-workers.[3]

In a typical experiment, 25 ml $Zr(O^nPr)_4$* was dissolved in 800 ml ethanol (0.10 M). In a second beaker, another solution containing 0.909 g Ca-Al ethoxide and 100 ml ethanol was prepared. When this was added to the first solution and mixed at room temperature, no chemical interaction occurred. The resultant solution was heated to 50°C, and another solution of 6.8 ml deionized water in 600 ml ethanol (0.63 M) was heated to the same temperature separately. Hydrolysis was then induced by adding the water/alcohol solution to the alkoxide/alcohol solution. No evidence of precipitation occurred within 2 minutes, 30 minutes, or even overnight. A

* Alfa Products

portion of the alcohol was distilled, leaving a clear gel, and the remainder of the alcohol was evaporated, leaving a powder. A portion of this was calcined at ~1000°C for 10 hours, transforming it into a very coarse solid.

III. Results

Calcination results indicate that a Ca-Al alkoxide was successfully synthesized. A more definite characterization will be made when molecular weight determination and nuclear magnetic resonance (NMR) results are obtained. The product's actual composition may explain why some of the product's calcium and aluminum oxides combined in a 5:3 ratio rather than the 1:1 ratio expected.

Hydrolysis of zirconium and Ca-Al alkoxides did not induce precipitation, leading instead to gel formation when the ethanol was evaporated. The gel was calcined at 1000°C for 10 hours, yielding a coarse solid. SEM analysis of the product revealed a dense material with very little grain boundary. Absence of shade contrast in the micrograph indicates no calcium-aluminum oxide at the boundary.

IV. Future Work

Future work on this coating system will deal with precipitation of the desired product as a powder rather than as a gel. By varying the concentrations of alkoxide and water solutions, the kinetics may be altered so powder of the desired composition will form.

V. References

1. B. Fegley, E. A. Barringer, and H. K. Bowen, J. Am. Ceram. Soc., 1984, 67(6), C113-16.

2. S. Govil and R. C. Mehrotra, Syn. React. Inorg. Metal-Org. Chem., 1975, 5(4), 267-77.

3. B. Fegley and E. A. Barringer, "Synthesis, Characterization, and Processing of Monosized Ceramic Powders," submitted to Better Ceramics Through Chemistry, 1984.

Table 1

IR Spectrum of Ca-Al Ethoxide $Ca[Al(OEt)_4]_2$

Band Position (cm^{-1})	Band Strength
2995-2825	vs
1460	s
1380	w
1170	m
1110	s
1070	vs
910	s
720	s
660	m
600	w
490	w

Key

vw - very weak

w - weak

m - medium

s - strong

vs - very strong

Ted McMahon

PREPARATION OF MONODISPERSE, EQUIAXED $2MgO.2Al_2O_3 \cdot 5SiO_2$ PARTICLES FROM ALUMINOSILICATE DOUBLE ALKOXIDE

I. Introduction

This report describes progress made in synthesizing uniform, submicron particles of cordierite ($2MgO.2Al_2O_3 \cdot 5SiO_2$), a lightweight, strong, refractory ceramic with a low coefficient of thermal expansion, using alkoxide precursors. Uniform particles are necessary in the creation of uniform ceramic microstructures, free of property-limiting flaws.

II. Experimental Procedure

Aluminosilicate synthesis, a preliminary step, was attempted here using Janavicius' method[1] for doping SiO_2 with B_2O_3 by partial hydrolysis. (Monodisperse, spherical SiO_2 could be doped with up to 29 wt% B_2O_3 using this method).

The general synthesis method involved adding two equivalents of ammoniated water (29% NH_3)* to a solution of one equivalent of tetraethyl orthosilicate (TEOS)** in alcohol, forming $Si(OEt)_2(OH)_2$. Aluminum alkoxide was then added to react with the partially hydrolyzed TEOS, yielding a product with a Si-O-Al linkage. The alkoxide was then fully hydrolyzed with excess ammoniated water.

This procedure was used for a range of final TEOS concentrations from 0.3M to 0.01M, over a range of Si:Al mole ratios from 10:1 to 5:4. Both the

---

* Mallinchralt NH_3 29.85%
** Aldrich

isopropoxide and sec-butoxide of aluminum $Al(OPr^i)_3$[†] and $Al(OBu^s)_3$,[#] respectively) were tried.

$Al(OPr^i)_3$ was used first, dissolved in toluene to make it soluble in the ammoniated TEOS/isopropanol solution. This procedure's results were unsatisfactory, though, and had to be discarded.

$Al(OBu^s)_3$ was therefore tried as an alternative: because it is a liquid, $Al(OBu^s)_3$ was expected to dissolve more readily in the TEOS/alcohol solution than had $Al(OPr^i)_3$. Although it was found unsuitable for use in a TEOS/ethanol system because it converts to the insoluble ethoxide on contact with ethanol, $Al(OBu^s)_3$ readily went into a TEOS/2-butanol solution.

III. Results

Powder particles produced from the $Al(OBu^s)_3$/TEOS/2-butanol solution were irregularly shaped and much smaller than the particle sizes of 0.1-0.5um hoped for.

IV. Future Work

IR spectroscopy will determine whether or not a triple alkoxide containing Si, Al, and Mg has indeed been synthesized. Kinetics of the hydrolysis reaction will then be studied using light scattering techniques, and the solvent's effect on hydrolysis and final powder characteristics determined.

---

† Chattem Chemicals
# Chattem Chemicals, high purity

V. References

1. L. V. Janavicius, "Formation and Processing of Monosized Borosilicate Powders," M.S. thesis, Mass. Inst. of Tech., Cambridge, MA (1984).

Anne Bagley

PREPARATION OF MONODISPERSE, EQUIAXED $2MgO \cdot 2Al_2O_3 \cdot 5SiO_2$ PARTICLES FROM MAGNESIUM-ALUMINUM DOUBLE ALKOXIDE

I. Introduction

This report describes progress made in synthesizing monodisperse, equiaxed particles of cordierite, $2MgO \cdot 2Al_2O_3 \cdot 5SiO_2$.

II. Experimental Procedure

Synthesis was originally attempted using solutions of individual alkoxides dissolved in their respective alcohols (e.g., $Mg(OEt)_2$,* $Al(OEt)_3$,** and tetraethyl orthosilicate (TEOS)# dissolved in ethanol). Immediate difficulties arose, however, in that the purchased alkoxides were insoluble in common alcohols, and their individual reaction times varied dramatically: Mg alkoxides reacted in seconds, while Si alkoxides were stable enough in water to be used under normal atmospheric conditions.

Double alkoxides were therefore used instead of single alkoxides. Besides being more soluble in alcohols, double alkoxides include two necessary elements in one compound, minimizing the system's complexity by effectively reducing its components from three to two.

A double alkoxide of Mg and Al was prepared using Mehrotra's method.[1] Mg metal was added to a solution of aluminum isopropoxide ($Al(Opr)_3$)† in excess isopropanol, with mercuric chloride serving as system catalyst.

---

* Apache Chemicals Inc., 95%
** Chattem Chemicals, high purity
\# Fisher Scientific Co.
† Chattem Chemicals, high purity

$$Mg + 2Al(OPr)_3 + 2PrOH \xrightarrow{HgCl_2} MgAl_2(OPr)_8 + H_2 \qquad (1)$$

Comparison of the resulting compound's IR spectra with Mehrotra's spectra showed the compound to be $MgAl_2(OPr)_8$. When this double alkoxide was hydrolyzed and heated to 800°C for 5 hours, X-ray diffraction showed the resulting compound to be spinel, $MgAl_2O_4$. Mehrotra suggests the reactions can be represented by the following equations.

$$MgAl_2(OPr)_8 + 8H_2O \longrightarrow MgAl_2(OH)_8 + 8PrOH \qquad (2)$$

$$MgAl_2(OH)_8 \longrightarrow MgAl_2O_4 + 4H_2O \qquad (3)$$

Under basic conditions, the double alkoxide (in final solution concentrations of 0.01 M to 0.3 M) reacted almost immediately with water to form a gel.

MgO and Al_2O_3 were incorporated into the silica in a manner similar to that used by Janavicius for doping SiO_2 with B_2O_3.[2] TEOS, which IR spectra showed to be already partially hydrolyzed, was further hydrolyzed with an NH_4OH/isopropanol solution. NH_4OH concentration varied between runs, from zero to a 2.5 molar ratio of water to Si. Double alkoxide was then added. Because the double alkoxide was utilized in its parent alcohol, its concentration had to be estimated from the starting agents' concentrations. The double alkoxide and TEOS solutions were allowed to mix for times varying from 10 minutes to 2.5 hours in the hope that the double alkoxide would react with the partially hydrolyzed TEOS to form a complex containing Mg, Al, and Si in the desired stoichiometric ratio.

The double alkoxide/TEOS mixture was further hydrolyzed with an NH_4OH/isopropanol solution. Final double alkoxide concentrations in this solution varied from 0.075M to 0.037M. Water diluted in isopropanol was then added in a molar excess of five times.

Each mixture reacted in seconds to form a gel, which was dried and then heated.

III. Results

The variations in NH_4OH concentration and mixing time appeared to have little effect on the final product. Samples heated to less than 1000°C showed no crystallinity. Heating at 1000°C for 15 hours enabled only major spinel peaks to be identified by X-ray diffraction, indicating that the sample consisted entirely of spinel. Heating to 1200°C for 3 hours produced X-ray diffraction results indicating that the sample contained about 75% cordierite and 25% spinel.

IV. Future Work

Further work is necessary to adjust the stoichiometry so that cordierite is the only final product. This can be done by distilling the double alkoxide from its parent alcohol so that solutions of more accurate molarity can be made. The effects of pH, alkoxide concentration, and different solvents should be studied so that particles, rather than gels, can be formed and their shape controlled.

In addition, experiments similar to those outlined above will be carried out using a purchased Al-Si double alkoxide and a Mg alkoxide.

References

1. R. C. Mehrotra, S. Goel, A. B. Goel, R. B. King, K. C. Nainin, "Preparation and Characterization of Some Volatile Isopropoxides of Aluminum and Alkaline Earth Metals." Inorg. Chem. Acta 29 (1978): 131-136.

2. L. V. Janavicius, "Formation and Processing of Monosized Borosilicate Powder," M.S. thesis, Mass. Inst. of Tech., Cambridge, MA (1984).

Paul White

SYNTHESIS OF NARROW SIZE DISTRIBUTION ZrO_2, $Y_2O_3 \cdot ZrO_2$, and $ZrO_2 \cdot Al_2O_3$ POWDERS

I. Introduction

This report describes progress made in synthesizing narrow size distribution powders to achieve more uniform packing of green pieces. Better-packed green pieces should produce final sintered pieces having uniform submicron microstructures.[1] Methods used for synthesizing narrow size distribution powders of ZrO_2, $Y_2O_3 \cdot ZrO_2$, and $ZrO_2 \cdot Al_2O_3$ are described below. ZrO_2 has important applications in sensoring devices; $Y_2O_3 \cdot ZrO_2$ and $ZrO_2 \cdot Al_2O_3$ are most noted for their high strength.

Powder characterizations were done by single point BET and density measurements, X-ray analysis, and chemical analyses that included inductively coupled plasma emission spectroscopy (ICP), proton-induced X-ray emission (PIXE), wet chemistry, and electron-probe microanalysis (EPMA).

II. Experimental Procedures, Results, and Discussions

ZrO_2

Experimental Procedure

Narrow size distribution zirconia was prepared by controlled hydrolysis of zirconium n-propoxide. When a 7.77×10^{-2} M $Zr^n(OPr)_4$ solution was mixed with a 5.37×10^{-1} M H_2O/dry ethanol solution at 50°C, a light-colored powder formed within 65 seconds. Stirring for an additional 20 minutes turned the mixture completely white. This mixture was centrifuged, and the supernatant decanted. The powder was then washed twice — some samples in ethanol, others in deionized water — to remove any unreacted alkoxide. Packing

samples were prepared by slip casting, for which powder dispersions were prepared at a pH of 10.0. Samples were then sintered at 1160°C.

Results

The powder yield from this process was ~48%. Figure 1 shows a TEM photograph of water-washed ZrO_2 prepared by this method. ZrO_2 particle surface areas, measured by single point BET, are given in Table 1 for powder treated three different ways. As indicated, surface area was strongly affected by both the solvent used to rinse the powder and the length of time the powder remained in solution afterwards. An average density of the crystallized powders is also included in Table 1.

X-ray analysis showed these powders to be amorphous, but calcining at 600°C for 6 hours transformed them to the monoclinic crystalline phase.

Table 2 is a representative ICP analysis of impurity levels in the ZrO_2 powder.

Figure 2 shows the top surface of a ZrO_2 compact. Packing densities of unfired pieces were about 62% of theoretical densities.

Figure 3 shows an SEM micrograph of ZrO_2's microstructure after sintering at 1160°C. Grain size is uniform and submicron.

Conclusions

Narrow size distribution ZrO_2 powders can be reproducibly synthesized. Powder packing was reproducible at ~62% of theoretical.

Sintering at temperatures of about 1160°C for approximately one hour yielded samples with uniform submicron microstructures.

$Y_2O_3 \cdot ZrO_2$ Experimental Procedure

Narrow size distribution ZrO_2 powders homogeneously doped with Y_2O_3 were prepared by coprecipitating $Zr^n(OPr)_4$ and $Y^i(OPr)_3$. $Y^i(OPr)_3$ was dissolved in $Zr^n(OPr)_4$, and the solution diluted with dry ethanol to yield concentrations of 7.34×10^{-2} M $Zr^n(OPr)_4$ and 1.13×10^{-2} M $Y^i(OPr)_3$. The alkoxide mixture was then hydrolized with a 1.0 M deionized H_2O solution so that the molar ratio of H_2O:$Zr^n(OPr)_4$ was 13.62:1. The mixture was then heated. Powder formed instantaneously at 50°C. Packing samples were prepared by slip casting, for which powder dispersions were prepared at a pH of 10.0. Sintering was done at 1100°C.

Results

The powder yield after washing was ~50%. Figure 4 shows a TEM photograph of H_2O-washed $Y_2O_3 \cdot ZrO_2$ taken at the same magnification as Figure 1.

Surface area measurements made on $Y_2O_3 \cdot ZrO_2$ varied by ± 20 m^2/g. An average measurement is included in Table 1.

X-ray diffraction showed the powder as prepared to be amorphous, but calcining at 1100°C for ~8 hr transformed the zirconia to the cubic form.

Table 3 details approximate impurity levels, determined by ICP.

EPMA analysis results, listed in Table 4, showed batch-to-batch reproducibility, and homogeneity within the sintered pieces.

Packing results for the $Y_2O_3 \cdot ZrO_2$ materials were similar to those obtained for ZrO_2; packing densities of unfired pieces were about 62% of theoretical.

Figure 5 shows an SEM micrograph of $Y_2O_3 \cdot ZrO_2$'s microstructure after sintering at 1100°C. Grain size is uniform and submicron.

Conclusions

Narrow size distribution $Y_2O_3 \cdot ZrO_2$ powders can be reproducibly synthesized. Powder packing was reproducible at ~62% of theoretical.

X-ray diffraction of $Y_2O_3 \cdot ZrO_2$ powder samples showed zirconia to be stabilized in the cubic form.

Sintering at temperatures of about 1100°C for approximately one hour yielded samples with uniform submicron microstructures. EPMA analysis of the sintered $Y_2O_3 \cdot ZrO_2$ samples showed the dopant to be homogeneously distributed throughout the sample.

$ZrO_2 \cdot Al_2O_3$

Experimental Procedure

Sized 0.2-0.3 μm Al_2O_3 was dried at 200°C for ~4 hr, then dispersed in dry ethanol. $Zr^n(OPr)_4$ was added to the dispersion and hydrolized with a H_2O/ethanol solution to precipitate ZrO_2 from the alkoxide as a coating on the Al_2O_3 particles. Dispersions used in packing were prepared at a pH of 10.0.

Reaction conditions are specified for three approximate compositions in Table 5.

Results

Figures 6a and 6b are bright- and dark-field TEM images of a 16 vol% zirconia-coated particle. The dark-field image shows an almost continuous zirconia layer surrounding the alumina particle.

Surface area measurements of the coated alumina show a large increase in surface area over uncoated Al_2O_3. Figure 7 shows that a plot of surface area versus volume % zirconia is linear, increasing with volume % zirconia.

Density measurements were performed on powders after calcining (600°C, ~6 hr). The calculated trend is plotted in Figure 8, assuming densities of 4.0 g/cm^3 for Al_2O_3 and 5.6 g/cm^3 for ZrO_2.

ICP analysis revealed the impurity levels listed in Table 6.

Chemical reproducibility, determined by wet chemistry and PIXE methods, is shown in Table 7.

Table 8 shows EPMA analysis data for a sintered $ZrO_2 \cdot Al_2O_3$ composite. These results demonstrate that coating uniformity leads to uniformity in the sintered product.

The top surface of a 16 vol% $ZrO_2 \cdot Al_2O_3$ composite is shown in Figure 9. Packing densities as high as 55% of theoretical were obtained. The uniform particle coating led to dispersion behavior similar to that of pure ZrO_2.

Figure 10 shows the microstructure of a 20 vol% $ZrO_2 \cdot Al_2O_3$ composite sintered at 1500°C for $1\frac{1}{2}$ hours. Grain sizes are largely submicron and nonuniform.

Conclusions

Uniformly coated, narrow size distribution $ZrO_2 \cdot Al_2O_3$ powders were synthesized reproducibly and packed to 55°C of theoretical. Sintered microstructures, though not of uniform grain size, were mostly submicron.

III. References

1. B. Fegley, E. A. Barringer, "Synthesis, Characterization, and Processing of Monosized Ceramic Powders," paper presented at Materials Research Society, Albuquerque, NM, 1984.

TABLE 1. Average Particle Surface Areas and Densities of ZrO_2 and $Y_2O_3 \cdot ZrO_2$

	ZrO_2	$Y_2O_3 \cdot ZrO_2$
Surface Area (m^2/g) H_2O-rinsed	127.58	74.11
Surface Area (m^2/g) H_2O-rinsed, allowed to stand ~1 month	42.66	-
Surface Area (m^2/g) EtOH-rinsed	21.90	-
Density	5.10	6.15

TABLE 2. Impurity Levels in ZrO_2 (Determined by ICP)

Element	ppm
Ca	<20
Mg	<10
Mn	<10
Mo	<20
Na	<50
Nb	<100
Ni	<30

Element	ppm
P	<50
Pb	<50
Sb	<50
Si	60-400
Sn	<50
Sr	<10
Ta	<100

Element	ppm
Ti	~350
V	<20
Zr	<20
K	<93
Hf	1.35%

TABLE 3. Impurity Levels in $Y_2O_3 \cdot ZrO_2$ Powder (Determined by ICP)

Element	ppm
Al	397
As	<24.7
B	96.7
Ba	<9.88
Be	<4.94
Ca	140
Cd	<9.88
Co	113
Cr	<66.0
Cu	<24.7

Element	ppm
Fe	144
Ga	<24.7
La	<9.88
Li	<9.88
Mg	21.6
Mn	<4.94
Mo	<24.7
Na	<49.4
Ni	<38.7
P	<24.7

Element	ppm
Pb	<24.7
Sb	<24.7
Se	<24.7
Si	692
Sn	<31.2
Sr	<4.94
Ti	0.602%
V	16.7
Zn	<14.8
Hf	1.42%

TABLE 4. Ratios of ZrO_2 to Y_2O_3 (Determined by EPMA) in Two Sintered Samples

#	PW #1 $ZrO_2 \cdot Y_2O_3$	PW #2 $ZrO_2 \cdot Y_2O_3$
1	5.75	5.79
2	5.79	5.80
3	5.69	5.83
4	5.77	5.60
5	5.76	5.85
6	5.82	5.59
7	5.81	5.74
8	5.76	-
9	5.79	-
10	5.80	-
average	5.77±0.04	5.74±0.12

TABLE 5. Reaction Conditions for $ZrO_2 \cdot Al_2O_3$ Composites

	~8 vol% ZrO_2	~16 vol% ZrO_2	~20 vol% ZrO_2
Initial [$Zr^n(OPr)_4$] (M)	6.54×10^{-2}	8.03×10^{-2}	7.84×10^{-2}
Initial [Al_2O_3] (M)	2.91×10^{-1}	1.78×10^{-1}	1.33×10^{-1}
Initial [H_2O] (M)	7.26×10^{-1}	5.24×10^{-1}	5.08×10^{-1}
$H_2O:Zr^n(OPr)_4$	11.11:1	6.54:1	6.48:1
Solvent	dry EtOH	dry EtOH	dry EtOH
Atmosphere	nitrogen	nitrogen	nitrogen
Reaction Temp. (°C)	50	50	50

TABLE 6. ICP Analysis of Impurity Levels* in Three $ZrO_2 \cdot Al_2O_3$ Samples

	# 1 (ppm)	# 2 (ppm)	# 3 (ppm)
As	<180	<156	174
Cu	16	7	9
Fe	130	86	87
Mg	20	17	19
P	<63	<55	<59
Pb	<38	<33	<36
Sb	<44	<39	<41
Se	<40	<35	<37
Si	216	522	821
Sn	<18	<19	<19
Ti	(wt %) 0.12	(wt %) 0.20	(wt %) 0.15

* B, Ba, Be, Ca, Cd, Co, Cr, Ga, La, Li, Mn, Mo, Na, Ni, Sr, Zn, Zr, K all below 12 ppm

TABLE 7. Chemical Reproducibility

Sample	Observed wt% ZrO_2	Analytical Method
PW #33	26.5 ± 0.5	wet chemistry
PW #38	27.0 ± 1.8	PIXE
PW #43	24.5 ± 1 6	PIXE

TABLE 8. EPMA Analysis of $ZrO_2 \cdot Al_2O_3$ †

Oxide	SW - AlZ-4B*	SW - AlZ - 4**
Al_2O_3	76.68±1.78	75.78±1.41
ZrO_2	22.44±1.79	22.90±1.63
HfO_2	0.28±0.10	0.70±0.23
ZnO	0.01±0.01	NA***
SiO_2	0.28±0.04	0.24±0.03
MnO	0.00±0.01	NA
CaO	0.03±0.01	0.02±0.01
FeO	0.07±0.04	0.09±0.02
PbO	0.01±0.02	0.00±0.00
Total	99.80±1.00	99.73±1.40

† Samples prepared from same batch of powder

* Average of 12 points

** Average of 11 points

*** Not analyzed

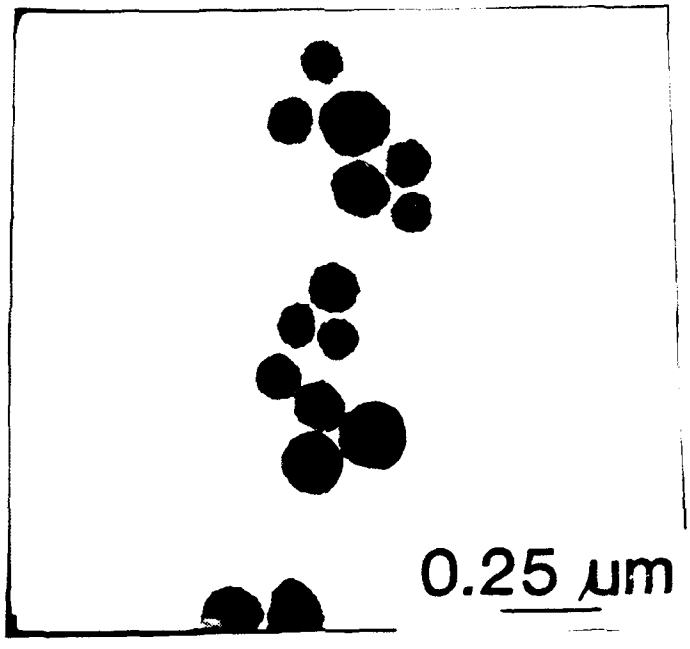

Figure 1. Water-washed ZrO_2 particles.

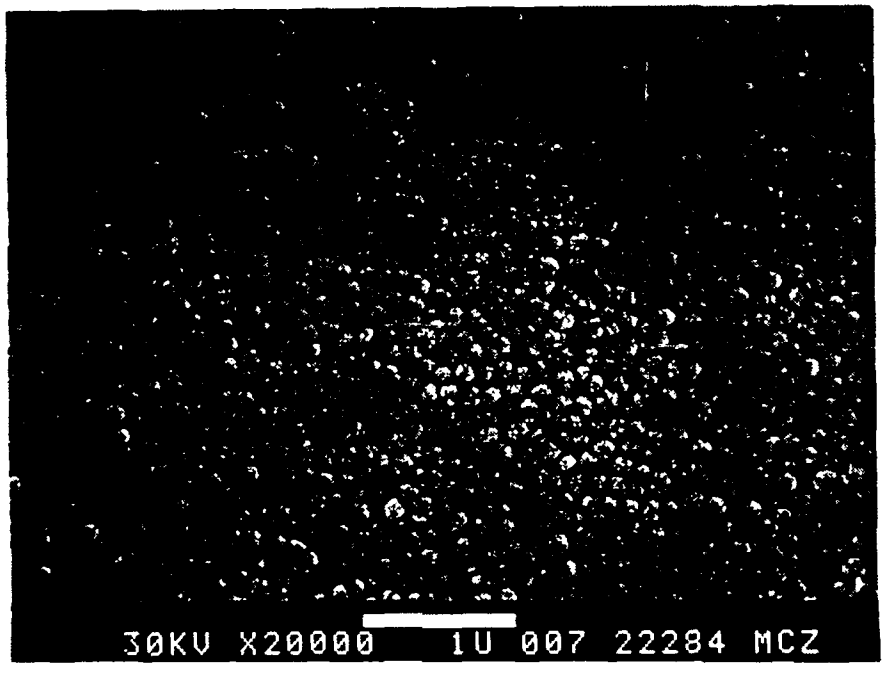

Figure 2. Top surface of ZrO_2 compacts (~65% of theoretical).

Figure 3. Top surface of sintered ZrO_2 piece (1160°C, ~1 hr).

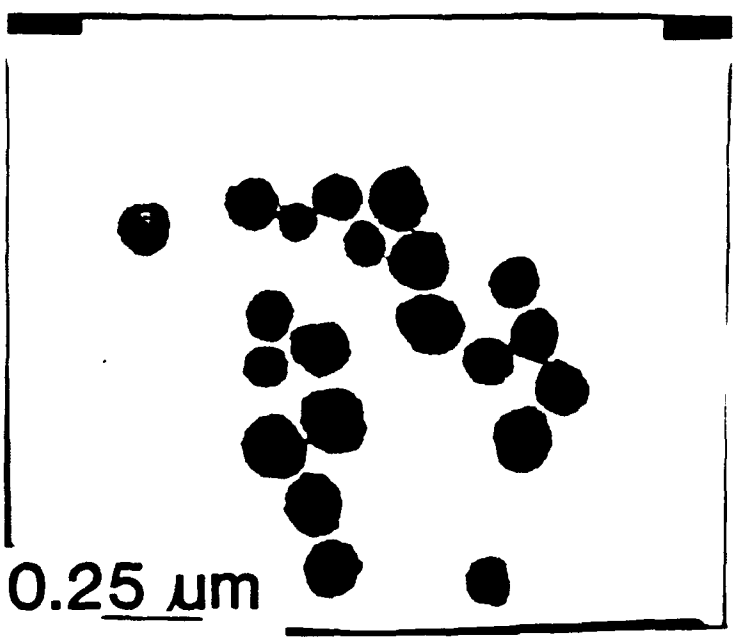

Figure 4. Water-washed Y_2O_3/ZrO_2.

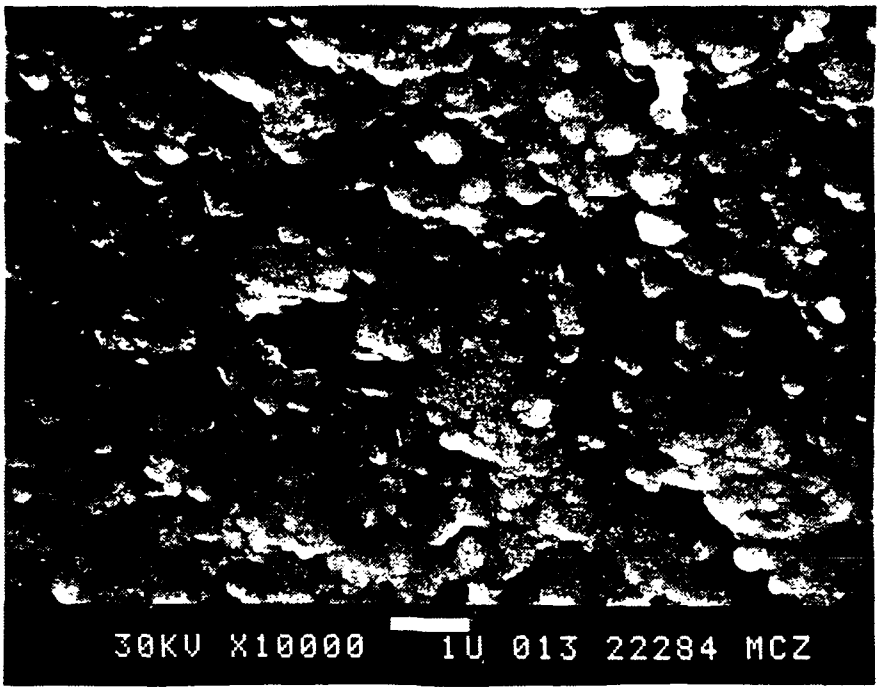

Figure 5. Top surface of sintered Y_2O_3/ZrO_2 (1100°C, ~1 hr).

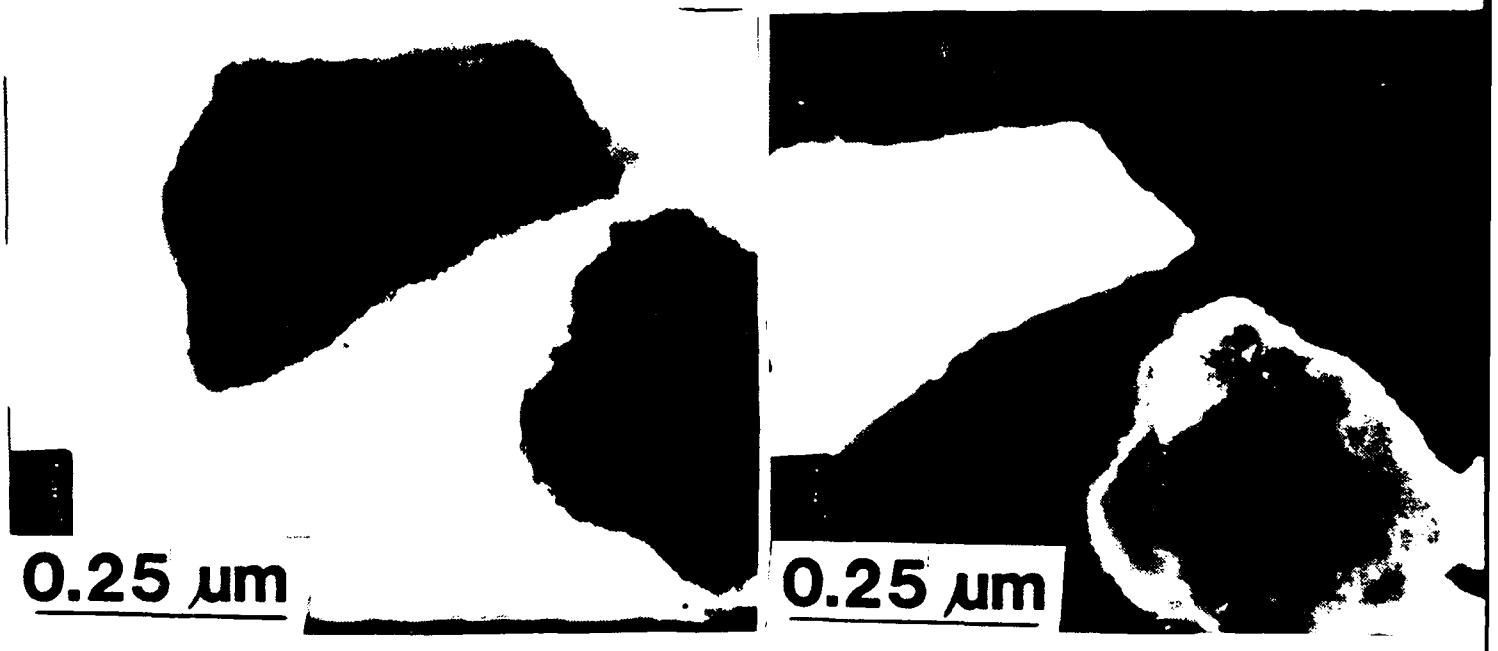

(A) (B)

Figure 6. (a) Bright field TEM image of Al_2O_3 particle coated with ZrO_2; (b) dark field TEM image of the same showing ZrO_2 coating on particle surface.

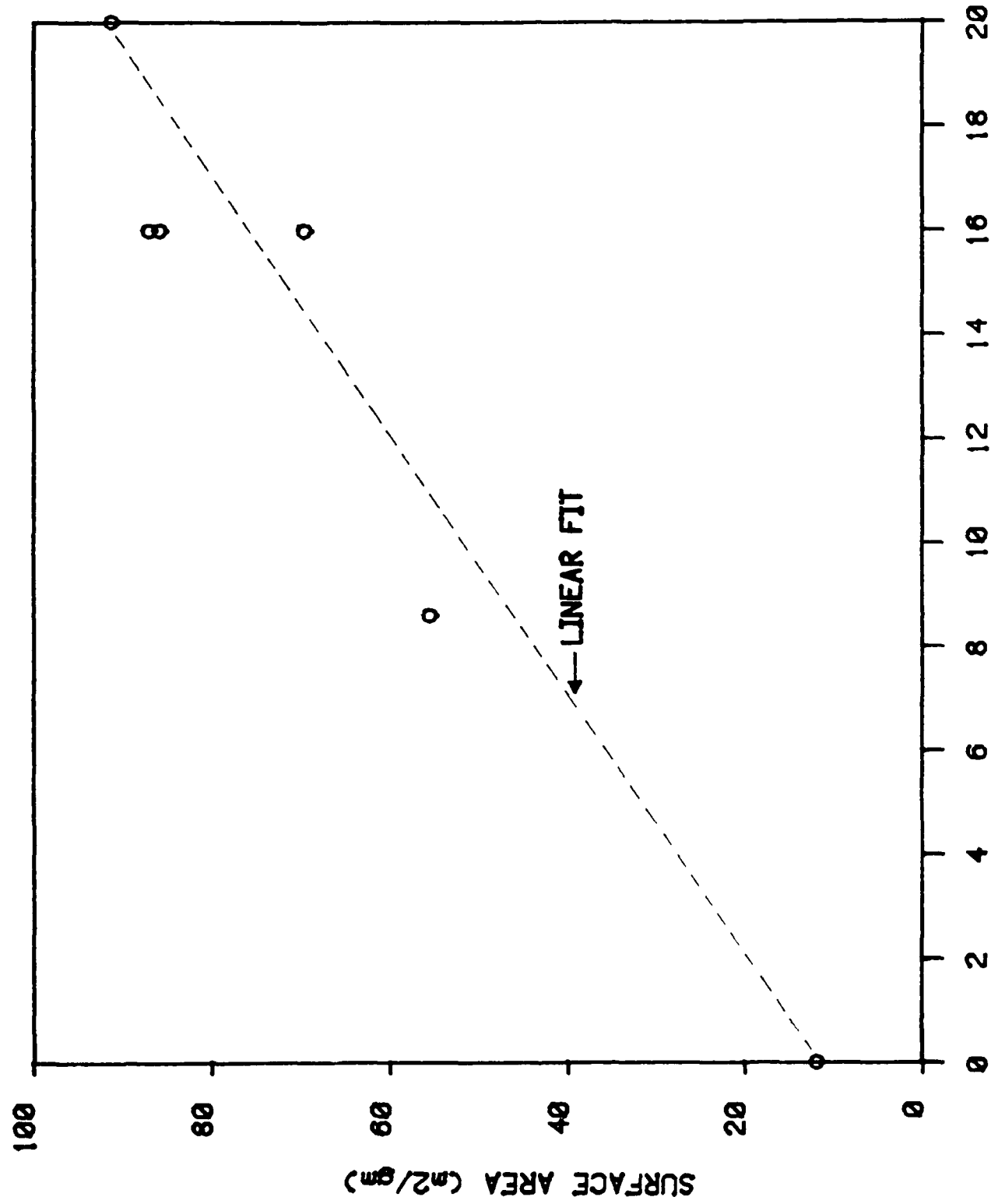

Figure 7. Surface area (m^2/g) versus volume % ZrO_2.

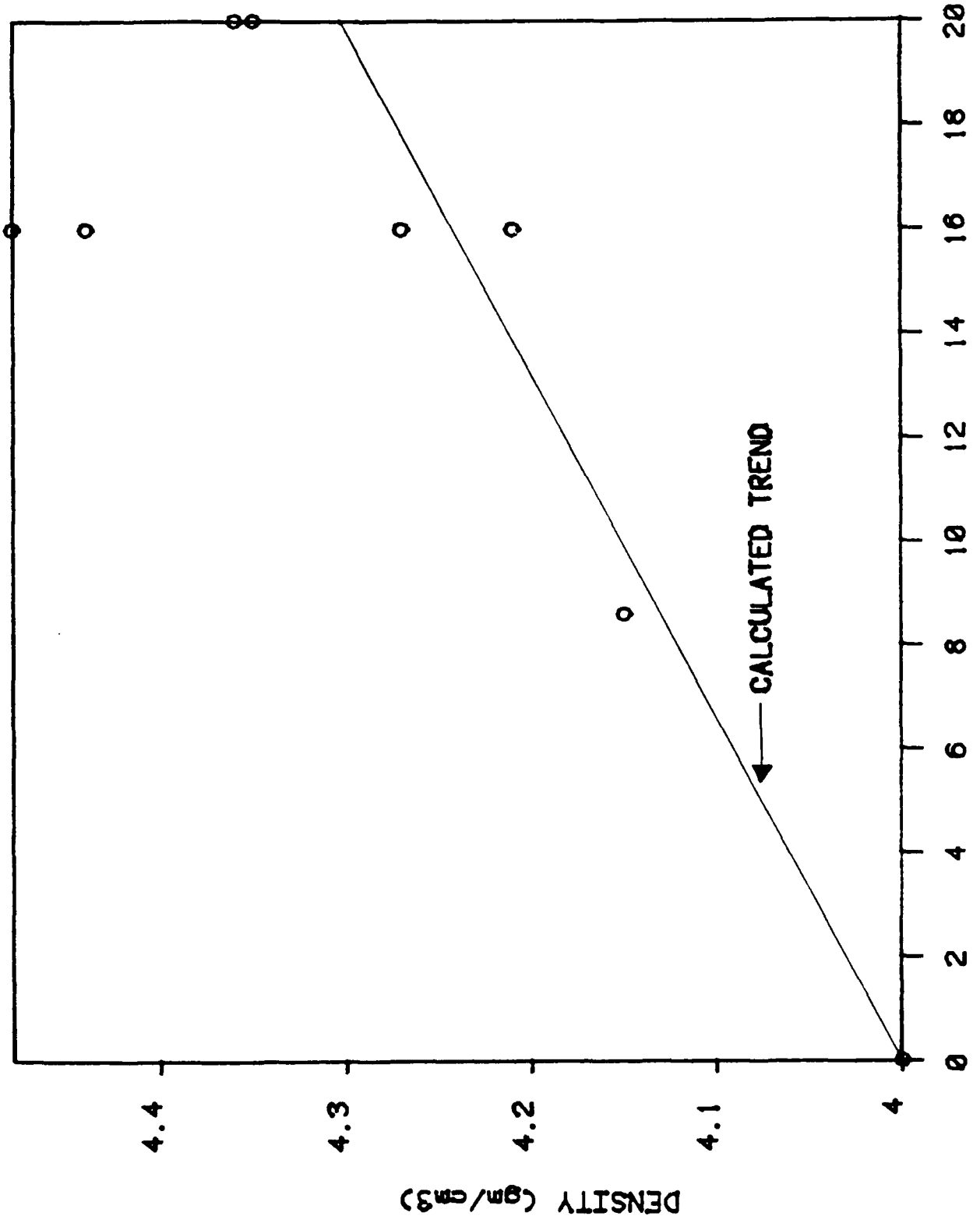

Figure 8. Density (g/cm^3) versus volume % ZrO_2.

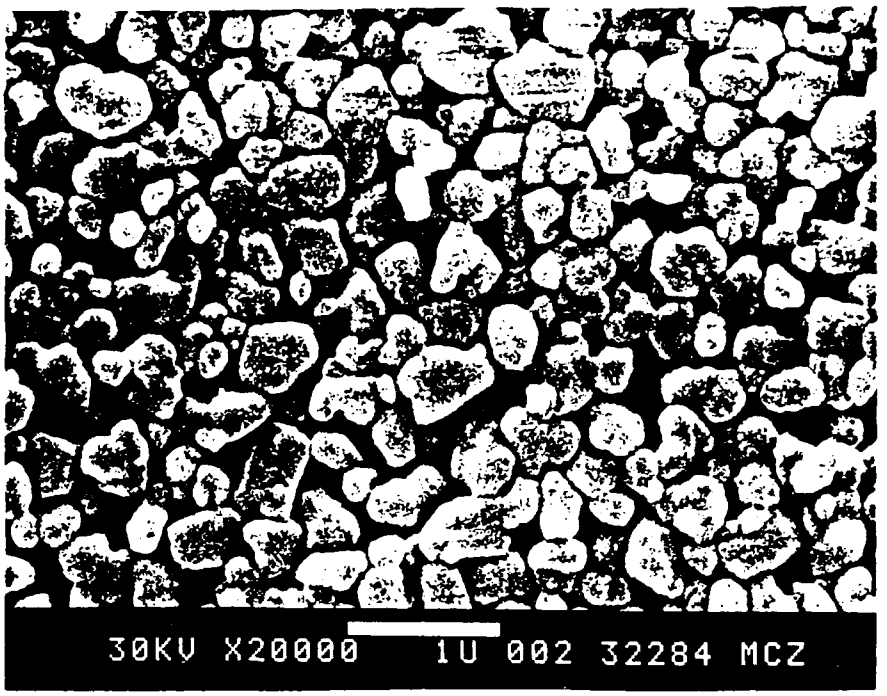

Figure 9. Top surface of ZrO_2/Al_2O_3 compact.

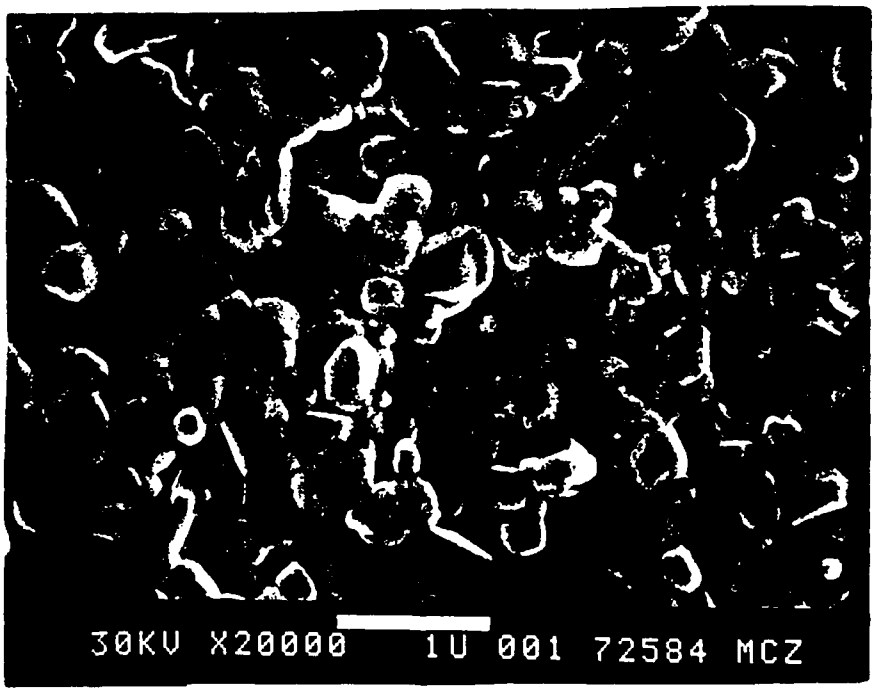

Figure 10. Top surface of sintered ZrO_2/Al_2O_3 piece (1500°C, $1^1/_2$hr).